



Mechanisms of platelet activation and receptor regulation in genetically modified mice

• • •

Mechanismen der Thrombozytenaktivierung und Rezeptorregulation in genetisch veränderten Mäusen

Doctoral thesis for a doctoral degree
at the Graduate School of Life Sciences,
Julius-Maximilians-Universität Würzburg,
Section Biomedicine

submitted by

Michael Popp

from Würzburg, Germany

Würzburg, 2016

Submitted on: _____

Office stamp

Members of the *Promotionskomitee*:

Chairperson: Prof. Dr. Manfred Gessler

Primary Supervisor: Prof. Dr. Bernhard Nieswandt

Supervisor (Second): PD Dr. Heike Hermanns

Supervisor (Third): Prof. Dr. Christoph Kleinschnitz

Date of Public Defense: _____

Date of Receipt of Certificates: _____

Table of contents

| | |
|--|-----------|
| Summary | IV |
| Zusammenfassung..... | VI |
| 1 Introduction | 1 |
| 1.1 Platelet activation and thrombus formation | 2 |
| 1.2 Platelet signaling upon activation..... | 3 |
| 1.2.1 (Hem)ITAM signaling | 3 |
| 1.2.2 GPCR signaling in platelets..... | 6 |
| 1.2.3 Small GTPases of the Rho family | 7 |
| 1.2.4 Calcium signaling in platelets | 9 |
| 1.3 Platelet integrin activation | 12 |
| 1.3.1 Hic-5..... | 12 |
| 1.4 BAR domain family proteins..... | 13 |
| 1.4.1 BIN2 | 14 |
| 1.5 Fcγ receptor signaling and immune thrombocytopenia..... | 14 |
| 1.6 Aim of the study..... | 17 |
| 2 Materials and Methods..... | 18 |
| 2.1 Materials | 18 |
| 2.1.1 Chemicals | 18 |
| 2.1.2 Kits | 21 |
| 2.1.3 Antibodies..... | 21 |
| 2.1.4 Buffers and media | 23 |
| 2.2 Methods..... | 27 |
| 2.2.1 Genetically modified mice..... | 27 |
| 2.2.2 Genotyping of mice | 28 |
| 2.2.3 Biochemistry | 37 |
| 2.2.4 <i>In vitro</i> analysis of platelet function | 39 |
| 2.2.5 <i>In vivo</i> analysis of platelet function..... | 44 |
| 2.2.6 Histology..... | 46 |
| 2.2.7 Microscopy..... | 46 |
| 2.2.8 Data analysis | 47 |

| | | |
|----------|---|-----------|
| 3 | Results | 48 |
| 3.1 | Bridging integrator 2 (BIN2) controls store-operated calcium entry in platelets and thrombotic and thrombo-inflammatory activity in mice | 48 |
| 3.1.1 | BIN2 interacts with STIM1 in platelets..... | 48 |
| 3.1.2 | BIN2 KO mice are viable and fertile, but display a mild macrothrombocytopenia..... | 50 |
| 3.1.3 | Defective SOCE in BIN2-deficient platelets..... | 52 |
| 3.1.4 | Defective (hem)ITAM-mediated activation of <i>Bin2</i> ^{fl/fl P14-Cre} platelets..... | 53 |
| 3.1.5 | Defective aggregate formation on collagen under flow and reduced coagulant activity of BIN2-deficient platelets | 55 |
| 3.1.6 | Lack of BIN2 has no influence on platelet spreading on fibrinogen and platelet integrin outside-in signaling <i>in vitro</i> | 56 |
| 3.1.7 | Impaired hemostasis and defective arterial thrombus formation in <i>Bin2</i> ^{fl/fl P14-Cre} mice | 57 |
| 3.1.8 | BIN2 plays an important role in the progression of ischemic stroke | 58 |
| 3.1.9 | Calpain-mediated degradation of BIN2..... | 59 |
| 3.2 | Normal platelet function in mice lacking hydrogen peroxide-induced clone-5 (Hic-5) 61 | |
| 3.2.1 | Hic-5 is dispensable for hematopoiesis and platelet morphology | 61 |
| 3.2.2 | Hic-5 is dispensable for inside-out signaling and thrombus formation <i>in vitro</i> | 62 |
| 3.2.3 | Lack of Hic-5 has no influence on platelet spreading on fibrinogen and platelet integrin outside-in signaling <i>in vitro</i> | 64 |
| 3.2.4 | Hic-5-deficient platelets have unaltered GPIb function..... | 65 |
| 3.2.5 | Unaltered <i>in vivo</i> thrombus formation in Hic-5-deficient mice..... | 65 |
| 3.3 | Non-redundant functions of small Rho GTPases RhoA and Rac1 in murine platelets 67 | |
| 3.3.1 | Non-redundant functions of RhoA and Rac1 for basic platelet parameters | 68 |
| 3.3.2 | Non-redundant functions of RhoA and Rac1 for integrin inside-out signaling | 69 |
| 3.3.3 | Non-redundant functions of RhoA and Rac1 for platelet spreading on fibrinogen and clot retraction <i>in vitro</i> | 70 |
| 3.3.4 | Combined deficiency of RhoA and Rac1 results in defective hemostasis and defective thrombus formation <i>in vivo</i> | 71 |
| 3.4 | Liver sinusoidal endothelial cells process antibody opsonized platelets through the inhibitory Fcγ receptor IIB in mice | 72 |
| 3.4.1 | FcγRs are required for anti-GPVI-induced transient thrombocytopenia and the generation of sGPVI..... | 72 |
| 3.4.2 | FcγRIIB, but not FcγRIII, is necessary to promote anti-GPVI-induced transient thrombocytopenia and the generation of sGPVI..... | 74 |
| 3.4.3 | JAQ1-opsonized platelets are retained primarily in the liver by FcγRIIB-expressing liver sinusoidal endothelial cells | 75 |
| 3.4.4 | Absence of endothelial ADAM10 does not prevent the generation of sGPVI | 77 |

| | | |
|----------|--|------------|
| 3.4.5 | Fc γ RIIB mediates the sequestration of anti-GPIIb/IIIa-opsonized platelets in the liver and contributes to the early phase of thrombocytopenia | 78 |
| 4 | Discussion | 79 |
| 4.1 | Bridging integrator 2 (BIN2) controls store operated calcium entry in platelets and thrombotic and thrombo-inflammatory activity in mice | 79 |
| 4.2 | Normal platelet function in mice lacking hydrogen peroxide-induced clone-5 (Hic-5) | 81 |
| 4.3 | Non-redundant functions of small Rho GTPases RhoA and Rac1 in murine platelets | 82 |
| 4.4 | Liver sinusoidal endothelial cells process antibody opsonized platelets through the inhibitory Fc γ receptor IIB in mice | 83 |
| 4.5 | Outlook and concluding remarks | 85 |
| 5 | References..... | 88 |
| 6 | Appendix..... | 100 |
| 6.1 | Abbreviations | 100 |
| 6.2 | Acknowledgements | 103 |
| 6.3 | Curriculum vitae | 104 |
| 6.4 | Publications | 105 |
| 6.5 | International Conferences | 105 |
| 6.6 | Affidavit..... | 106 |
| 6.7 | Eidesstattliche Erklärung..... | 106 |

Summary

This work summarizes the results of studies on several major aspects of platelet activation and platelet receptor regulation. Therefore, this thesis is divided into four parts.

Platelet activation and aggregation at sites of vascular injury is critical to prevent excessive blood loss, but may also lead to life-threatening ischemic disease states, such as myocardial infarction and stroke. Agonist-induced elevation in cytosolic Ca^{2+} concentrations is essential for platelet activation in hemostasis and thrombosis. The principal route of Ca^{2+} influx in platelets is store-operated calcium entry (SOCE). The calcium sensor molecule stromal interaction molecule 1 (STIM1) regulates SOCE by activating the membrane calcium channel protein Orai1, but the exact mechanisms of this interaction are not fully understood. Using affinity chromatography to screen for STIM1 interacting proteins in platelets, bridging integrator 2 (BIN2), an adapter protein belonging to the family of BAR proteins that is mainly expressed in the hematopoietic system, was identified. Newly generated BIN2 KO mice were viable and fertile but their platelets displayed markedly impaired SOCE in response to thapsigargin (TG) as well as agonists acting on immunoreceptor tyrosine-based activation motif (ITAM) or G protein-coupled receptors. This SOCE defect resulted in impaired (hem)ITAM induced platelet activation, aggregate formation under flow and procoagulant activity. As a consequence, mice lacking BIN2 in platelets were protected from occlusive arterial thrombus formation and thrombo-inflammatory cerebral infarct progression in a model of experimental stroke. These results identify BIN2 as a critical regulator of platelet SOCE in thrombosis and thrombo-inflammatory disease.

Integrin $\alpha\text{IIb}\beta 3$ plays a central role in the adhesion and aggregation of platelets. Integrin activation requires the transmission of a signal from the small cytoplasmic tails of the α or β subunit to the large extracellular domains resulting in conformational changes of the extracellular domains to enable ligand binding. It was hypothesized that Hic-5 is a novel regulator of integrin $\alpha\text{IIb}\beta 3$ activation in mice. As demonstrated in the second part of this thesis, lack of Hic-5 had no detectable effect on platelet integrin activation and function *in vitro* and *in vivo* under all tested conditions. These results indicate that Hic-5 is dispensable for integrin $\alpha\text{IIb}\beta 3$ activation and consequently for arterial thrombosis and hemostasis in mice.

The Rho GTPase family members RhoA and Rac1 play major roles in platelet activation at sites of vascular injury. Little is known about possible redundant functions of these Rho GTPases in regulating platelet function. To investigate functional redundancies of RhoA and Rac1 in platelet production and function, mice with MK- and platelet-specific double-deficiencies in RhoA and Rac1 were generated. RhoA/Rac1 double-deficiency phenocopied the respective single knockouts without any additional effects in the double-knockout animals,

demonstrating for the first time a functional non-redundancy of RhoA and Rac1 in platelet function.

Antibodies against platelet glycoproteins (GP) trigger platelet destruction in immune thrombocytopenia (ITP) by binding to Fc γ receptors (Fc γ Rs) on immune cells. However, antibodies against the platelet collagen receptor GPVI exert powerful anti-thrombotic action *in vivo* by inducing ectodomain shedding of the receptor associated with a transient thrombocytopenia. As shown in the final part of this thesis, blockade or deficiency of the inhibitory Fc γ RIIB abolished sequestration of anti-GPVI opsonized platelets in the hepatic vasculature and GPVI shedding. This process was mediated by liver sinusoidal endothelial cells (LSEC), the major Fc γ RIIB expressing cell type in the body. Furthermore, LSEC Fc γ RIIB mediated hepatic platelet sequestration and contributed to thrombocytopenia in mice treated with antibodies against α IIb β 3, the major target antigen in human ITP. These results reveal a novel and unexpected function of hepatic Fc γ RIIB in the processing of antibody-opsonized platelets.

Zusammenfassung

Diese Arbeit fasst Untersuchungen zu verschiedenen Aspekten der Aktivierung von Thrombozyten und deren Rezeptorregulation zusammen. Daher ist diese Doktorarbeit in vier Teile gegliedert.

Die Aktivierung und Aggregation von Thrombozyten nach einer Gefäßverletzung ist entscheidend, um einen übermäßigen Blutverlust zu vermeiden, kann aber auch zu lebensbedrohlichen ischämischen Erkrankungen, wie beispielsweise Myokardinfarkt und Schlaganfall, führen. Bei der Aktivierung der Thrombozyten kommt es zu einem Anstieg der zytosolischen Ca^{2+} -Konzentration. Der Ca^{2+} -Einstrom in die Thrombozyten erfolgt hauptsächlich durch den „*store operated calcium entry*“ (SOCE). Der Calciumsensor „*stromal interaction molecule 1*“ (STIM1) reguliert den SOCE indem er das Ionenkanal-bildende Protein Orai1 in der Plasmamembran aktiviert. Der genaue Mechanismus dieser Interaktion ist jedoch noch nicht vollständig aufgeklärt. Durch den Einsatz von Affinitätschromatographie, um Interaktionspartner von STIM1 zu identifizieren, wurde „*bridging integrator 2*“ (BIN2) gefunden. BIN2 ist ein Adapterprotein, aus der Familie der BAR Proteine, welches hauptsächlich von Zellen des hämatopoetischen Systems exprimiert wird. BIN2-defiziente Mäuse sind lebensfähig und fruchtbar, aber ihre Thrombozyten zeigten einen deutlich verminderten SOCE. Diese Reduktion zeigte sich sowohl nach der Stimulation mit Thapsigargin, aber auch nach der Stimulation mit Agonisten, die „*immunoreceptor tyrosine-based activation motif*“ (ITAM-) oder G-Protein gekoppelte Rezeptoren aktivieren. Der defekte SOCE führte zu verminderter (hem)ITAM-induzierter Thrombozytenaktivierung, reduzierter Thrombenbildung im Flusskammersystem und verminderter prokoagulanter Aktivität. Dies hatte zur Folge, dass Mäuse mit thrombozytenspezifischer BIN2-Defizienz vor arterieller Thrombose und, in einem Schlaganfallmodell, vor thrombo-inflammatorischer Infarktprogression geschützt sind. Diese Ergebnisse zeigen, dass BIN2 ein wichtiger Regulator des SOCE in Thrombozyten bei Thrombosen und thrombo-inflammatorischen Erkrankungen ist.

Das Integrin $\alpha\text{IIb}\beta 3$ spielt bei der Adhäsion und Aggregation von Thrombozyten eine wichtige Rolle. Um das Integrin zu aktivieren, bedarf es einer Signalübertragung von den kleinen zytoplasmatischen Teilen der α und β Untereinheiten zu den großen extrazellulären Domänen, was zu deren Konformationsänderung führt und schließlich die Ligandenbindung ermöglicht. Es besteht die Hypothese, dass Hic-5 an der Regulation des Integrins $\alpha\text{IIb}\beta 3$ in murinen Thrombozyten beteiligt ist. Wie im zweiten Teil dieser Arbeit gezeigt werden konnte, hat eine Hic-5 Defizienz jedoch weder *in vitro* noch *in vivo* Einfluss auf die Aktivierung und Funktion des Integrins $\alpha\text{IIb}\beta 3$ in Thrombozyten. Diese Ergebnisse zeigen, dass Hic-5 für die Aktivierung des Integrins $\alpha\text{IIb}\beta 3$ und folglich auch für die arterielle Thrombose und Hämostase in Mäusen entbehrlich ist.

Kleine GTPasen der Rho-Proteinfamilie, wie z.B. RhoA und Rac1 spielen bei der Thrombozytenaktivierung bei Gefäßverletzungen eine wichtige Rolle. Dennoch ist wenig über redundante Funktionen von RhoA und Rac1 bei der Steuerung der Thrombozytenfunktion bekannt. Um eine mögliche funktionelle Redundanz von RhoA und Rac1 zu untersuchen, wurden MK- und thrombozytenspezifische RhoA und Rac1 doppelt-defiziente Tiere gezüchtet. Die Thrombozyten der Tiere zeigten die Phänotypen einer RhoA- und Rac1-Defizienz, ohne dass weitere Effekte bemerkbar waren. Diese Ergebnisse zeigen zum ersten Mal, dass es keine funktionelle Redundanz von RhoA und Rac1 bei der Regulation der Thrombozytenfunktion gibt.

Antikörper, die gegen Glykoproteine auf Thrombozyten gerichtet sind, führen bei einer Immunthrombozytopenie (ITP) durch die Bindung an Fc γ Rezeptoren auf Immunzellen, zu einer Zerstörung der Thrombozyten. Eine Ausnahme sind Antikörper gegen den Kollagenrezeptor GPVI der Thrombozyten. Hier führen diese Antikörper zu einem starken antithrombotischen Schutz *in vivo*, indem sie das sog. „Shedding“ der Ektodomäne des Rezeptors und nur eine vorübergehende Thrombozytopenie auslösen. Im letzten Teil dieser Arbeit konnte gezeigt werden, dass sowohl die Blockade, also auch das vollständige Fehlen des inhibitorischen Fc γ RIIB, die Sequestrierung von anti-GPVI-opsonierten Thrombozyten und das Shedding von GPVI verhindert. Für diese Prozesse ist speziell der Fc γ RIIB auf „*liver sinusoidal endothelial cells*“ (LSEC) ursächlich. Ferner konnte gezeigt werden, dass Fc γ RIIB auf LSECs auch für die Sequestrierung von Thrombozyten und die Thrombozytopenie in Mäusen, die mit Antikörpern gegen α IIb β 3, dem Hauptantigen bei humaner ITP, behandelt wurden, verantwortlich ist. Diese Ergebnisse enthüllen eine neue und unerwartete Funktion des hepatischen Fc γ RIIB bei der Reaktion auf Antikörper-opsonierte Thrombozyten.

1 Introduction

Platelets are small anucleate discoid-shaped blood cells which safeguard the integrity of the vascular system. Upon damage to the vessel wall, like upon traumatic injury or pathological alteration of the endothelial layer, such as found in atherosclerosis, platelets come into contact with thrombogenic components of the exposed extracellular matrix (ECM). They become rapidly activated, secrete their granule contents and form a plug that seals the wound to limit blood loss and prevents infection.

Platelets have a diameter of 3-4 μm in humans and 1-2 μm in mice. Their life span is restricted to 10 days in humans and up to 5 days in mice. Aged, dysfunctional or pre-activated platelets are cleared from the circulation by resident macrophages, primarily in the spleen and liver.¹ New platelets are permanently produced by their bone-marrow resident precursors, the megakaryocytes (MKs), to maintain a normal range of circulating platelets ($150\text{-}400 \times 10^3$ platelets μL^{-1} in humans and $\sim 1,000 \times 10^3$ platelets μL^{-1} in mice).^{2,3} A current model suggests that MKs extend long cytoplasmic protrusions, proplatelets, into sinusoidal blood vessels, where the tip of these structures is shed and becomes further fragmented into platelets by shear forces in the circulation.^{4,5} Impaired platelet production or increased platelet clearance may result in low platelet counts, termed thrombocytopenia. Several (hereditary) disorders, such as Wiskott-Aldrich syndrome or leukemia, are accompanied by impaired platelet production, while immune diseases, such as idiopathic thrombocytopenic purpura, or non-immune diseases, such as hypersplenism, cause an increased platelet clearance.⁶⁻⁹

Platelets have only limited capacity for *de novo* protein synthesis, as they lack a nucleus. Circulating platelets already contain all organelles including mitochondria, the open canalicular system (OCS), the dense tubular system and different types of granules: α -granules, dense granules and lysosomes. Lysosomes store enzymes necessary for the degradation of proteins, carbohydrates and lipids. Dense granules contain mainly non-proteinaceous compounds that support platelet aggregation, e.g. adenine nucleotides, polyphosphates and Ca^{2+} . α -granules contain more than 300 different proteins, such as adhesion proteins (most notably fibrinogen, P-selectin, von Willebrand factor (vWF)), coagulation factors, growth factors and chemokines (e.g. platelet factor (PF) 4).^{10,11}

In pathological conditions, uncontrolled thrombus formation may lead to thrombotic vessel occlusion with obstruction of blood flow, loss of oxygen supply and subsequent tissue damage¹², such as in myocardial infarction and ischemic stroke, which currently represent the leading causes of death and permanent disability worldwide.¹³ Therefore, platelet activation needs to be tightly regulated by a complex interplay between activating and inhibitory mechanisms that ensure controlled spatial and temporal responses.

1.1 Platelet activation and thrombus formation

At sites of vascular injury, subendothelial matrix components or proteins adsorbed onto exposed tissue, including vWF, fibrillar collagens, fibronectin and laminins, are exposed to the flowing blood which initiates platelet adhesion and activation.¹⁴ The multi-step process of platelet activation and thrombus formation can be divided into three major steps: tethering, activation and firm adhesion (Figure 1).

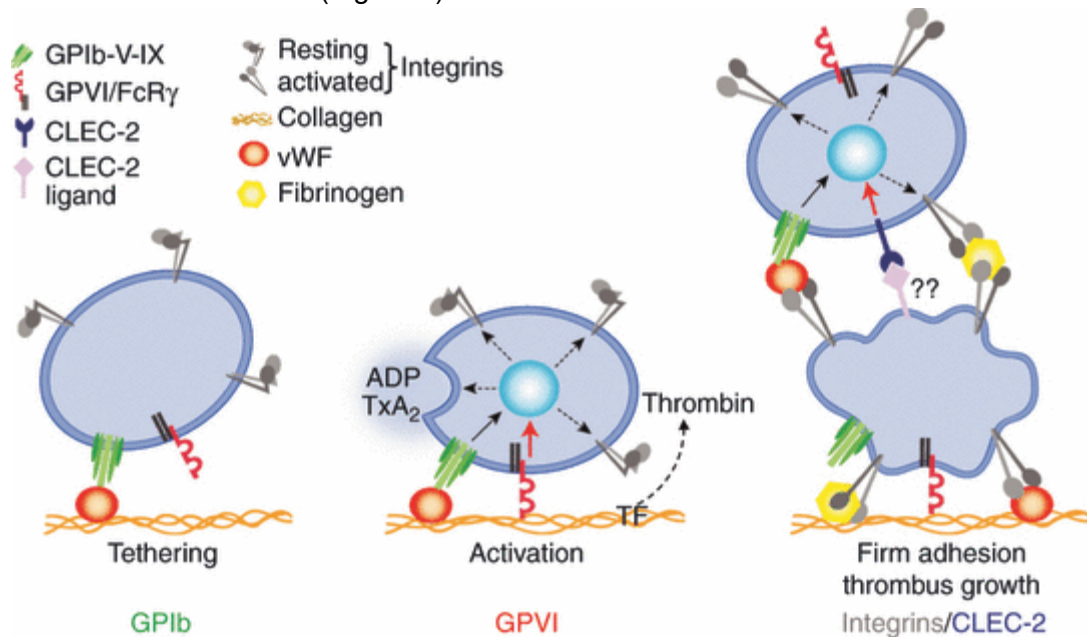


Figure 1. Model of platelet adhesion to the ECM and subsequent thrombus formation. At sites of vascular injury, initial contact (tethering) of platelets with components of the ECM predominantly depends on the interaction between GPIb and vWF, leading to deceleration of platelets. The deceleration enables GPVI-collagen interactions, which trigger cellular activation and conversion of integrins to a high-affinity state. Released second-wave mediators (such as ADP and TxA₂) and locally produced thrombin further stimulate platelet activation. Finally, activated platelet integrins facilitate firm platelet adhesion to the ECM. Enhanced release of soluble second-wave agonists amplifies integrin activation on adherent platelets and sustains thrombus growth. ADP, adenosine diphosphate; TxA₂, thromboxane A₂; vWF, von Willebrand factor; CLEC-2: C-type lectin-like receptor 2. Taken from: Nieswandt *et al.*, 2011.¹⁴⁰

Under conditions of high shear, as found in small arteries and arterioles, platelets are decelerated by the transient interaction of vWF, which is immobilized on collagen fibers, and the platelet receptor complex glycoprotein (GP) Ib-V-IX.¹⁵ The binding of GPIb to vWF is insufficient to mediate stable adhesion, but the subsequent tethering of platelets enables binding of GPVI, the central activating collagen receptor.¹⁶ GPVI binds collagen with low affinity and is unable to mediate stable adhesion by itself.¹⁴ It rather induces platelet activation by intracellular signaling processes via an immunoreceptor tyrosine-based activation motif (ITAM) in the associated Fc receptor (FcR) γ -chain.¹⁷ The activation leads to subsequent release of secondary mediators, most importantly thromboxane A₂ (TxA₂) and adenosine diphosphate (ADP). Another consequence of platelet activation is the increased activity of platelet scramblases leading to exposure of negatively charged phosphatidylserine (PS) on the platelet surface. PS provides a platform for the assembly of two major coagulation factor complexes

and subsequent thrombin production, which is amplified through the exposure of locally produced tissue factor (TF).^{18,19} ADP, TxA₂ and thrombin participate in further cellular activation by inducing various signaling pathways via G protein-coupled receptors (GPCRs)²⁰, which amplifies and sustains initial activation and recruits new platelets from the blood stream into the growing thrombus. The described signaling events converge in the “final common pathway” of platelet activation: integrins on the platelet surface shift from a low to a high affinity state, which enables firm ligand binding. The activated integrins transduce outside-in signals which cause cytoskeletal rearrangements, spreading and clot retraction.²¹

1.2 Platelet signaling upon activation

There are two major downstream signaling pathways that are activated after ligand binding to platelet receptors (Figure 2). Both culminate in the activation of phospholipase C (PLC) isoforms leading to hydrolysis of phosphatidyl-inositol-4,5-bisphosphate (PIP₂) to inositol-3,4,5-trisphosphate (IP₃) and diacylglycerol (DAG) which results in elevation of cytosolic Ca²⁺ concentration, integrin activation, platelet shape change, aggregation and secretion. One pathway is triggered by GPVI and C-type lectin-like receptor 2 (CLEC-2) and involves tyrosine phosphorylation cascades downstream of the receptor-associated ITAM, or hemITAM, respectively, leading to full platelet activation. Soluble agonists, such as thrombin, ADP, and TxA₂ stimulate receptors that couple to heterotrimeric G proteins and induce distinct downstream signaling pathways.²⁰ G_q proteins activate PLCβ leading to Ca²⁺ mobilization and activation of protein kinase C (PKC).²² G_{12/13} proteins regulate multiple pathways, of which the Rho/Rho-kinase pathway, leading to myosin light chain phosphorylation and platelet shape change, is the best studied one.²³ The α-subunit of G_i family proteins inhibits adenylyl cyclase, while its βγ complexes can regulate several channels and enzymes, most notably phosphatidylinositol-3-kinases (PI3Ks).²⁴

1.2.1 (Hem)ITAM signaling

The ITAM was initially described by Reth *et al.*²⁵ ITAMs contain a short amino acid sequence that consist of a duplicate of the sequence YXXL/I (Y: tyrosine, L: leucine, I: isoleucine, X: any amino acid) with six to eight intervening residues.²⁶ The resulting structure of ITAMs is critical for their function as scaffold protein for other signaling molecules that are recruited to activated receptors (Figure 3). ITAMs are found in T and B cell receptor (TCR and BCR) chains, but also in Fc receptors, like FcγRIII. The ITAM-bearing receptors on murine platelets are GPVI and CLEC-2, whereas the latter only contains half an ITAM in its cytoplasmic tail and is therefore termed a (hem)ITAM receptor. Human platelets express additionally FcγRIIA. Platelet activation through FcγRIIA has important implications in the pathogenesis of several diseases related to immune-mediated thrombocytopenia and thrombosis syndromes.²⁷

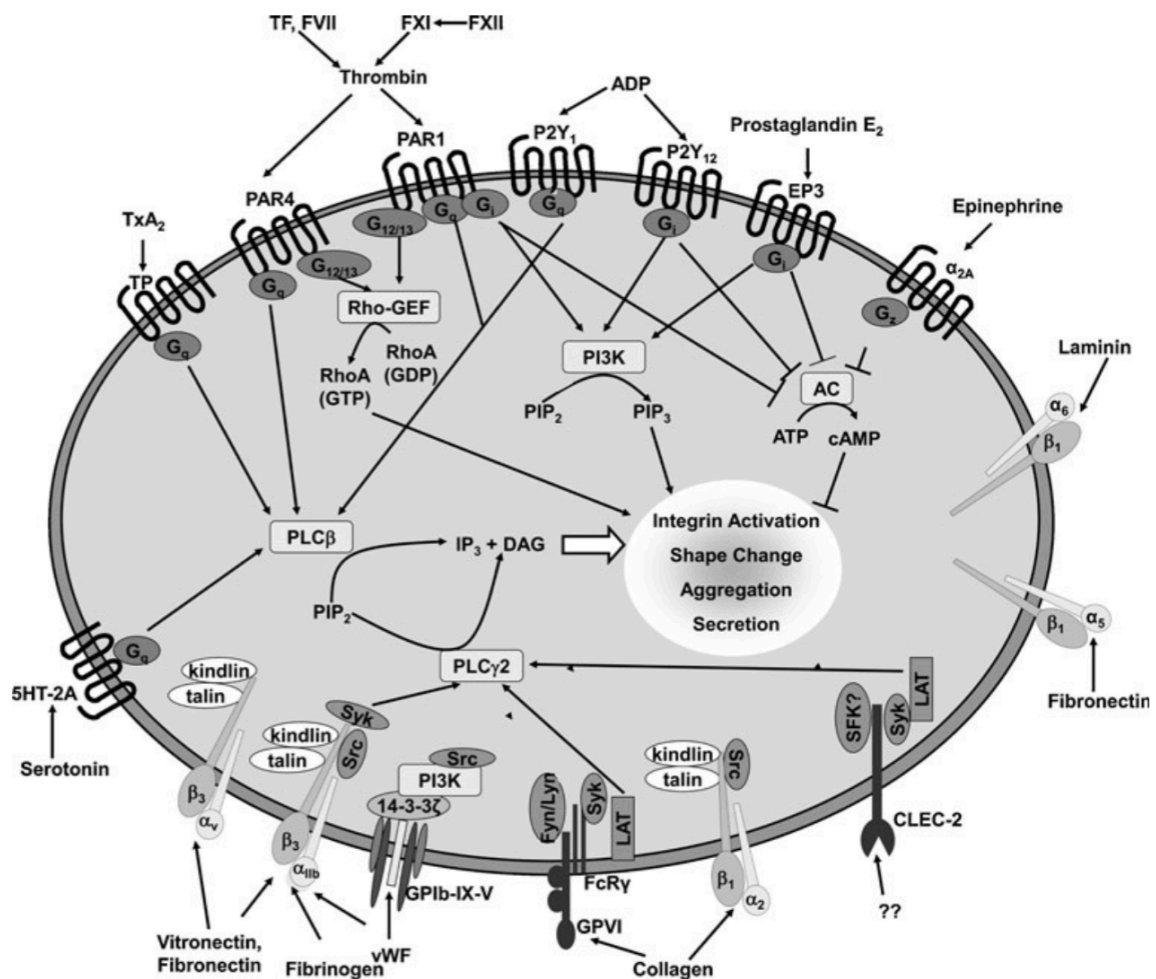


Figure 2. Major signaling pathways in platelets. Soluble agonists, including ADP, TxA₂ and thrombin, mediate effects via receptors that couple to heterotrimeric G proteins (G_q, G_{12/13}, G_i) and activate downstream effectors. Adhesion receptors, such as GPIb, CLEC-2 and active integrins, induce PLC γ 2 activation upon ligand binding. Both signaling pathways culminate in integrin activation, platelet shape change, aggregation and secretion. PI3K, phosphatidylinositol-3-kinase; PIP₂, phosphatidylinositol-4,5-bisphosphate; PIP₃, phosphatidylinositol-3,4,5-trisphosphate; IP₃, inositol-3,4,5-trisphosphate; AC, adenylyl cyclase; DAG, diacylglycerol; PLC, phospholipase C; CLEC-2: C-type lectin-like receptor 2; PAR, protease-activated receptor; ADP, adenosine diphosphate; GDP, guanosine diphosphate; GTP, guanosine triphosphate; GEF, guanine nucleotide exchange factor; RhoA, Ras homolog gene family, member A; Fg, fibrinogen; TF, tissue factor; TxA₂, thromboxane A₂; vWF, von Willebrand factor; LAT, linker for activation of T cells; Syk, spleen tyrosine kinase; SFK, Src family kinase. Taken from: Stegner and Nieswandt, 2010.⁵⁴

1.2.1.1 GPVI

GPVI is a 58-kDa type I transmembrane protein that is constitutively associated with the Fc receptor γ (FcR γ) chain. The FcR γ chain is essential for GPVI function because it is not only required for GPVI expression in platelets but also contains the ITAM that is required for GPVI mediated signal transduction.^{28,29} GPVI has been estimated to be expressed on the cell surface with a number of 4,000 to 6,000 copies per platelet, partially in a monomeric and dimeric form

with one GPVI molecule associated with one FcR γ -chain dimer.^{30,31} Only the dimeric form of the receptor ectodomain (GPVI-Fc) binds collagen with high affinity.³² Stimulation of GPVI has been shown to result in rapid formation of disulfide-linked dimers.^{32,33} Ligand-induced crosslinking of GPVI triggers tyrosine phosphorylation of the FcR γ -chain on its ITAMs by the Src family kinases (SFK) Fyn and Lyn. The phosphorylation stimulates recruitment and subsequent activation of the tandem SH2 domain-containing tyrosine kinase Syk. Phosphorylation of Syk initiates a downstream signaling cascade, involving the adaptors linker of activated T cells (LAT) and SH2 domain containing leukocyte protein of 76 kDa (SLP-76), and culminates in activation of numerous effector molecules, including PLC γ 2 and PI3K.³⁰

GPVI has emerged as an attractive potential target for antithrombotic therapy, as its deficiency, blockade or antibody-induced depletion provides powerful protection from experimental arterial thrombosis without affecting platelet hemostatic functions.^{34,35} The most powerful approach to target GPVI function in mice *in vivo* is based on the immunodepletion of the receptor in circulating platelets by antibodies directed against its ectodomain. The targeted GPVI down-regulation, which occurs very efficiently in human and murine platelets,^{36,37} strictly depends on signaling through the receptor.^{34,38} The major mechanism of GPVI depletion is ectodomain shedding, presumably by metalloproteinases of the α disintegrin and metalloproteinase (ADAM) family, which is accompanied by a transient drop in platelet count.³⁸ Under conditions of defective platelet signaling, i.e. in the absence of LAT or PLC γ 2, the receptor is still down-regulated *in vivo*, but this occurs through internalization/intracellular degradation, which is not associated with a drop in platelet count.³⁹ It is important to mention, that different anti-GPVI antibodies of the IgG class efficiently deplete the receptor *in vivo*, while they do not affect GPVI surface expression in platelets *in vitro*,³⁹ indicating the involvement of a non-platelet compartment. Investigation of this compartment is one of the aims of this thesis.

1.2.1.2 CLEC-2

In contrast to GPVI, CLEC-2, a ~32 kDa type II transmembrane protein, contains half an ITAM in its cytoplasmic tail ((hem)ITAM). CLEC-2 binds the endogenous ligand podoplanin, which is not expressed within the vasculature, and the snake venom toxin rhodocytin.^{16,40} CLEC-2 is expressed as a homodimer on resting platelets and cellular activation is induced after receptor clustering upon ligand binding.⁴¹ Similar to GPVI, CLEC-2 deficiency has only a minor influence on hemostasis, but prevents formation of stable vessel occluding thrombi.^{42,43} GPVI and CLEC-2 have some important redundant functions in hemostasis and the maintenance of vascular integrity at sites of inflammation.^{44,45} It is noteworthy that CLEC-2 is also involved in several processes beyond thrombosis and hemostasis, including the separation of lymphatics from the blood vasculature, the maintenance of high endothelial venule barrier function and the formation of lymph nodes.⁴⁶⁻⁴⁹

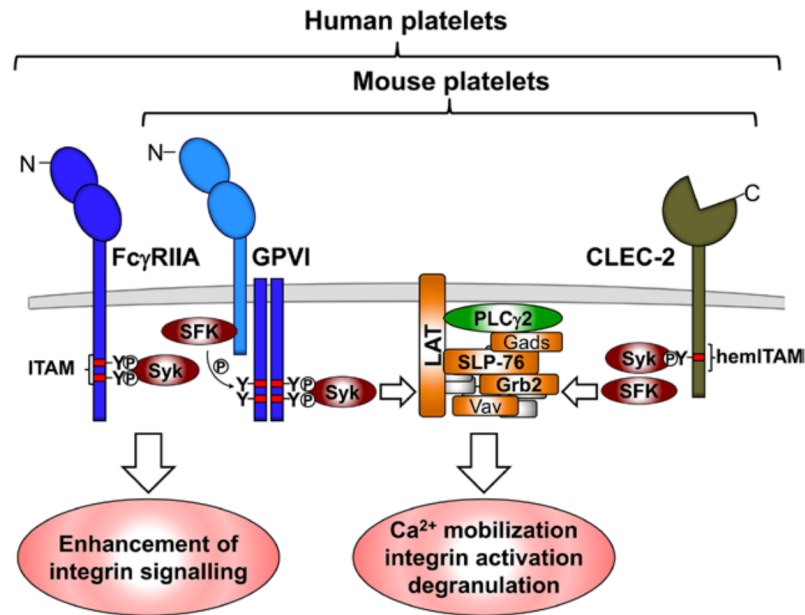


Figure 3. (hem)ITAM signaling in platelets. The type I transmembrane protein GPVI is constitutively associated with the ITAM-bearing Fc γ chain. Ligand binding induces phosphorylation of the ITAM by SFKs, followed by the recruitment and activation of Syk. Phosphorylated Syk triggers a downstream signaling cascade, consisting of kinases, adaptor and effector molecules. The pathway culminates in the activation of PLC γ 2. The C-type lectin-like receptor 2 (CLEC-2) lacks the Fc γ chain and contains half an ITAM (hemITAM) in its cytoplasmic tail. Following hemITAM phosphorylation, Syk and SFKs cooperatively modulate a signaling cascade similar to that found downstream of GPVI. The Fc receptor Fc γ RIIA, which is expressed on human, but not on mouse platelets, also signals through an ITAM and contributes to integrin outside-in signaling through Syk. SFK, Src family kinase; Syk, spleen tyrosine kinase; LAT, linker for activation of T cells; Grb2, growth factor receptor-bound protein 2; Gads, Grb2-related adaptor downstream of Shc; SLP-76, SH2 domain containing leukocyte protein 76; PLC γ 2, phospholipase C γ 2. Taken from: Stegner *et al.*, 2014.²⁷

1.2.2 GPCR signaling in platelets

As mentioned above, most soluble agonists initiate platelet activation through G protein-coupled receptors (GPCRs). ADP is an essential amplifier of platelet activation. Released from damaged endothelial cells and from platelet granules, ADP binds to its receptors P2Y₁, coupled to G_q, and P2Y₁₂, coupled to G_{12/13}.⁵⁰ Another important second wave mediator released by stimulated platelets is TxA₂. TxA₂ binds to the G_q- and G_{12/13}-coupled thromboxane-prostanoid receptors TP α and TP β .⁵¹ The most potent soluble agonist is thrombin. Besides its role in platelet activation, thrombin also converts plasma fibrinogen into fibrin to stabilize the thrombus. Thrombin is a serin protease, generated by both, the intrinsic and the extrinsic coagulation pathway at sites of vascular injury.⁵² Thrombin activates the protease-activated receptors (PAR) 1 and 4 (human) or 3 and 4 (mouse) by proteolytic cleavage of their N-terminus, which exposes a so-called tethered ligand that activates the cleaved receptors to stimulate mainly G_q and G_{12/13}, but also G_i.⁵³

Other soluble agonists are epinephrine, signaling via the G_z -coupled α_{2A} -adrenergic receptor, prostaglandin E_2 via G_i -coupled EP3 receptor and serotonin, utilizing the G_q -coupled 5-hydroxytryptamine 2A receptor.⁵⁴

On the other hand, antagonists like endothelium-derived nitric oxide (NO) and prostacyclin (PGI_2) inhibit platelet activation. While NO activates guanylyl cyclase to generate cyclic guanosine monophosphate (cGMP), PGI_2 signals via the G_s -coupled IP receptor to stimulate adenylyl cyclase, inducing cyclic adenosine monophosphate (cAMP) formation.⁵⁴

1.2.3 Small GTPases of the Rho family

Mammalian Rho GTPases serve as signaling mediators in the regulation of diverse cellular processes, especially the control of cytoskeletal rearrangements. They comprise a family of 20 proteins which belong to the Ras superfamily of monomeric 20-25 kDa guanosine-5'-triphosphate (GTP) binding proteins.⁵⁵ Rho GTPases act as molecular switches, cycling between a GTP-bound (active) and a guanosine diphosphate (GDP-) bound (inactive) state (Figure 4). Guanine nucleotide-exchange factors (GEFs) promote the exchange of GDP to GTP. As small GTPases lack intrinsic GTPase-activating domains, GTPase-activating proteins (GAPs) mediate the hydrolysis of GTP to GDP and thus inhibit Rho GTPase activation. Rho proteins may also be regulated by guanine nucleotide-dissociation inhibitors (GDIs), keeping Rho GTPases in the inactive state and thus prevent spontaneous activation.⁵⁶ In their active form, Rho GTPases interact with specific effectors and can activate downstream signaling events. Among the Rho family members, the GTPases RhoA, Cdc42 and Rac1 are best characterized for their role as key regulators in the dynamics of the actin cytoskeleton in platelets upon activation and play key roles in platelet aggregation, secretion, spreading and thrombus formation.⁵⁷⁻⁵⁹

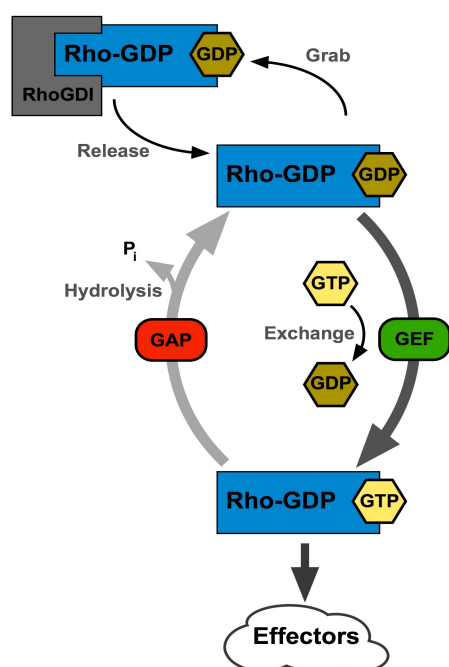


Figure 4: Activation and regulation of Rho GTPases. Rho GTPases cycle between an inactive, GDP-bound, and an active, GTP-bound, state in which they can interact with effector molecules. GEFs mediate the exchange of GDP to GTP. GAPs trigger the hydrolysis of Rho GTP to GDP and inactivate GTPase function. GDIs induce sequestering of Rho proteins away from regulators and target proteins and thus prevent activation. GDP, guanosine diphosphate; GTP, guanosine triphosphate; GEF, guanine nucleotide-exchange factor; GAP, GTPase-activating protein; GDI, guanine nucleotide-dissociation inhibitor. Modified from: Aslan, McCarty, 2013.¹⁹⁴

1.2.3.1 RhoA in platelets

RhoA (Ras homolog gene family, member A) is involved in focal adhesion formation and actomyosin contractions.⁶⁰ In platelets, G_{13} regulates the Rho/Rho-kinase pathway, resulting in myosin light chain (MLC) phosphorylation and initiation of platelet shape change. G_{13} directly activates p115RhoGEF that promotes RhoA-GTP formation.²³ In this active form, RhoA interacts with its downstream effector Rho-associated protein kinase (ROCK). ROCK phosphorylates and inhibits the myosin light chain (MLC) phosphatase, leading to increased MLC phosphorylation, and thereby resulting in subsequent actomyosin contractions that promote platelet shape change from discoid to spherical form. An alternative pathway, which is promoted through G_q signaling, stimulates MLC kinase activation and directly triggers MLC phosphorylation.^{23,61} Studies in MK-/platelet-specific RhoA-deficient mice revealed that RhoA plays roles in platelet shape change and G_{13} -mediated integrin $\alpha IIb\beta 3$ activation, granule release, clot retraction and thrombus formation. *In vivo* RhoA deficiency resulted in reduced thrombus formation, prolonged tail bleeding time and partial protection from ischemic stroke, establishing RhoA as an important regulator of platelet function in thrombosis and hemostasis.⁵⁷

1.2.3.2 Rac1 in platelets

In general, Rac (Ras-related C3 botulinum toxin substrate) proteins have important functions in lamellipodia formation.⁵⁵ However, Rac1 is the only isoform expressed in platelets.⁶² Studies on knockout mice confirmed that Rac1 is essential for lamellipodia formation during integrin $\alpha IIb\beta 3$ -mediated spreading and for signal transduction downstream of GPVI and CLEC-2.^{58,62} Rac1 acts as a co-activator of PLC γ 2, independently of tyrosine phosphorylation, to regulate Ca^{2+} and diacylglycerol-regulated guanine-nucleotide-exchange factor I (CalDAG-GEFI) and P2Y₁₂-dependent activation of the Ras-related small GTPase, Ras-proximate-1 (Rap1), leading to integrin $\alpha IIb\beta 3$ activation.^{58,63} Another pool of Rac1, downstream of PLC γ 2 and calcium signaling, has been proposed to activate downstream effectors, such as the WASP-family verprolin homologous protein (WAVE) and actin-related proteins 2/3 (Arp2/3) system or p21-activated kinases (PAK) and thereby regulating platelet secretion, aggregation and spreading events.⁶³ Rac1-deficient platelets display defective thrombus formation on collagen under flow conditions. This defect translates into a protection in collagen-dependent models of arterial thrombosis, but also prolonged bleeding times, demonstrating that Rac1 is essential for ITAM-dependent PLC γ 2 activation in platelets and that this is critical for thrombus formation *in vivo*.^{58,62}

Studies have shown that Rac1 activity can be blocked using the inhibitors NSC23766 and EHT1864.^{64,65} However, these inhibitors have been recently demonstrated to exert profound

off-target effects, questioning the use of these inhibitors for biochemical studies at the used concentrations and as therapeutic agents.⁶⁶

1.2.3.3 Cdc42

Cdc42 (cell division control protein 42 homolog) has been established as a regulator of filopodia formation, exocytosis and secretion in many cell types, like neurons and embryonic stem cells (ESCs).^{55,56} So far, two different mouse knockouts were used to study the role of Cdc42 in platelets. Platelets from mice deficient for Cdc42 only in platelets and megakaryocytes (*Cdc42^{fl/fl} Pfl4-Cre*), showed a specific defect in platelet filopodia formation on vWF. Surprisingly, filopodia formation on the surfaces of fibrinogen and collagen-related peptide (CRP) was unaltered. These results suggested a unique signaling role of Cdc42 downstream of GPIb, but not GPVI or α IIb β 3. Unexpectedly, lack of Cdc42 in platelets resulted in increased secretion from α - and dense granules, together with enhanced thrombus formation *in vitro* and *in vivo* and prolonged tail bleeding times.⁵⁹ Platelets from mice lacking Cdc42 in all hematopoietic cells (*Cdc42^{fl/fl} Mx-Cre*) showed a defect in filopodia formation on fibrinogen and reduced granule secretion, but also prolonged tail bleeding times.⁶⁷ These data revealed that Cdc42 is required for platelet filopodia formation, secretion and aggregation and therefore plays a critical role in platelet mediated hemostasis and thrombosis. However, there is no apparent mechanistic explanation for the discrepancies between the two animal knockouts.

The hypothesis that the newly characterized Rho GTPase Rif (RhoF) would compensate for the lack of Cdc42 in filopodia formation could not be confirmed, as RhoF is dispensable for filopodia formation and platelet function in general (Goggs *et al.*, 2013⁶⁸ and Dütting *et al.*, unpublished).

Although Rho GTPases have partially overlapping signaling pathways and binding partners, only little is known about functional redundancies of different Rho GTPases in platelet production and function. Only recently, a redundant function of Rac1 and Cdc42 has been demonstrated in the regulation of microtubule dynamics and (pro-)platelet formation by the use of MK-/platelet-specific double-deficient mice.⁶⁹ The analysis of possible redundant functions of RhoA and Rac1 in platelet function is one of the aims of this thesis.

1.2.4 Calcium signaling in platelets

Calcium (Ca^{2+}) is a crucial second messenger for cellular processes in nearly all cells.⁷⁰ Especially in platelets, the elevation of intracellular Ca^{2+} levels [Ca^{2+}]_i is the central step for shape change, degranulation and integrin activation.^{71,72} Upon platelet activation, elevation of [Ca^{2+}]_i occurs from the release of Ca^{2+} from intracellular stores, the dense tubular system

(DTS, the equivalent of the endoplasmic reticulum, ER, in platelets), or from the entry of extracellular Ca^{2+} through the plasma membrane (PM).

1.2.4.1 Store-operated calcium entry (SOCE)

Signaling via (hem)ITAM receptors and integrins but also activation by PI3K downstream of G_i leads to the activation of PLC γ 2, whereas GPCRs coupled to G_q (stimulation via thrombin, ADP and TxA₂) activate PLC β .⁵⁴ Both PLC isoforms hydrolyze the membrane phospholipid PIP₂ into IP₃ and DAG. IP₃ releases Ca^{2+} from the intracellular stores by activating IP₃-sensitive Ca^{2+} channels located in the ER in platelets. The subsequent reduced Ca^{2+} concentration in the ER is detected by the EF-hand motif of the calcium sensor stromal interaction molecule 1 (STIM1), which opens the store-operated calcium (SOC) channel, calcium release-activated calcium modulator 1 (Orai1, CRACM1), in the plasma membrane to allow entry of extracellular Ca^{2+} (Figure 5).^{73,74}

The calcium sensor STIM1 is a type I single transmembrane protein containing two N-terminal EF hand domains, a sterile α -motif (SAM) domain, the transmembrane region, two coiled-coil regions, and at the C-terminal end, a serine/proline-rich and a lysine-rich domain. The EF hand domains in the ER bind Ca^{2+} . Upon store release, STIM1 redistributes to “puncta” and opens the SOC channels in the PM.^{75,76} *Stim1^{Sax/+}* mice have a mutation in the EF hand of STIM1, resulting in gain-of-function.⁷⁷ This mutation resulted in permanently opened SOC channels in the PM of platelets, which leads to elevated basal Ca^{2+} levels compared with wild-type controls. These platelets were in a preactivated state and were rapidly cleared from the circulation resulting in macrothrombocytopenia and a bleeding phenotype. Platelets of *Stim1^{-/-}* mice showed an almost complete lack of SOCE and severely impaired Ca^{2+} responses to all major platelet agonists, but $\alpha\text{IIb}\beta$ 3 activation was largely intact. *In vivo*, STIM1-deficient mice were protected from arterial thrombosis and ischemic brain infarction, but bleeding times were only mildly prolonged.⁷⁸

Orai1 is a plasma membrane protein with four predicted transmembrane domains and intracellular C- and N-termini. Orai1 multimerizes with itself to create the channel. Although human and murine platelets express all three isoforms of the Orai channel family (Orai1-3), Orai1 is the predominant isoform in both species.^{79,80} Analysis of Orai1-deficient platelets revealed a ~90% reduction in SOCE compared to wild-type controls, similar to the results from STIM1-deficient mice. Due to a normal Ca^{2+} store content and agonist-induced Ca^{2+} store release, *Orai1^{-/-}* platelets reach consistently higher $[\text{Ca}^{2+}]_i$ than *Stim1^{-/-}* platelets. Nevertheless, Orai1-deficient mice were protected in models of arterial thrombosis and ischemic brain infarction, with only mildly prolonged bleeding times.⁸¹

1.2.4.2 Other Ca²⁺ entry mechanisms

Besides SOCE, there are also other calcium entry mechanisms. The non-store-operated calcium entry (non-SOCE) is mediated by DAG, which can directly activate Ca²⁺ channels, like TRPC6 in the plasma membrane. TRPC6 is a member of the canonical subfamily of the transient receptor potential (TRP) channels.⁸² A study in TRPC6-deficient mice showed, that DAG activated Ca²⁺ influx was abolished in the mutant platelets, but no reductions in SOCE or agonist induced Ca²⁺ responses were found. Furthermore, TRPC6 had no major functional relevance for hemostasis and thrombosis.⁸³ A different study in *Orai1^{-/-}/Trpc6^{-/-}* mice could show that SOCE was further reduced in these platelets, compared to *Orai1^{-/-}* platelets, indicating that TRPC6 operates in crosstalk with Orai1 through Orai1-induced DAG production via phospholipase activation.⁸⁴

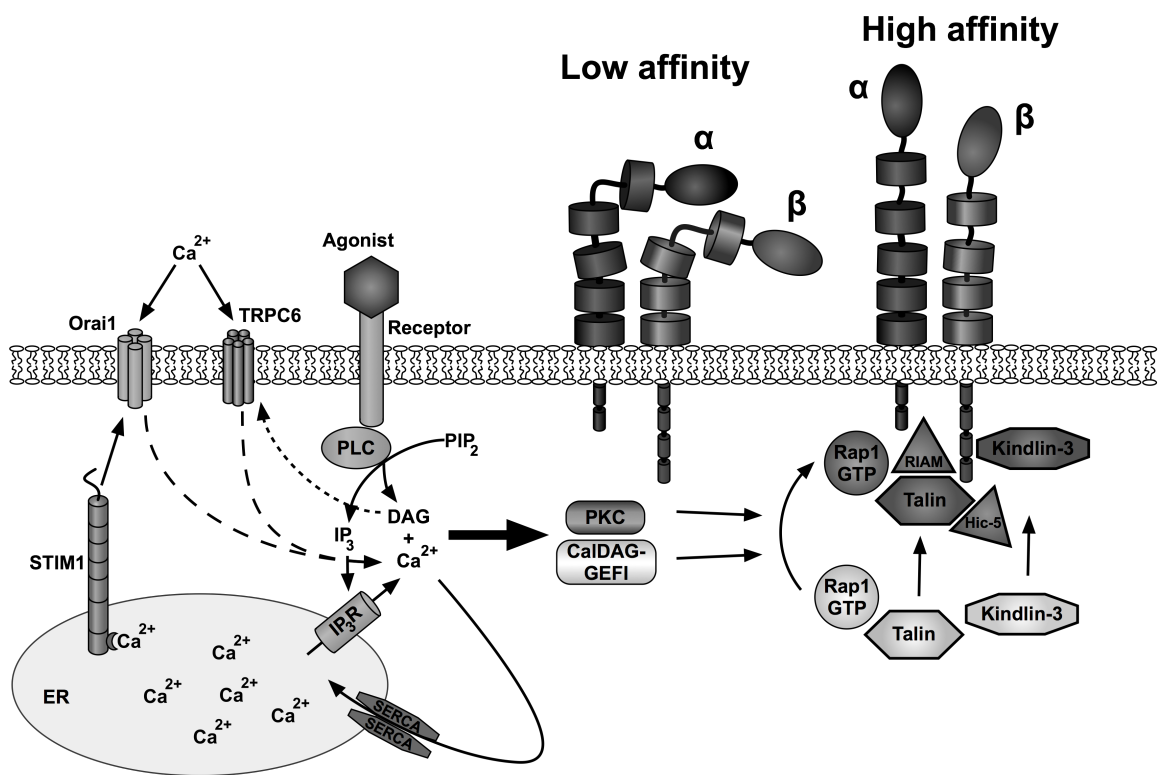


Figure 5: Calcium signaling and a model of integrin activation in platelets. Agonist stimulation triggers PLC activation and the formation of IP₃ and DAG. **Left:** IP₃ releases Ca²⁺ from the intracellular stores (dense tubular system, DTS – the equivalent of the endoplasmic reticulum, ER, in platelets) and in turn STIM1 opens Orai1 channels in the plasma membrane, a process called store-operated calcium entry (SOCE). DAG mediates non-SOCE through canonical transient receptor potential channel 6 (TRPC6). Not depicted: receptor-operated (ROC) channels. The counteracting mechanisms involve sarcoplasmic/endoplasmic reticulum Ca²⁺ ATPases (SERCAs) and plasma membrane Ca²⁺ ATPases (PMCAs; not depicted), which pump Ca²⁺ back into the stores or through the plasma membrane out of the cell, respectively. **Right:** DAG and Ca²⁺ activate PKC and CalDAG-GEFI, leading to activation and translocation of Rap1 to the plasma membrane. The Rap1 effector molecule RIAM interacts with both Rap1-GTP and talin-1, thereby unmasking the integrin-binding site in talin-1. Binding of talin-1 disrupts the salt bridge between the transmembrane regions of the α and β integrin subunits, which results in a conformational change in the extracellular domains and ligand binding. This final step requires also binding of functional kindlin-3 to the NPXY motif of the integrin β tail, but it is not clear whether this occurs simultaneously with talin-1 binding or sequentially. Hic-5 is an adaptor molecule interacting with talin-1. Modified from Varga-Szabo *et al.*, 2009 and Nieswandt *et al.*, 2009.^{87,213}

The purinoceptor P2X₁ is the channel for receptor-operated calcium entry (ROCE). The natural agonist of P2X₁ is adenosine triphosphate (ATP). P2X₁ seems to be an amplifier for signals mediated by GPCR agonists or collagen, especially at low concentrations, but could also enhance PLC-mediated activation processes.⁸⁵ Aggregation, as well as granule release, was reduced in P2X₁-deficient platelets compared to wild-type platelets, but the mutant platelets responded normally to GPCR agonists and higher doses of collagen. *In vivo*, the mutant mice were protected in a model of thrombosis in small arteries.⁸⁶

1.3 Platelet integrin activation

Integrins enable platelets to establish firm adhesion contacts to components of the ECM plasma proteins and other receptors.⁸⁷ These heterodimeric transmembrane receptors are composed of α and β subunits and serve as bidirectional signaling molecules.⁸⁸ Platelets express three $\beta 1$ integrins, binding to collagen ($\alpha 2\beta 1$), fibronectin ($\alpha 5\beta 1$), and laminin ($\alpha 6\beta 1$) as well as the $\beta 3$ integrins, $\alpha v\beta 3$ binding to vitronectin and the major platelet integrin $\alpha IIb\beta 3$ (also known as GPIIb/IIIa).^{89,90} Integrin $\alpha IIb\beta 3$ is the receptor for several ligands, each containing an arginine-glycine-aspartic acid (RGD) sequence, such as fibrinogen, fibrin, vWF, fibronectin, thrombospondin and vitronectin.⁹¹

In response to cellular activation, $\alpha IIb\beta 3$ shifts from a low- to a high-affinity state (Figure 5). This process requires the transmission of signals from the small cytoplasmic tails to the large extracellular domains of the integrin subunits.⁹² Several proteins have been proposed to be involved in the regulation of integrin activation.⁹³ The recruitment and binding of talin (Tln) 1 and kindlins to NPYX-motifs at the intracellular tail of the integrin β -subunit and their function in $\alpha IIb\beta 3$ activation have been extensively studied.⁹⁴⁻⁹⁹ Also CalDAG-GEFI and its downstream effector the small GTPase Rap1 critically affect $\alpha IIb\beta 3$ activation.¹⁰⁰⁻¹⁰³ However, a functional role for the proposed proteins in integrin activation *in vivo* could not be confirmed in all cases as, for example, in the case of Rap1-GTP-interacting adaptor molecule (RIAM).¹⁰⁴

1.3.1 Hic-5

Hydrogen peroxide-induced clone-5 (Hic-5) was identified as a gene inducible by transforming growth factor $\beta 1$ (TGF $\beta 1$) as well as hydrogen peroxide in a differential screen of cDNA libraries from the mouse osteoblastic cell line MC3T3-E1. The authors of that study speculated that Hic-5 may have a role in the growth-inhibitory pathway associated with *in vitro* senescence and that down-regulation of Hic-5 contributes to tumorigenesis.¹⁰⁵ In human platelets, Hic-5 localizes to focal adhesions and interacts with talin.¹⁰⁶ Hic-5 contains four LIM domains at the C-terminus and shares high homology with paxillin that has been shown to localize to focal adhesions and to interact with talin in platelets as well.¹⁰⁷ LIM domains (named after the initial discovery in the proteins Lin11, Isl-1 and Mec-3¹⁰⁸) are cysteine rich regions composed of two

zinc fingers, mediating protein-protein interactions. These domains were originally identified in homeodomain proteins and have been subsequently found in both cytoplasmic and nuclear proteins.¹⁰⁹ For paxillin, it has been recently shown that it negatively regulates platelet signaling pathways resulting in augmented α IIb β 3 activation upon stimulation of GPVI and GPCRs.¹¹⁰ However, the role of Hic-5 as a novel regulator of integrin α IIb β 3 activation and platelet aggregation in mice is controversial and will be discussed in this thesis.^{111,112}

1.4 BAR domain family proteins

BAR proteins are an evolutionary conserved family of adaptor proteins characterized by a common N-terminal domain termed the BAR domain, named after a shared sequence motif initially defined in the BIN1, amphiphysin and yeast RVS167/161 proteins.¹¹³ The BAR domains, α -helix rich domains of ~260 amino acid residues, typically form a dimer generation with a distinct curved surface (Figure 6).¹¹⁴ The dimers bind to the negatively-charged phospholipids in the plasma membrane and support tubulation of curved membranes, but also bind various regulatory proteins in the cytosol and the nucleus, like small GTPases.¹¹⁵ These proteins function in diverse cellular processes, including membrane dynamics, actin organization, cell growth control, immunity, and tumor suppression.¹¹⁶ BAR proteins are divided into three subfamilies, defined by their BAR/N-BAR (N-BAR: N-terminal amphipathic helix), F-BAR (extended Fes-CIP4 homology (EFC)/FCH-BAR), or I-BAR (IRSp53-MIM homology domain/inverse-BAR) domains.¹¹⁷

The three bridging integrator proteins (BIN1-3) are BAR/N-BAR proteins. BIN1 and BIN3 are ubiquitously expressed in mammalian cells. Different splice variants of BIN1, also known as Amphiphysin II, are expressed in neurons, muscle cells or tumor cells. The ubiquitous and muscle-specific isoform localizes to the nucleus as well as to the cytosol, a property essential for anticancer functions, which could be also shown in an animal model.^{113,118,119} In addition, Bin1 has been shown to localize to cardiac T-tubules where it facilitates cytoskeleton-based calcium channel trafficking to the T-tubule membrane. The cardiac deletion of BIN1 in mice led to decreased folding of T-tubules, without affecting overall cardiomyocyte morphology. The deletion rather resulted in free diffusion of local extracellular calcium and potassium ions, prolonging action-potential duration and increasing susceptibility to ventricular arrhythmias.^{120,121} BIN3 is expressed in all tissues, but only poorly in the brain. Animal studies have shown functions of BIN3 in lens development and cancer suppression during aging.¹²²

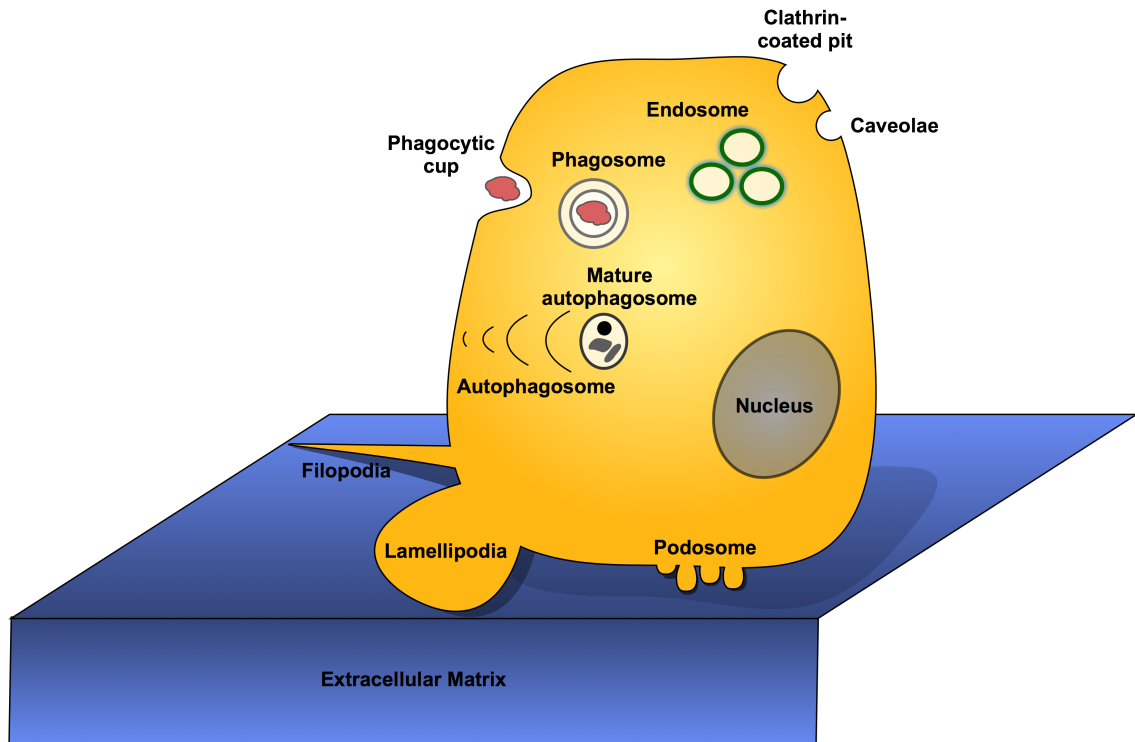


Figure 6: Subcellular structures influenced by BAR proteins. BAR proteins induce membrane deformation, based on the geometries of basic-charged amino acid residues that correspond to the structures of the membrane binding surface of the BAR domain. BAR or F-BAR proteins bind to the membrane to generate invaginations, such as caveolae and clathrin-coated pits. I-BAR proteins deform the membrane to generate protrusions, such as filopodia and lamellipodia. Modified from Safari and Suetsugu, 2012.²¹⁴

1.4.1 BIN2

Bridging integrator-2 (BIN2) was identified by Ge and Prendergast as a member of the BAR protein family, due to the high degree of conservation between the N-terminal region of BIN2 and the BAR domains of BIN1 and amphiphysin.¹²³ In contrast to the N-terminus, the C-terminal extension in INn2 is highly variable between species and unrelated to either BAR family adaptors or other known proteins. BIN2 lacks a C-terminal SH3 domain that is found in all other BAR adaptor proteins, except for Rvs161, which does, however, also lack a C-terminal extension. While BIN1 and BIN3 are ubiquitously expressed, BIN2 is predominantly found in hematopoietic cells.¹²³ Recently, a siRNA-knockdown of BIN2 in leukocytes has been shown to result in decreased cell migration, but increased phagocytosis, whereas overexpression of BIN2 led to decreased phagocytosis. Besides these initial data, nothing is known about the *in vivo* function of BIN2.¹²⁴ The analysis of an animal model of BIN2-deficiency and the consequence of BIN2-deficiency in platelets is one of the aims in this thesis.

1.5 Fc γ receptor signaling and immune thrombocytopenia

Immune thrombocytopenia (ITP) is an acquired autoimmune disorder, characterized by low platelet counts ($< 100 \times 10^9$ platelets L^{-1}) and increased bleeding risk.¹²⁵ ITP can either occur

as a primary effect in the absence of other causes or as a consequence of disorders that may be associated with thrombocytopenia. Secondary ITP can be an effect of chronic infections, such as *Helicobacter pylori*, Hepatitis C virus and HIV or other autoimmune disorders, such as systemic lupus erythematosus, rheumatoid arthritis and antiphospholipid syndrome.¹²⁶ The pathophysiology of ITP is complex, but the primary event is caused by immunoglobulin G (IgG) autoantibodies against platelet surface glycoproteins, resulting in strongly enhanced Fc γ R-mediated phagocytosis and destruction by macrophages in the reticuloendothelial system within the spleen (Figure 7 and ¹²⁷). The two most common antigens of anti-platelet antibodies in patients suffering from ITP are GPIb, the von Willebrand factor receptor, and the major platelet integrin α IIb β 3 (GPIIb/IIIa).¹²⁸ Anti-GPIb antibodies induce Fc-independent platelet destruction, while anti-GPIIb/IIIa antibodies efficiently trigger Fc-dependent platelet clearance.^{129–131} However, it should be noted that autoantibodies are not detectable in up to 50% of ITP patients while remission in ITP can occur despite the continued presence of platelet autoantibodies.⁶ Recent studies have shown that these autoantibodies not only opsonize platelets, but can also inhibit and destroy megakaryocytes, the progenitor cells of platelets.¹³² Another mechanism leading to thrombocytopenia is T cell-mediated peripheral platelet destruction and inhibition/destruction of megakaryocytes.¹³³ Although regulatory T cells (Tregs) only represent 5-10% of peripheral CD4⁺ T cells, there is growing evidence for the role of Tregs in ITP. Normally, Tregs, play essential roles in self-tolerance by suppressing both cell-mediated (CD8⁺ T cell) and antibody-mediated (CD19⁺ B cell) responses. Circulating Tregs in patients with acute and chronic ITP have been previously shown to be significantly reduced compared to healthy controls, but also show impaired regulatory activity inducing a shift in self-tolerance (summarized in¹²⁶).

As already indicated above, macrophages are key players in the pathology of ITP, as they clear antibody-opsonized platelets from the circulation via their Fc γ Rs, but also serve as antigen-presenting cells (APCs) to further promote the production of autoantibodies and activation CD8⁺ cytotoxic T cells.^{127,134} Mice express three activating Fc γ Rs (Fc γ RI, Fc γ RIII, Fc γ RIV) and one inhibitory Fc γ R (Fc γ RIIB), while humans express six different Fc γ receptors (RI, RIIA-C, RIIIA-B).^{135,136} Fc γ RIIB is the only known inhibitory Fc γ R. It transmits inhibitory signals through an immunoreceptor tyrosine-based inhibitory motif (ITIM) contained in its cytoplasmic region. All activating murine Fc γ R need the FcR γ -chain with its ITAM as signal transducing unit and for proper assembly of the entire Fc γ R.¹³⁵ The activatory and inhibitory Fc γ Rs bind IgG with different affinity and subclass specificity. Fc γ RIII exclusively binds IgG1, while Fc γ RIV prefers IgG2a and IgG2b antibodies.¹³⁵ Of note, clinical data, along with information gained from animal models, suggest that the high-affinity Fc γ RI does not play a relevant role in ITP, as this receptor is constantly saturated.¹³⁵ The receptors are widely

expressed throughout the hematopoietic system. Innate immune effector cells, such as monocytes, macrophages, dendritic cells (DCs), basophils and mast cells, express both activating and inhibitory Fc γ Rs. In mice, monocytes and macrophages express all three activating (Fc γ RI, Fc γ RIII, Fc γ RIV) and the inhibitory Fc γ RIIB.¹³⁵ It is noteworthy that the majority of Fc γ RIIB is found in liver sinusoidal endothelial cells (LSECs) which, however, lack activating Fc γ Rs.¹³⁷ LSECs separate hepatocytes from the blood in the sinusoidal lumen by forming a fenestrated endothelium which lacks a basement membrane establishing the space of Disse between the endothelial lining and the hepatocytes. Fc γ RIIB on LSECs is the critical scavenging receptor that mediates capture and removal of viruses and soluble immune complexes (sIC).¹³⁸ However, a role of Fc γ RIIB in the processing of antibody-opsonized blood cells, including platelets, has not been reported to date and the investigation of this role is one aim of this thesis.

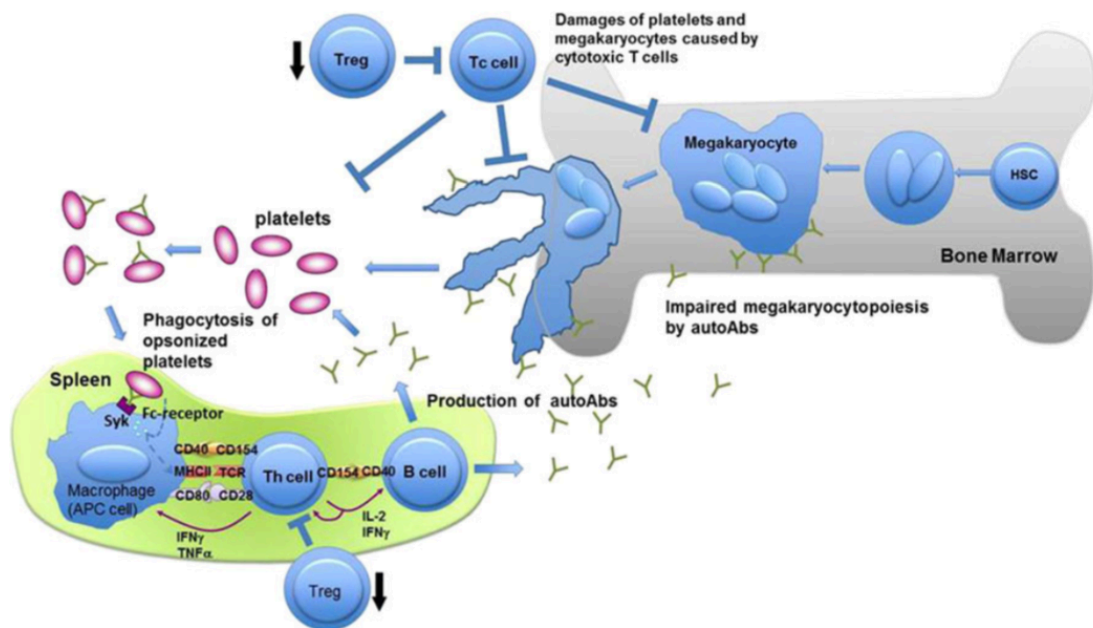


Figure 7: Simplified scheme of the pathophysiology of immune thrombocytopenia. The occurrence of antiplatelet autoantibodies remains the central pathogenetic mechanism. Autoantibodies opsonize platelets which are phagocytosed and destroyed by macrophages predominantly in the spleen. Peptide fragments expressed with MHC class II stimulate helper T cells, following activation of autoreactive B cells. Impaired regulatory T cell function fails to control self-tolerance. Autoantibodies also impair megakaryocyte function. Additionally, autoreactive cytotoxic T cells may destroy platelets and megakaryocytes. Taken from: Kashiwagi and Tomiyama, 2013.²¹⁵

1.6 Aim of the study

Given the key role of platelets in normal hemostasis as well as in thrombotic disorders, further understanding of signaling pathways in platelets and regulation of platelet receptors is essential in order to identify potential new targets and possibilities for antithrombotic therapy. The BAR protein BIN2 is expressed in platelets and other hematopoietic cells, but only little is known about its function and potential *in vitro* and *in vivo* functions in platelets. The first part of this thesis deals with the analysis of a mouse model of BIN2-deficiency and the consequence of BIN2-deficiency in platelets.

The paxillin family member Hic-5 is proposed as an important regulator of the activation of the major platelet integrin α IIb β 3, essential for firm platelet adhesion and thrombus formation. However, the importance of Hic-5 in platelet function is controversial. The second aim of this thesis was to analyze the role of Hic-5 as regulator of integrin α IIb β 3 activation and platelet aggregation.

The Rho GTPase family members RhoA and Rac1 play major roles in platelet activation at sites of vascular injury. Little is known about possible redundant functions of these Rho GTPases in regulating platelet function. The third aim of this thesis was to analyze redundant functions of the Rho GTPases RhoA and Rac1 in platelet function.

The last part of this thesis deals with the analysis of antibody-mediated modulation of platelet receptor function in thrombotic disease. GPVI has emerged as an attractive potential target for antithrombotic therapy, as its deficiency, blockade or antibody-induced depletion provides powerful protection from experimental arterial thrombosis without affecting platelet hemostatic functions. While different anti-GPVI antibodies of the IgG class efficiently deplete the receptor *in vivo* they do not affect GPVI surface expression in platelets *in vitro*. This indicates the involvement of a non-platelet compartment. The data obtained in the course of this thesis reveal a so far unknown role of Fc γ RIIB in the processing of antibody-opsonized blood cells including platelets.

2 Materials and Methods

2.1 Materials

2.1.1 Chemicals

| Reagent | Company |
|--|---|
| Acetic acid | Roth (Karlsruhe, Germany) |
| Acetylsalicylic acid (ASA) | Bayer (Leverkusen, Germany) |
| Adenosine diphosphate (ADP) | Sigma-Aldrich (Schnelldorf, Germany) |
| Agarose | Roth (Karlsruhe, Germany) |
| Amersham [®] Hyperfilm [®] , ECL | GE Healthcare (Freiburg, Germany) |
| 3-amino-9-ethylcarbazole (AEC) solution | EUROPA (Cambridge, UK) |
| Alexa F488 | Molecular Probes (Eugene, USA) |
| Alexa F647 | Molecular Probes (Eugene, USA) |
| Ammonium persulfate (APS) | Roth (Karlsruhe, Germany) |
| Apyrase (Grade III) | Sigma-Aldrich (Schnelldorf, Germany) |
| Aquatex [®] aqueous mounting medium | VWR Int. GmbH (Vienna, Austria) |
| β -mercaptoethanol (β -ME) | Roth (Karlsruhe, Germany) |
| Botrocetin | Pentapharm Ltd. (Basel, CH) |
| Bovine serum albumin (BSA) | AppliChem (Darmstadt, Germany) |
| Bradford protein assay | Bio-Rad (Munich, Germany) |
| Cacodylate | AppliChem (Darmstadt, Germany) |
| Calcium chloride | Roth (Karlsruhe, Germany) |
| Calpeptin | Merck Millipore (Darmstadt, Germany) |
| Chloroform | AppliChem (Darmstadt, Germany) |
| Chlodrosomes | Clodronate Liposomes (Haarlem, The Netherlands) |
| Chrono-Lume luciferase reagent | Chrono-log (Havertown, PA, USA) |
| Collagen Horm [®] suspension + SKF sol. | Takeda (Linz, Austria) |
| Convulxin (CVX) | Alexis Biochemicals (San Diego, USA) |
| Cryo-Gel | Leica Biosystems (Wetzlar, Germany) |
| Dade [®] Innovin (tissue factor) | Siemens Healthcare Diagnostics (Deerfield, IL, USA) |
| 4',6-diamidino-2-phenylindole (DAPI) | Life Technologies (Darmstadt, Germany) |
| Dimethyl sulfoxide (DMSO) | Sigma-Aldrich (Steinheim, Germany) |
| Dry milk, fat-free | AppliChem (Darmstadt, Germany) |
| Deoxynucleotide triphosphates (dNTP) mix | Life Technologies (Darmstadt, Germany) |
| DyLight-488 | Pierce (Rockford, USA) |

| Reagent | Company |
|--|--|
| DyLight-649 | Pierce (Rockford, USA) |
| Enhanced chemiluminescence (ECL) detection substrate | MoBiTec (Göttingen, Germany) |
| Ethylenediaminetetraacetic acid (EDTA) | AppliChem (Darmstadt, Germany) |
| Ethylene glycol tetraacetic acid (EGTA) | Sigma-Aldrich (Schnelldorf- Germany) |
| Epon 812 | Roth (Karlsruhe, Germany) |
| Ethanol | Roth (Karlsruhe, Germany) |
| Ethidium bromide | Roth (Karlsruhe, Germany) |
| Fentanyl | Janssen-Cilag (Neuss, Germany) |
| Fibrinogen from human plasma (# F3879) | Sigma-Aldrich (Schnelldorf, Germany) |
| Fibrinogen from human plasma (# F4883) | Sigma-Aldrich (Schnelldorf, Germany) |
| Flumazenil | AlleMan Pharma (Pfullingen, Germany) |
| Fluorescein-isothiocyanate (FITC) | Molecular Probes (Oregon, USA) |
| Fluoroshield™ | Sigma-Aldrich (Schnelldorf, Germany) |
| Fluoroshield™ with DAPI | Sigma-Aldrich (Schnelldorf, Germany) |
| Formalin 37% | Roth (Karlsruhe, Germany) |
| Fura-2/AM | Life Technologies (Darmstadt, Germany) |
| GeneRuler DNA Ladder Mix | Life Technologies (Darmstadt, Germany) |
| Glucose | Roth (Karlsruhe, Germany) |
| Glutaraldehyde solution (25%) | Science Services (Munich, Germany) |
| Hematoxylin solution (# MHS32) | Sigma-Aldrich (Schnelldorf, Germany) |
| Heparin sodium | Ratiopharm (Ulm, Germany) |
| 4-(2-hydroxyethyl)-1-piperazine-ethanesulfonic acid (HEPES) | Life Technologies (Darmstadt, Germany) |
| IGEPAL®CA-630 | Sigma-Aldrich (Schnelldorf, Germany) |
| Immobilon-P transfer membrane, PVDF | Merck Millipore (Darmstadt, Germany) |
| Indomethacin | Sigma-Aldrich (Schnelldorf, Germany) |
| Integrilin® (Eptifibatide) | Millennium Pharmaceuticals Inc. (Cambridge, USA) |
| Ionomycin | Merck Millipore (Darmstadt, Germany) |
| Iron-III-chloride hexahydrate (FeCl ₃ ·6H ₂ O) | Roth (Karlsruhe, Germany) |
| Isofluran CP® | cp-pharma (Burgdorf, Germany) |
| Isopropanol | Roth (Karlsruhe, Germany) |
| Ketamine | Parke-Davis (Berlin, Germany) |
| Loading Dye solution, 6x | Fermentas (St. Leon-Rot, Germany) |
| Magnesium chloride | Roth (Karlsruhe, Germany) |
| Medetomidine | Pfizer (Karlsruhe, Germany) |
| Methanol | Roth (Karlsruhe, Germany) |

| Reagent | Company |
|---|--|
| Midazolam | Roche (Grenzach-Wyhlen, Germany) |
| Midori Green Advanced DNA stain | Nippon Genetics Europe (Düren, Germany) |
| Naloxon | AlleMan Pharma (Pfullingen, Germany) |
| NuPAGE [®] LDS Sample Buffer (4x) | Life Technologies (Darmstadt, Germany) |
| NuPAGE [®] Novex [®] 4-12% Bis-Tris Gels, 1mm, 10 well, 15 well | Life Technologies (Darmstadt, Germany) |
| Osmium tetroxide | Merck Millipore (Darmstadt, Germany) |
| PageRuler Prestained Protein Ladder (# 26616, 26619) | Life Technologies (Darmstadt, Germany) |
| Paraformaldehyde (PFA) | Sigma-Aldrich (Schnelldorf, Germany) |
| Phenol/chloroform/isoamyl alcohol | Roth (Karlsruhe, Germany) |
| Phalloidin-Atto647N | Sigma-Aldrich (Schnelldorf, Germany) |
| Pluronic F-127 | Life Technologies (Darmstadt, Germany) |
| Poly-L-lysine (PLL) | Sigma-Aldrich (Schnelldorf, Germany) |
| Propidium iodide | Life Technologies (Darmstadt, Germany) |
| Prostacyclin (PGI ₂) | Calbiochem (Bad Soden, Germany) |
| Protease Inhibitor Cocktail (# P8340) | Sigma-Aldrich (Schnelldorf, Germany) |
| Proteinase K, recombinant, PCR grade (20 mg mL ⁻¹) | Life Technologies (Darmstadt, Germany) |
| RNase A (# R4875) | Sigma-Aldrich (Schnelldorf, Germany) |
| R-phycoerythrin (PE) | EUROPA (Cambridge, UK) |
| Rotiphorese [®] Gel 30 (37,5:1) acrylamide | Roth (Karlsruhe, Germany) |
| SeeBlue [®] Plus2 pre-stained standard | Life Technologies (Darmstadt, Germany) |
| Sodium azide | Sigma-Aldrich (Schnelldorf, Germany) |
| Sodium carbonate | Sigma-Aldrich (Schnelldorf, Germany) |
| Sodium chloride | AppliChem (Darmstadt, Germany) |
| Sodium citrate | AppliChem (Darmstadt, Germany) |
| Sodiumdihydrogenphosphate | Roth (Karlsruhe, Germany) |
| Sodium dodecyl sulfate (SDS) | Sigma-Aldrich (Schnelldorf, Germany) |
| Sodium hydroxide | AppliChem (Darmstadt, Germany) |
| Sodium orthovanadate | Sigma-Aldrich (Schnelldorf, Germany) |
| Streptavidin-HRP (# 016-030-084) | Jackson ImmunoResearch (West Grove, PA, USA) |
| Sucrose | Sigma-Aldrich (Schnelldorf, Germany) |
| <i>Taq</i> DNA polymerase (5 U L ⁻¹ without BSA) | Life Technologies (Darmstadt, Germany) |
| N,N,N',N'-Tetramethylethylenediamine (TEMED) | Roth (Karlsruhe, Germany) |
| Thapsigargin (TG) | Life Technologies (Darmstadt, Germany) |

| Reagent | Company |
|---|---------------------------------------|
| Thrombin from human plasma | Roche Diagnostics (Mannheim, Germany) |
| Tissue Tek | Sigma-Aldrich (Schnelldorf, Germany) |
| TMB Substrate Reagent Set | Sakura Finetek (Staufen, Germany) |
| Tris(hydroxymethyl)aminomethane (TRIS) | BD Biosciences (Heidelberg, Germany) |
| Triton X-100 | Roth (Karlsruhe, Germany) |
| TRizol [®] | Sigma-Aldrich (Schnelldorf, Germany) |
| Tween [®] 20 | Invitrogen (Karlsruhe, Germany) |
| U46619 | Roth (Karlsruhe, Germany) |
| Water, nuclease-free | Enzo Life Sciences (Lörrach, Germany) |
| Western Lightning [®] Plus-ECL | Roth (Karlsruhe, Germany) |
| | PerkinElmer (Baesweiler, Germany) |

Collagen-related peptide (CRP) was kindly provided by Paul Bray (Baylor College, USA). Rhodocytin (RC) was a generous gift from Dr. Johannes Eble (University Hospital, Frankfurt, Germany). All other non-listed chemicals were obtained from AppliChem (Darmstadt, Germany), Roth (Karlsruhe, Germany) or Sigma-Aldrich (Schnelldorf, Germany). Annexin A5 was generously provided by Jonathan F. Tait (Medical Center Washington, USA) and conjugated in our lab. Primers were obtained from Metabion (Planegg-Martinsried, Germany).

2.1.2 Kits

| Kits | Company |
|--|---------------------------------|
| IP-One ELISA assay | Cisbio (Codolet, France) |
| SuperScript [®] First-Strand Synthesis System | Invitrogen (Karlsruhe, Germany) |

2.1.3 Antibodies

2.1.3.1 Commercially purchased antibodies

| Antibody | Host organism | Company |
|----------------------|---------------|--|
| anti- β -actin | Rabbit | Sigma-Aldrich (Schnelldorf, Germany) |
| anti-BIN2 | Rabbit | Proteintech (Manchester, United Kingdom) |
| | Rabbit | Sigma-Aldrich (Schnelldorf, Germany) |
| anti-CD29 (9EG7) | Rat | BD Biosciences (Heidelberg, Germany) |
| anti-CD3 | Rat | BD Biosciences (Heidelberg, Germany) |
| anti-CD45R/B220 | Rat | BioLegend (San Diego, USA) |
| anti-CD105 | Rat | BioLegend (San Diego, USA) |
| anti-GAPDH | Rabbit | Sigma-Aldrich (Schnelldorf, Germany) |
| anti-Hic-5 | Mouse | BD Biosciences (Heidelberg, Germany) |

| Antibody | Host organism | Company |
|------------------------------------|----------------------|--------------------------------------|
| anti-LAT | Rabbit | Cell Signaling (Denver, USA) |
| anti-leupaxin | Rabbit | BioLegend (San Diego, USA) |
| anti-Ly-6G/C (Gr1) | Rat | BioLegend (San Diego, USA) |
| anti-paxillin | Rabbit | Biorbyt (Cambridge, United Kingdom) |
| anti-phospho-LAT (Y191) | Rabbit | Cell Signaling (Denver, USA) |
| anti-phospho-PLC γ 2 (Y759) | Rabbit | Cell Signaling (Denver, USA) |
| anti-phospho-Syk (Y525/526) | Rabbit | Cell Signaling (Denver, USA) |
| anti-phospho-Tyrosine (4G10) | Mouse | Merck Millipore (Darmstadt, Germany) |
| anti-PLC γ 2 | Rabbit | Santa Cruz (Heidelberg, Germany) |
| anti-Rac1 | Rabbit | Merck Millipore (Darmstadt, Germany) |
| anti-RhoA | Mouse | Cytoskeleton (Denver, USA) |
| anti-STIM1 | Rabbit | Cell Signaling (Denver, USA) |
| anti-Syk | Rabbit | Cell Signaling (Denver, USA) |
| anti-TER-119 | Rat | BioLegend (San Diego, USA) |
| anti-vWF | Mouse | DAKO (Hamburg, Germany) |
| Antibody conjugates | Host organism | Company |
| anti- α -tubulin-Alexa F488 | Mouse | Invitrogen (Karlsruhe, Germany) |
| anti-mouse IgG-Cy3 | Donkey | Jackson Immuno (Suffolk, UK) |
| anti-mouse IgG-HRP | Rat | DAKO (Hamburg, Germany) |
| anti-rabbit IgG-Cy3 | Goat | Jackson Immuno (Suffolk, UK) |
| anti-rabbit IgG-Alexa F488 | Donkey | Invitrogen (Karlsruhe, Germany) |
| anti-rabbit IgG-HRP | Goat | Cell Signaling (Denver; USA) |
| anti-rat IgG-FITC | Rabbit | Dianova (Hamburg, Germany) |
| anti-STIM1-Atto550 | Rabbit | alomone labs (Jerusalem, Israel) |

2.1.3.2 Monoclonal rat antibodies generated or modified in our laboratory

| Antibody | Clone | Isotype | Antigen | Reference |
|-----------------|--------------|----------------|--------------------------------------|---|
| 2.4G2 | - | | CD16/CD32 (Fc γ RIIb/RIII) | Clone HB-197 purchased from ATCC; |
| p0p4 | 15E2 | IgG2b | GPIb α | 139 |
| p0p3 | 7A9 | IgG2a | GPIb α | 139 |
| p0p1 | 3G6 | IgG1 | GPIb β | 139 |
| DOM2 | 89H11 | IgG2a | GPV | 129 |
| p0p6 | 56F8 | IgG2b | GPIX | 129 |
| JAQ1 | 98A3 | IgG2a | GPVI | 140 |

| Antibody | Clone | Isotype | Antigen | Reference |
|-----------------|--------------|----------------|---------------------|------------------|
| JAQ3 | 0E3 | IgG2a | GPVI | 141 |
| INU1 | 11E9 | IgG1 | CLEC-2 | 43 |
| ULF1 | 97H1 | IgG2a | CD9 | unpublished |
| LEN1 | 12C6 | IgG2b | $\alpha 2$ | 22 |
| EDL1 | 57B10 | IgG2a | $\beta 3$ | 139 |
| JON2 | 14A3 | IgG2a | $\alpha IIb\beta 3$ | 129 |
| JON/A | 4H5 | IgG2b | $\alpha IIb\beta 3$ | 142 |
| MWReg30 | 5D7 | IgG1 | $\alpha IIb\beta 3$ | 143 |
| WUG 1.9 | 5C8 | IgG1 | P-selectin | 141 |

2.1.4 Buffers and media

If not stated otherwise, all buffers were prepared in deionized water obtained from a MilliQ Water Purification System (Millipore, Schwalbach, Germany). pH was adjusted with HCl or NaOH.

Blocking buffer (Western blot)

BSA or fat-free dry milk 5%
in Washing Buffer (see below)

Blocking buffer (Immunohistochemistry)

Tween 20[®] 0.1%
BSA 3%
Rat / Goat serum 3%
in PBS

Cacodylate buffer, pH 7.2

Sodium cacodylate 0.1 M

Coating buffer (ELISA), pH 9.5

NaHCO₃ 85 mM
Na₂CO₃ 15 mM

Karnovsky fixation buffer, pH 7.2

Paraformaldehyde 2%
Glutardialdehyde 2.5%
Cacodylate 0.1 M

Laemmli buffer (for SDS-PAGE)

TRIS 40 mM

| | |
|---|-------------------------|
| Glycine | 0.95 M |
| SDS | 0.5% |
| Loading dye (6x) for analysis of PCR products | |
| TRIS (150 mM) | 33% |
| Glycerin | 60% |
| Bromophenolblue | 0.04% |
| Lysis buffer for DNA isolation | |
| TRIS | 100 mM |
| EDTA (0.5 M) | 5 mM |
| NaCl | 200 mM |
| SDS | 0.2 % |
| Proteinase K (20 mg mL ⁻¹) | 100 µg mL ⁻¹ |
| Lysis buffer for platelet lysates, pH 8.0 | |
| Tris, pH 7.4 | 15 mM |
| NaCl | 155 mM |
| EDTA | 1 mM |
| NaN ₃ | 0.005% |
| Igepal [®] CA-630 | 1% |
| protease inhibitor cocktail | 1% |
| Lysis buffer (2x) for tyrosine phosphorylation studies, pH 7.5 | |
| NaCl | 300 mM |
| TRIS | 20 mM |
| EGTA | 2 mM |
| EDTA | 2 mM |
| NaF | 10 mM |
| Na ₃ VO ₄ | 4 mM |
| Igepal [®] CA-630 | 2 % |
| protease inhibitor cocktail | |
| MOPS (3-(N-morpholino)propanesulfonic acid) buffer (20x) | |
| MOPS | 1 M |
| TRIS | 1 M |
| SDS | 69.3 mM |
| EDTA | 20.5 mM |
| PBS (Phosphate-buffered saline), pH 7.14 | |
| NaCl | 137 mM |

| | |
|--|---------|
| KCl | 2.7 mM |
| KH ₂ PO ₄ | 1.5 mM |
| Na ₂ HPO ₄ x 2H ₂ O | 8 mM |
| PBS/EDTA (for platelet lysates) | |
| EDTA | 5 mM |
| in PBS | |
| PHEM buffer, pH 6.8 | |
| PIPES | 100 mM |
| HEPES | 5.25 mM |
| EGTA | 10 mM |
| MgCl ₂ | 20 mM |
| PHEM complete buffer, pH 7.2 | |
| PHEM Fixation Buffer | |
| Igepal [®] CA-630 | 0.1% |
| in PHEM | |
| PHEM fixation buffer | |
| PFA | 4% |
| in PHEM | |
| RIPA buffer | |
| NaCl | 150 mM |
| Sodium deoxycholate | 0.5 % |
| SDS | 0.1 % |
| TRIS, pH 8.0 | 50 mM |
| Na ₃ VO ₄ | 2 mM |
| Igepal [®] CA-630 | 1 % |
| protease inhibitor cocktail | |
| SDS sample buffer, 2x | |
| β-Mercaptoethanol (for red. Conditions) | 10% |
| TRIS (1.25 M), pH 6.8 | 10% |
| Glycerin | 20% |
| SDS | 4% |
| Bromophenolblue | 0.02% |
| Separating gel buffer (SDS-PAGE), pH 8.8 | |
| TRIS/HCl | 1.5 M |

Sodium citrate, pH 7.0

Sodium citrate 0.129 mM

Stacking gel buffer (SDS-PAGE), pH 6.8

TRIS/HCl 0.5 M

Stripping buffer (Western blot, "mild"), pH 2.0

Glycine 25 mM

SDS 1%

in PBS

TAE buffer (50x)

TRIS 0.2 M

Acetic acid 5.7%

EDTA (0.5 M) 10%

TBS (TRIS-buffered saline), pH 7.3

NaCl 137 mM

TRIS/HCl 20 mM

TE-buffer

TRIS 10 mM

EDTA 1 mM

Transfer-buffer (semi-dry blot)

TRIS ultra 48 mM

Glycine 39 mM

Methanol 20%

TRIS-EDTA-buffer, pH 9.0

TRIS 10 mM

EDTA 1 mM

Tween 20[®] 0.05%

Tyrode's buffer, pH 7.3

NaCl 137 mM

KCl 2.7 mM

NaHCO₃ 12 mM

NaH₂PO₄ 0.43 mM

Glucose 0.1 %

HEPES 5 mM

BSA 0.35%

CaCl₂ 2 mM

| | |
|--------------------------------------|-------|
| MgCl ₂ | 1 mM |
| Washing buffer (ELISA) | |
| Tween 20 [®] | 0.05% |
| in PBS | |
| Washing buffer (Western Blot) | |
| Tween 20 [®] | 0.1% |
| in TBS | |

2.2 Methods

2.2.1 Genetically modified mice

The generation of *Bin2^{fl/fl}* mice was as follows: A 9.96 kb region used to construct the targeting vector was first subcloned into a ~2.4 kb backbone vector (pSP72, Promega) from a positively identified 129 BAC clone (bmQ365K17). The region was designed such that the 5' homology arm extends about 2.83 Kb 5' to the 3' end of the LoxP-FRT flanked Neo cassette. The 3' homology arm ends 3' to single LoxP cassette and is 6.52 Kb long. The LoxP-FRT flanked Neo cassette was inserted 403 bp upstream of exon 3. The single LoxP site was inserted 157 bp downstream of exon 3. The target region comprises 615 bp and includes exon 3. DNA of the targeting vector was linearized by NotI digestion and then transfected by electroporation of BA1 (C57Bl/6 x 129/SvEv) (Hybrid) embryonic stem cells. After selection with G418, surviving clones were expanded for PCR analysis to identify recombinant ES clones. 5 positive clones were identified and expanded. Targeted iTL BA1 (C57BL/6N x 129/SvEv) hybrid embryonic stem cells were microinjected into blastocysts of pseudo-pregnant C57BL/6 females. Highly chimeric offspring was mated to C57BL/6 FLP mice to remove the Neo cassette (Neo deletion in somatic cells) and backcrossed to C57BL/6 females resulting in *Bin2^{fl/+}* mice with Neo deletion in germ cells. Constitutive knockout mice were generated by mating with CMV-Cre and for MK-/platelet-specific knockout mice with Pf4-cre mice.^{144,145} Intercrossing of the respective offspring resulted in *Bin2^{-/-}*-mice or *Bin2^{fl/fl} Pf4-Cre* mice, respectively. *Bin2^{fl/fl}* littermates served as controls.

Tgfb1i1^{+/-} mice were generated by injection of embryonic stem cell clone EPD0817_1_D04 (Knockout Mouse Project [KOMP] Repository) into blastocysts of pseudo-pregnant C57BL/6 females to generate germ line chimeras. Male chimeras were bred to C57BL/6 females to generate *Tgfb1i1^{+/-}* mice, which were intercrossed to produce *Tgfb1i1^{-/-}* mice and littermate wild-type controls.

C57BL/6JRj mice maintained under specific-pathogen-free conditions were obtained at an age of 6-9 weeks from JANVIER LABS (Le Genest-Saint-Isle, France). Mice with a constitutive

knockout for GPVI (*Gp6^{-/-}*), Fc γ RIIB (*Fcgr2b^{-/-}*) and Fc γ RIII (*Fcgr3^{-/-}*) were described earlier in ^{39,146,147} and backcrossed on C57Bl/6J background for at least 10 generations.

RhoA^{fl/fl} and *Rac1^{fl/fl}* mice were generated as previously described.^{57,58} *RhoA^{fl/fl}* and *Rac1^{fl/fl}* mice were intercrossed with mice carrying the platelet factor 4 (Pf4)-Cre transgene (*Pf4-Cre*)¹⁴⁵ to generate *RhoA^{fl/fl}/Rac1^{fl/fl}Pf4-Cre* mice. *RhoA^{fl/fl}/Rac1^{fl/fl}* mice served as control.

All animal experiments were approved by the district government of Lower Franconia (Bezirksregierung Unterfranken).

2.2.2 Genotyping of mice

2.2.2.1 Isolation of genomic mouse DNA

Ear punches were incubated overnight at 56°C and 900 rpm or for 3 h at 56°C and 1,400 rpm in 500 μ L of lysis buffer. Cellular proteins and lipids were removed by the addition of 500 μ L of phenol/chloroform/isoamyl alcohol (25:24:1). Samples were mixed well and centrifuged for 10 min at 10,000 rpm in an Eppendorf 5417R tabletop centrifuge at RT. After centrifugation, the aqueous nucleic acid containing upper phase was transferred into a new tube containing 500 μ L isopropanol to precipitate the DNA. Subsequently, the nucleic acids were spun down by centrifugation for 15 min at 14,000 rpm and 4°C. The pellet was washed and dehydrated by the addition of 500 μ L 70% ethanol with subsequent centrifugation for 15 min at 14,000 rpm. Before dissolving the pellet in 50 μ L TE buffer, the pellet was allowed to dry for 30 min at 37°C.

2.2.2.2 PCR (Polymerase chain reaction)

Separate PCR reactions were performed to amplify the *WT/floxed RhoA*, *Rac1*, *Bin2* or the targeted *Fcgr2b*, *Fcgr3*, *Bin2*, *Tgfb1i1* loci and to control the presence of the Cre-recombinase cassette under control of the *Pf4* or *CMV* promoter. GPVI-deficient mice were genotyped by flow cytometry.

PCR mix for *Bin2* WT/floxed and targeted *Bin2* allele

| | |
|---------------|--|
| 1.0 μ L | DNA sample |
| 2.5 μ L | 10x Taq Buffer (+KCl, -MgCl ₂) |
| 2.5 μ L | MgCl ₂ [25 mM] |
| 1 μ L | dNTPs [10 mM] |
| 0.1 μ L | forward Primer [100 pM] |
| 0.1 μ L | reverse Primer [100 pM] |
| 0.25 μ L | native Taq-Polymerase [5 U μ L ⁻¹] |
| 17.55 μ L | H ₂ O |

PCR mix for *CMV-Cre*

| | |
|--------------------|---|
| 0.5 μL | DNA sample |
| 2.5 μL | 10x Taq Buffer (+KCl, -MgCl ₂) |
| 1.5 μL | MgCl ₂ [25 mM] |
| 1 μL | dNTPs [10 mM] |
| 0.1 μL | forward Primer [100 pM] |
| 0.1 μL | reverse Primer [100 pM] |
| 0.5 μL | native Taq-Polymerase [5 U μL^{-1}] |
| 18,8 μL | H ₂ O |

PCR program for *CMV-Cre*

| Temperature [°C] | Time [s] | Repeats |
|------------------|----------|-----------|
| 95 | 300 | 1 cycle |
| 95 | 30 | 35 cycles |
| 67 | 30 | 35 cycles |
| 72 | 60 | 35 cycles |
| 72 | 300 | 1 cycle |
| 22 | ∞ | 1 cycle |

Primer *CMV-Cre*

| | |
|---------|--|
| CMV_fwd | 5' GCC TGC ATT ACC GGT CGA TGC AAC GA 3' |
| CMV-rev | 5' GTG GCA GAT GGC GCG GCA ACA CCA TT 3' |

Expected band size: 700 bp for positive samples.

PCR mix for *Fcgr2b*

| | |
|---------------------|---|
| 1 μL | DNA sample |
| 2.5 μL | 10x Taq Buffer (+KCl, -MgCl ₂) |
| 2.5 μL | MgCl ₂ [25 mM] |
| 1 μL | dNTPs [10 mM] |
| 0.25 μL | 1:10 diluted forward Primer [100 pM] WT |
| 0.5 μL | 1:10 diluted forward Primer [100 pM] KO |
| 0.5 μL | 1:10 diluted reverse Primer [100 pM] |
| 0.5 μL | native Taq-Polymerase [5 U μL^{-1}] |
| 16.25 μL | H ₂ O |

PCR program for *Fcgr2b*

| Temperature [°C] | Time [s] | Repeats |
|------------------|----------|-----------|
| 95 | 300 | 1 cycle |
| 95 | 30 | 35 cycles |
| 67 | 60 | 35 cycles |
| 72 | 60 | 35 cycles |
| 72 | 300 | 1 cycle |
| 22 | ∞ | 1 cycle |

Primer *Fcgr2b*

Fcgr2b_wt_fwd 5' TTG ACT GTG GCC TTA AAC GTG TAG 3'

Fcgr2b_ko_fwd 5' CTC GTG CTT TAC GGT ATC GCC 3'

Fcgr2b_rev 5' AAA CTC GAC CCC CCG TGG ATC 3'

Expected band sizes: 161 bp for *WT* allele and 232 bp for targeted *Fcgr2b* allele.

PCR mix for *Fcgr3*

| | |
|---------|---|
| 1 µL | DNA sample |
| 2.5 µL | 10x Taq Buffer (+KCl, -MgCl ₂) |
| 2.5 µL | MgCl ₂ [25 mM] |
| 1 µL | dNTPs [10 mM] |
| 0.5 µL | 1:10 diluted forward Primer [100 pM] WT or KO |
| 0.5 µL | 1:10 diluted reverse Primer [100 pM] |
| 0.5 µL | native Taq-Polymerase [5 U µL ⁻¹] |
| 16.5 µL | H ₂ O |

PCR program for *Fcgr3-WT*

| Temperature [°C] | Time [s] | Repeats |
|------------------|----------|-----------|
| 95 | 180 | 1 cycle |
| 95 | 30 | 35 cycles |
| 58 | 30 | 35 cycles |
| 72 | 60 | 35 cycles |
| 72 | 300 | 1 cycle |
| 22 | ∞ | 1 cycle |

PCR program for *Fcgr3-KO*

| Temperature [°C] | Time [s] | Repeats |
|------------------|----------|-----------|
| 95 | 300 | 1 cycle |
| 95 | 30 | 35 cycles |
| 68 | 30 | 35 cycles |
| 72 | 60 | 35 cycles |
| 72 | 300 | 1 cycle |
| 22 | ∞ | 1 cycle |

Primer *Fcgr3*

| | |
|--------------|-----------------------------------|
| Fcgr3_wt_fwd | 5' CTA CAT CCT CCA TCT CTC TAG 3' |
| Fcgr3_ko_fwd | 5' GCA CGA GAC TAG TGA GAC GTG 3' |
| Fcgr3_rev | 5' GTG GCT GAA AAG TTG CTG CTG 3' |

Expected band sizes: 238 bp for *WT* allele and 550 bp for targeted *Fcgr3* allele.

PCR mix for *Pf4-Cre*

| | |
|----------|---|
| 2.0 µL | DNA sample |
| 2.5 µL | 10x Taq Buffer (+KCl, -MgCl ₂) |
| 2.5 µL | MgCl ₂ [25 mM] |
| 0.5 µL | dNTPs [10 mM] |
| 1 µL | 1:10 diluted forward Primer [100 pM] |
| 1 µL | 1:10 diluted reverse Primer [100 pM] |
| 0.25 µL | native Taq-Polymerase [5 U µL ⁻¹] |
| 15.25 µL | H ₂ O |

PCR program for *Pf4-Cre*

| Temperature [°C] | Time [s] | Repeats |
|------------------|----------|-----------|
| 95 | 300 | 1 cycle |
| 95 | 30 | 35 cycles |
| 48.5 | 30 | 35 cycles |
| 72 | 45 | 35 cycles |
| 72 | 300 | 1 cycle |
| 22 | ∞ | 1 cycle |

Primer Pf4-Cre

Pf4_fwd 5' CCC ATA CAG CAC ACC TTT TG 3'

Pf4_rev 5' TGC ACA GTC AGC AGG TT 3'

Expected band size: 450 bp for positive samples.

PCR mix for Rac1

| | |
|----------|---|
| 1 µL | DNA sample |
| 2.5 µL | 10x Taq Buffer (+KCl, -MgCl ₂) |
| 2.5 µL | MgCl ₂ [25 mM] |
| 1 µL | dNTPs [10 mM] |
| 1 µL | 1:10 diluted forward Primer [100 pM] |
| 1 µL | 1:10 diluted reverse Primer [100 pM] |
| 0.25 µL | native Taq-Polymerase [5 U µL ⁻¹] |
| 15.75 µL | H ₂ O |

PCR program for Rac1

| Temperature [°C] | Time [s] | Repeats |
|------------------|-------------------|-----------|
| 95 | 300 | 1 cycle |
| 95 | 30 | 10 cycles |
| 63 | 30 | 10 cycles |
| | (-1°C each cycle) | |
| 72 | 30 | 10 cycles |
| 95 | 30 | 35 cycles |
| 53 | 30 | 35 cycles |
| 72 | 30 | 35 cycles |
| 72 | 300 | 1 cycle |
| 22 | ∞ | 1 cycle |

Primer Rac1

Rac1_fwd 5' GTC TTG AGT TAC ATC TCT GG 3'

Rac1_rev 5' CTG ACG CCA ACA ACT ATG C 3'

Expected band sizes: 236 bp for *WT* allele and 318 bp for floxed *Rac1* allele.

PCR mix for *RhoA*

| | |
|--------------|--|
| 1 μ L | DNA sample |
| 2 μ L | 10x Taq Buffer (+KCl, -MgCl ₂) |
| 0.6 μ L | MgCl ₂ [25 mM] |
| 0.4 μ L | dNTPs [10 mM] |
| 0.2 μ L | diluted forward Primer [100 pM] |
| 0.2 μ L | reverse Primer [100 pM] |
| 0.2 μ L | native Taq-Polymerase [5 U μ L ⁻¹] |
| 20.6 μ L | H ₂ O |

PCR program for *RhoA*

| Temperature [°C] | Time [s] | Repeats |
|------------------|----------|-----------|
| 95 | 120 | 1 cycle |
| 95 | 30 | 35 cycles |
| 55 | 30 | 35 cycles |
| 72 | 30 | 35 cycles |
| 72 | 300 | 1 cycle |
| 22 | ∞ | 1 cycle |

Primer *RhoA*

| | |
|-----------|-------------------------------------|
| JVH11_for | 5' AGC CAG CCT CTT GAC CGA TTT A 3' |
| JVH15_rev | 5' TGT GGG ATA CCG TTT GAG CAT 3' |

Expected band sizes: 297 bp for *WT* allele and 393 bp for floxed *RhoA* allele.

PCR mix for *Tgfb1i1*

| | |
|---------------|--|
| 1.0 μ L | DNA sample |
| 2.5 μ L | 10x Taq Buffer (+KCl, -MgCl ₂) |
| 2.5 μ L | MgCl ₂ [25 mM] |
| 1 μ L | dNTPs [10mM] |
| 0.1 μ L | forward Primer WT [100 pM] |
| 0.1 μ L | reverse Primer WT [100 pM] |
| 0.1 μ L | forward Primer KO [100 pM] |
| 0.1 μ L | reverse Primer KO [100 pM] |
| 0.25 μ L | native Taq-Polymerase [5 U μ L ⁻¹] |
| 17.35 μ L | H ₂ O |

PCR program for *Tgfb1i1*

| Temperature [°C] | Time [s] | Repeats |
|------------------|----------|-----------|
| 95 | 300 | 1 cycle |
| 95 | 30 | 35 cycles |
| 58 | 30 | 35 cycles |
| 72 | 30 | 35 cycles |
| 72 | 300 | 1 cycle |
| 22 | ∞ | 1 cycle |

Primer *Tgfb1i1*

| | |
|----------------|----------------------------------|
| Tgfb1i1_wt_fwd | 5' GGG ACG GGG CGT AGA TAA AG 3' |
| Tgfb1i1_wt_rev | 5' ACA CCC ATT CAC ACA CTG GA 3' |
| Tgfb1i1_ko_fwd | 5' TAG ATA GAG ATG GCG CAA CG 3' |
| Tgfb1i1_ko_rev | 5' ACA CCC ATT CAC ACA CTG GA 3' |

Expected band sizes: 329 bp for the *WT* allele and 212 bp for the targeted *Tgfb1i1* allele.

2.2.2.3 RNA preparation from platelets

For each genotype, at least three animals were bled under isoflurane anesthesia up to 1 mL into 300 μ L heparin (in TBS [20 U mL⁻¹]) and prepared as described in 2.2.4.1. The pellets were resuspended and pooled in a total volume of 250 μ L lysis buffer, vortexed and incubated for 10 min at RT. After the addition of 1 mL TRIzol[®] reagent, the samples were incubated for 10 min at RT. Further, 250 μ L of chloroform were added and the samples were incubated for 10 min at RT and afterwards centrifuged for 10 min at 10,000 rpm (Eppendorf 5417R) and 4°C. The upper phase was then transferred into a tube containing 1 mL of chloroform/isoamyl alcohol (24:1), vortexed for 2 min and centrifuged for 10 min at 10,000 rpm and 4°C. Thereafter, the upper phase was pipetted into a new tube containing 1 mL of ice cold isopropanol, mixed well and incubated for 30 min on ice. The nucleic acids were pelleted by centrifugation for 10 min at 14,000 rpm (Eppendorf 5417R) and 4°C, washed once with 70% ethanol (10 min, 14,000 rpm, 4°C), dried at RT for 30 min and finally resuspended in 20 μ L RNase free water. The RNA content of the samples was determined using a NanoDrop (Thermo Scientific, Wilmington, USA) device.

2.2.2.4 Semiquantitative reverse transcription PCR (RT-PCR)

For reverse transcription PCR, two different mastermixes were prepared:

Mastermix 1:

| | |
|--------|--|
| 1.0 µg | RNA |
| 1 µL | oligo dT Primer [0.5 µg µL ⁻¹] |
| 1 µL | dNTPs [10 mM] |
| x µL | ad 12 µL H ₂ O |

Mastermix 1 was denaturated for 5 min at 65°C and subsequently cooled on ice.

Mastermix 2:

| | |
|------|-----------------------------------|
| 4 µL | 5x First-Strand Buffer |
| 2 µL | 0.1 M DTT |
| 1 µL | RNAseOUT [40 U µL ⁻¹] |

Mastermix 1 and 2 were pooled and 1 µL of SuperScript[®] II Reverse Transcriptase [200 U µL⁻¹] was added. Amplification was performed for 50 min at 42°C in a thermomixer and afterwards the reaction was stopped by incubation of the samples at 70°C for 15 min. The generated cDNAs were stored at -20°C. The mRNA expression levels were determined by PCR, optimal annealing temperature for the primers used was identified via gradient PCR. *Gapdh* expression levels were used as control.

PCR mix for semi-quantitative RT-PCR

| | |
|-----------|---|
| 2.0 µL | cDNA sample |
| 2.0 µL | 10x Taq Buffer (+KCl, -MgCl ₂) |
| 1.2 µL | MgCl ₂ [25 mM] |
| 0.4 µL | dNTPs [10 mM] |
| 0.1 µL | forward Primer [100 pM] |
| 0.1 µL | reverse Primer [100 pM] |
| 0.125 µL | native Taq-Polymerase [5 U µL ⁻¹] |
| 14.075 µL | H ₂ O |

PCR program for semi-quantitative RT-PCR

| Temperature [°C] | Time [s] | Repeats |
|------------------|----------|-----------|
| 95 | 300 | 1 cycle |
| 95 | 30 | 10 cycles |
| 48-70 | 30 | 35 cycles |
| 72 | 60 | 35 cycles |
| 72 | 300 | 1 cycle |
| 22 | ∞ | 1 cycle |

RT-PCR Primer

Tgfb1i1 (annealing temperature 58°C)

Tgfb1i1_RT_fwd 5' TTT TGG CCG CTG CCT TTA AC 3'

Tgfb1i1_RT-rev 5' AGG CTT GCA TAC TGT GCT GT 3'

Expected band size: 319 bp for the *WT* allele.

GAPDH (annealing temperature 61°C)

GAPDH_RT_forw 5' GCA AAG TGG AGA TTG TTG CCA T 3'

GAPDH_RT_rev 5' CCT TGA CTG TGC CGT TGA ATT T 3'

Expected band size: 108 bp for the *WT* allele.

2.2.2.5 Agarose gel electrophoresis

The PCR products were separated on 1% agarose gels. In parallel, a marker with a range from 100 to 10,000 bp was run on the gels to control the size of the products. 1.5 g of agarose were added to 150 mL TAE buffer and boiled in microwave for approximately 3 min. The dissolved agarose was allowed to cool down to 60°C, DNA was stained by the addition of 50 $\mu\text{L L}^{-1}$ ethidium bromide or Midori Green™ and the gel was poured into a sleigh containing a comb. The cast gel was then laid into a chamber filled with TAE buffer. The PCR products were diluted in 6x Loading Dye and 20 μL per sample were loaded onto the gels. The samples were separated for 30-45 min at 130 V. For big gels, 4 g agarose was dissolved in 400 mL TAE buffer. The big gels were run at 160 V. Finally, the DNA/ethidium bromide/Midori Green™ was visualized under ultra violet light and pictures were taken with a camera (Herolab GmbH, Germany).

2.2.3 Biochemistry**2.2.3.1 Western blot (Immunoblotting)**

PRP was prepared as described in 2.2.4.1. To remove residual serum albumin, platelets were washed twice with 5 mM EDTA in PBS. For Western blotting, platelet counts of washed platelet were determined using a Sysmex KX 21-N cell analyzer (Sysmex Deutschland GmbH) and counts were adjusted to 1.0×10^6 platelets per μL using lysis buffer. After an incubation time of 10 min on ice, the samples were mixed with an equal volume of reducing 2x Loading Dye and boiled for 5 min at 95°C. The denatured platelet lysates were then separated by sodium dodecyl sulfate (SDS) - polyacrylamide gel electrophoresis (PAGE) and blotted onto polyvinylidenedifluoride (PVDF) membranes. Membranes were incubated with blocking buffer for 1 h at RT and incubated with the respective antibodies overnight at 4°C. For visualization,

horseradish peroxidase-conjugated secondary antibodies and enhanced chemiluminescence solution were used.

2.2.3.2 Protein phosphorylation studies

Washed platelets [$7 \times 10^5 \mu\text{L}^{-1}$] from wild-type and knockout mice were prepared as described in 2.2.4.1. To avoid protein dephosphorylation by phosphatases present in certain preparations of BSA, platelets were washed once with Tyrode's buffer with BSA and all subsequent washing steps were carried out in Tyrode's buffer without BSA. To prevent aggregation, 2 U mL^{-1} apyrase, 5 mM EDTA and $10 \mu\text{M indomethacin}$ were added to the platelet suspension. Platelets were stimulated in suspension with 0.1 U mL^{-1} thrombin, $0.5 \mu\text{g mL}^{-1}$ convulxin, or $2 \mu\text{g mL}^{-1}$ rhodocytin under constant stirring conditions at 37°C . Stimulation was stopped by addition of 1:1 ice cold lysis buffer. Lysates were centrifuged at $14,000 \text{ rpm}$ to remove cell debris. NuPAGE[®] 4x LDS buffer supplemented with β -mercaptoethanol was added to the supernatant. Samples were incubated at 70°C for 10 min and separated by SDS-PAGE on NuPAGE[®] 4-12% Bis-Tris gradient gels (Invitrogen) under reducing conditions. Gels were run in 1x MOPS buffer at 4°C and proteins subsequently transferred onto a PVDF membrane. Membranes were blocked for 1h at RT and then incubated o/n at 4°C with anti-phosphotyrosine antibody, clone 4G10, or with phospho-specific antibodies. Rabbit anti-mouse immunoglobulins-HRP or goat-anti-rabbit-IgG HRP-conjugated antibodies and ECL were used for visualization. Respective non-phosphorylated proteins were used as loading control.

2.2.3.3 Ex vivo sGPVI ELISA

Mice were retroorbitally injected with $2 \mu\text{g g}^{-1}$ bodyweight JAQ1_{biotin} or vehicle. At the indicated time points $100 \mu\text{L}$ of blood was withdrawn from the retro-orbital plexus in $100 \mu\text{L}$ heparin [20 U mL^{-1}]. Plasma was separated by two subsequent centrifugations ($2,800 \text{ rpm}$ and $14,000 \text{ rpm}$, 5 min, RT) and was incubated on JAQ3-coated [$10 \mu\text{g mL}^{-1}$] plates for 1 h at 37°C . After extensive washing, plates were incubated with HRP-labeled streptavidin for 45 min at 37°C and developed using TMB. The reaction was stopped by addition of $2 \text{ N H}_2\text{SO}_4$ and absorbance at 450 nm was recorded on a Multiskan (Thermo Scientific). Plasma from JAQ1_{biotin} treated *Gp6*^{-/-} mice served as control.

2.2.3.4 Protein lysates from tissue

Animals were anesthetized, sacrificed by cervical dislocation and organs were immediately removed, washed once with sterile PBS and cut into small pieces of $\sim 30 \text{ mg}$. The tissue pieces were transferred into $200 \mu\text{L}$ of RIPA buffer, homogenized using a pestle and lysed on ice for 30 min. Cell fragments were pelleted by centrifugation for 10 min at 4°C and $14,000 \text{ rpm}$ (Eppendorf 5417R). The supernatants were transferred to new tubes and protein concentration

was determined by Bio-Rad Bradford assay. Equal amounts of protein were analyzed by Western blot analysis (see 2.2.3.1).

2.2.3.5 Mass spectrometry (MS) analysis of the STIM1 interactome

Experiments were conducted by Dr. Thomas Premisler from the Institute of Physiology, University of Würzburg, Würzburg, Germany. SDS-PAGE of elution samples, gel silver staining, tryptic digestion of differential protein spots and sample preparation for subsequent mass spectrometry (MS) analysis was performed as published previously.¹⁵¹ Tryptic peptides were separated on an Ultimate nano-high performance liquid chromatography (HPLC) system (Dionex, Idstein, Germany) as reported by Premisler *et al.*¹⁵² and directly eluted into the online electrospray ionization (ESI) ion source of a Qtrap 4000 (Applied Biosystems, Darmstadt, Germany) and an LTQ XL (Thermo Fisher Scientific, Dreieich, Germany) mass analyzer, respectively. Full MS survey scans from 350 to 2,000 m/z were acquired and the three most intense peaks were subjected to collision-induced dissociation MS/MS. Mass spectra were recorded via the Analyst 1.4 (QTrap) and the Xcalibur 2.1.0 (LTQ) operating software including the mascot.dll 1.6b5 (QTrap) and the extract_msn (LTQ) plug-in for conversion of LC-MS raw data into Mascot generic format. Applying the Mascot™ search algorithm for MS/MS spectra (Mascot Daemon 2.2.02 software platform and Mascot server version 2.2.04), the generated data were searched against the UniProtKB/ Swiss-Prot database (www.uniprot.org, 11/2009, human subset), with Mascot parameters being set as published.¹⁵² All MS/MS spectra with a minimum Mascot score of 34 (P-value of 0.05) were taken into consideration for further interpretation and were additionally validated manually.

2.2.4 In vitro analysis of platelet function

2.2.4.1 Purification of platelets from whole blood of mice

Mice were bled under isoflurane anesthesia up to 1 mL in 300 μ L heparin [20 U mL⁻¹] or ACD buffer. 300 μ L of heparin [20 U mL⁻¹] were added and the samples were centrifuged for 6 min at 800 rpm. Subsequently, the upper phase and the buffy coat with some erythrocytes were transferred into 300 μ L heparin [20 U mL⁻¹]. To further purify the platelets, centrifugation was repeated (6 min, 800 rpm) and only the upper phase without any erythrocytes was pipetted into a new tube containing 2 μ L of apyrase [0.02 U mL⁻¹, f.c.] and 5 μ L PGI₂ [0.1 μ g mL⁻¹, f.c.]. Platelets were spun down (5 min, 2,800 rpm), resuspended in 1 mL of Tyrode's buffer without Ca²⁺, containing 2 μ L of apyrase [0.02 U mL⁻¹, f.c.] and 5 μ L PGI₂ [0.1 μ g mL⁻¹, f.c.] and allowed to rest for 5 min at 37°C. The washing step was repeated twice, before the pellet was resuspended in an appropriate volume of Ca²⁺-free Tyrode's buffer containing apyrase [0.02 U mL⁻¹, f.c.] and the platelets were allowed to rest for 30 min prior to experiments.

2.2.4.2 Purification of platelets from whole blood of humans and co-localization studies

Fresh blood samples of patients and healthy volunteers were collected in 1/10 volume of ACD and centrifuged for 10 min at 200 g. PRP without any erythrocytes was collected, supplemented with 2 μL of apyrase [0.02 U mL^{-1} , f.c.] and 5 μL PGI₂ [$0.1 \mu\text{g mL}^{-1}$, f.c.], per mL PRP. Prior to immunofluorescence staining, platelets were pelleted by centrifugation for 10 min at 800 g and washed twice with Tyrode's-HEPES buffer containing 2 μL apyrase [0.02 U mL^{-1} , f.c.] and 5 μL PGI₂ [$0.1 \mu\text{g mL}^{-1}$, f.c.]. The samples were allowed to rest for 30 min at 37°C.

For co-localization studies, platelets were fixed on poly-L-Lysine or allowed to spread on fibrinogen without stimulus for 30 minutes. Platelets were stained with phalloidin Atto647N and the indicated antibodies and visualized by confocal microscopy. Co-localization was determined by Pearson's R value with the help of Fiji¹⁴⁸ by thresholding the staining of BIN2 and STIM1 of platelets using the same settings for all samples.

2.2.4.3 Determination of platelet size and count by flow cytometry

50 μL of blood was withdrawn from the retro-orbital plexus in 300 μL heparin [20 U mL^{-1}]. The sample was filled up with 650 μL Tyrode's buffer without Ca²⁺ (1:20 dilution). Platelet count and size were assessed by incubating diluted, heparinized blood with fluorophore-conjugated antibodies directed against platelet-specific epitopes and subsequently analyzed using flow cytometry (FACSCalibur, BD Biosciences). Forward scatter (FSC) and the counts per second were determined. Alternatively, platelet count and size were measured in heparinized blood in a Sysmex analyzer.

2.2.4.4 Assessment of platelet glycoprotein expression by flow cytometry

The expression levels of the most prominent platelet glycoproteins were determined by incubating heparinized blood with fluorophore-conjugated monoclonal antibodies and fluorescence intensities were analyzed by flow cytometry. The expression levels were expressed as mean fluorescence intensity (MFI).

2.2.4.5 Detection of platelet integrin activation and degranulation by flow cytometry

This experiment monitors the signaling-dependent activation of $\alpha\text{IIb}\beta\text{3}$ integrins and the process of degranulation (determined by P-selectin exposure). 50 μL of blood were withdrawn under isoflurane anesthesia, diluted in 300 μL heparin [20 U mL^{-1}] and washed twice (5 min, 2,800 rpm) with 1 mL of Ca²⁺-free Tyrode's buffer. After the final washing step, the washed blood was resuspended in an appropriate volume of Ca²⁺-containing Tyrode's buffer. Washed blood was incubated with fluorophore-conjugated antibodies directed against activated β1 integrins (9EG7-FITC) or $\alpha\text{IIb}\beta\text{3}$ integrins (PE-conjugated JON/A) and against P-selectin

(FITC- labeled WUG 1.9). Subsequently, the samples were activated with different agonists such as ADP, U46619 (a stable thromboxane A₂ analogue), thrombin, CRP and the snake venom toxins convulxin (CVX) and rhodocytin (RC). The reaction was stopped after incubation for 7 min at 37°C and 7 min at RT by the addition of 500 µL PBS.

2.2.4.6 Aggregometry

In aggregometry, light transmission of a washed platelet suspension was monitored over time (10 min) using a four-channel aggregometer (APACT, Laborgeräte und Analysensysteme, Hamburg). 1.5×10^5 platelets per µL in 150 µL Ca²⁺-containing Tyrode's buffer supplied with 100 µg mL⁻¹ human fibrinogen were activated with different concentrations of agonists (1.6 µL, 100-fold-concentrated), specific for GPVI signaling, such as collagen, CRP and CVX, or GPCR-related agonists represented by ADP, U46619 (U46) or thrombin. For stimulation with thrombin, Ca²⁺-containing Tyrode's buffer without human fibrinogen was used. Aggregation studies with ADP were performed in PRP [1.5×10^5 platelets per µL]. Aggregation was expressed as arbitrary units. Light transmission of 160 µL Tyrode's buffer with Ca²⁺ (and fibrinogen) was set as 100% aggregation.

2.2.4.7 Luminometric measurement of ATP release

Washed platelets [80 µL with 5×10^5 platelets µL⁻¹] were diluted into 160 µL Tyrode-HEPES buffer containing 2 mM Ca²⁺ and incubated with Luciferase-Luciferin reagent under stirring conditions (1200 rpm), followed by addition of an agonist. ATP release and aggregation were measured simultaneously in a Lumi-aggregometer (Chrono-Log, Havertown, PA, USA).

2.2.4.8 Platelet adhesion under flow conditions

Rectangular coverslips (24 x 60 mm) were coated overnight at 37°C with 70 µg mL⁻¹ fibrillar type I collagen and prior to the experiment blocked for 1 h with 1% BSA. Mice were bled up to 1 mL in 300 µL heparin [20 U mL⁻¹], the blood was diluted 3:1 with Ca²⁺-containing Tyrode's buffer and incubated for 5 min at 37°C with DyLight-488-conjugated anti-GPIX derivative [0.2 µg mL⁻¹]. A transparent flow chamber with a slit depth of 50 µm was covered with a collagen-coated and BSA-blocked cover slip and perfused for 4 min with the diluted whole blood using a pulse-free pump and different wall shear rates, reflecting the blood flow in different vessel types (1,000 s⁻¹, 1,700 s⁻¹). Subsequently, the chamber was washed for 75 s with Tyrode's buffer at the same shear rate and at least five phase-contrast and fluorescent pictures were taken using a Zeiss Axiovert 200 inverted microscope (40x/0.60 objective) equipped with a CoolSNAP-EZ camera (Visitron). The recorded phase-contrast and fluorescence pictures were analyzed offline using Metavue software.

2.2.4.9 Analysis of phosphatidylserine (PS)-exposing platelets

Under flow conditions:

Rectangular cover slips (24 x 60 mm) were coated with 200 $\mu\text{g mL}^{-1}$ fibrillar type I collagen (Horm) and blocked with 1% BSA. Heparinized whole blood was supplemented with additional 5 U mL^{-1} heparin and perfused over collagen coated coverslips through transparent flow chamber at a shear rate of 1000 s^{-1} as described above. The flow chamber was rinsed for 4 min with Tyrode-HEPES buffer containing 2 mM CaCl_2 , 5 U mL^{-1} heparin, and 0.25 $\mu\text{g mL}^{-1}$ annexin A5-DyLight 488. The flow chamber was rinsed for additional 2 min with Tyrode-HEPES buffer supplemented with 2 mM CaCl_2 and 5 U mL^{-1} heparin, before phase-contrast and fluorescence images were obtained using a Zeiss Axiovert 200 inverted microscope (40x objective, NA = 0.75; Zeiss Oberkochen, Germany) and analyzed offline using Metavue software (Visitron, Puchheim, Germany). Procoagulant activity was defined as the ratio of surface coverage of PS-exposing platelets (annexin A5-DyLight 488 staining of platelets) to the total surface covered by platelets.

Under static conditions:

Washed platelets were diluted into Tyrode-HEPES buffer containing 2 mM CaCl_2 [50 μL with 0.5×10^5 platelets μL^{-1}] and incubated with agonists for 15 min at 37°C in the presence of saturating amounts of Alexa F488-coupled annexin A5. Reactions were stopped by the addition of 500 μL Tyrode-HEPES buffer containing 2 mM Ca^{2+} , data were immediately collected on a FACSCalibur (BD Biosciences, Heidelberg, Germany) and analyzed using FlowJo v7 software (FlowJo, LLC, Ashland OR, USA).

2.2.4.10 Platelet spreading on fibrinogen

The ability of platelets to adhere and form filopodia and lamellipodia on a fibrinogen-coated surface, in response to thrombin, was assessed by a spreading assay. Rectangular coverslips (24 x 50/60 mm) were coated with 10 μg human fibrinogen [100 μL of 100 $\mu\text{g mL}^{-1}$] overnight at 4°C in a humid chamber. Slides were blocked with 1% BSA in PBS for 1 h at RT. 30 μL of washed platelets [3×10^5 per μL] were mixed with 70 μL Tyrode's buffer containing 2 mM Ca^{2+} , activated with 0.01 U mL^{-1} thrombin and immediately allowed to spread on the fibrinogen-coated coverslips at RT. After different time intervals, the adherent platelets were fixed with 300 μL 4% PFA for 5 min and differential interference contrast (DIC) microscopy pictures were taken using an inverted microscope Zeiss HBO 100 (Axiovert 200M, Zeiss). For analysis, the phase abundance of the different spreading stages (1, resting; 2, formation of filopodia; 3, formation of filopodia and lamellipodia; 4, fully spread) was determined.

2.2.4.11 Platelet spreading on von Willebrand factor

The involvement of GPIb signaling during spreading was specifically addressed by allowing platelets [3×10^5 per μL] to spread on a vWF matrix. Coverslips were coated overnight at 4°C with anti-human vWF antibody [$4 \mu\text{g mL}^{-1}$], blocked for 1 h with 1% BSA in PBS and afterwards incubated with 100 μL heparinized mouse plasma for 2 h at 37°C . 30 μL washed platelets [0.3×10^6 per μL] were mixed with 70 μL Ca^{2+} -containing Tyrode's buffer and incubated for 10 min with integrilin [$40 \mu\text{g mL}^{-1}$] to block $\alpha\text{IIb}\beta_3$ integrins. Platelets were stimulated with botrocetin [$2 \mu\text{g mL}^{-1}$] to enhance GPIb binding and allowed to adhere. Spreading was stopped after the respective time points by the addition of 300 μL 4% PFA in PBS. Analysis was performed by DIC microscopy.

2.2.4.12 Platelet clot retraction

Mice were bled up to 700 μL in 70 μL sodium citrate [0.129 mM] and PRP was isolated by centrifugation at 1,800 rpm for 5 min. Plasma was collected and platelets were resuspended in 1 mL Ca^{2+} -free Tyrode's buffer supplemented with 2 μL of apyrase [0.02 U mL^{-1} , f.c.] and 5 μL PGI_2 [$0.1 \mu\text{g mL}^{-1}$, f.c.]. Platelet count was determined and 7.5×10^7 platelets were resuspended in 250 μL plasma. PRP [3×10^5 platelets per μL] was recalcified by adding 20 mM CaCl_2 and supplemented with 1 μL of red blood cells to visualize the clot. Clot formation was initiated by the addition of 4 U mL^{-1} thrombin (Sigma). Clot formation and retraction was recorded up to 4 h and the residual serum volume was determined.

2.2.4.13 Measurement of inositol-1-phosphate (IP_1)

Washed platelets were adjusted to the final concentration of $0.6 \times 10^6 \mu\text{L}^{-1}$ in a modified phosphate-free Tyrode's buffer containing 50 mM LiCl_2 , 2 mM Ca^{2+} , indomethacin [10 μM] and apyrase [2 U mL^{-1}] were also added. Platelets were activated with the indicated agonists for 5 minutes at 37°C with constant shaking at 450 rpm. After stimulation, platelets were lysed in the buffer supplied with the kit. 50 μL of lysed platelets were used for the IP_1 ELISA assay according to the manufacturer's protocol (Cisbio, France).

2.2.4.14 Intracellular calcium measurements

Platelet intracellular Ca^{2+} measurements were performed as described.⁷⁸ Platelets isolated from whole blood (see 2.2.4.1) were washed and suspended in Tyrode's buffer without Ca^{2+} . Washed platelets [$2 \times 10^5 \mu\text{L}^{-1}$] were loaded with Fura-2/AM [5 μM] in the presence of Pluronic F-127 [0.2 $\mu\text{g mL}^{-1}$] for 30 minutes at 37°C . After 30 minutes platelets were washed and resuspended in Tyrode's buffer containing no or 1 mM Ca^{2+} . Stirred platelets were activated with different agonists, and fluorescence was measured with a LS 55 fluorimeter (PerkinElmer, Rodgau, Germany). Excitation was alternated between 340 and 380 nm, and

emission was measured at 509 nm. Each measurement was calibrated using Triton X-100 and EDTA.

2.2.4.15 Thrombin generation assay

Thrombin generation was quantified in citrate-anticoagulated PRP [1×10^8 platelets μL^{-1}]. PRP preparations were pooled from 2-4 mice with the same genotype. To activate platelets, the samples were incubated with CRP [$20 \mu\text{g mL}^{-1}$] or ionomycin [$20 \mu\text{M}$] for 10 min at 37°C . After stimulation, samples (4 vol) were transferred to a polystyrene 96-well plate already containing 1 vol of thrombin calibrator or PRP reagent (20 mM HEPES, 140 mM NaCl, 0.5% BSA, 18 pM tissue factor [3 pM f.c.]). Coagulation was started by adding 1 vol fluorescent thrombin substrate (2.5 mM Z-GGR-AMC, 20 mM HEPES, 140 mM NaCl, 200 mM CaCl_2 , and 6% BSA). Thrombin generation was measured according to the calibrated automated thrombogram method.^{149,150} Samples were run in duplicates.

2.2.5 *In vivo* analysis of platelet function

2.2.5.1 Tail bleeding time

Mice were anesthetized by intraperitoneal injection of triple narcotics (Midazolam [$5 \mu\text{g g}^{-1}$], Medetomidine [$0.5 \mu\text{g g}^{-1}$], Fentanyl [$0.05 \mu\text{g g}^{-1}$]) and a 1 mm segment of the tail tip was removed using a scalpel. Tail bleeding was monitored by gently absorbing blood on filter paper at 20 s intervals without making contact with the wound site. Bleeding was determined to have ceased when no blood was observed on the paper. When indicated, acetylsalicylic acid (ASA) [$1 \mu\text{g g}^{-1}$ bodyweight] was administered to the animals prior to the experiment. Experiments were stopped after 20 min by cauterization and anesthesia was antagonized by injection of Atipam [$2.5 \mu\text{g g}^{-1}$], Flumazenil [$0.5 \mu\text{g g}^{-1}$] and Naloxon [$1.2 \mu\text{g g}^{-1}$]. For the saline model, 1 mm of the tail tip was amputated, and the tails were immersed in 0.9% isotonic saline at 37°C . The time to complete arrest of bleeding (no blood flow for 1 minute) was determined.

2.2.5.2 FeCl_3 -induced injury of mesenteric arterioles

The mesentery of 3- to 4-week old anesthetized mice (ketamine/xylazine [$100/5 \text{ mg kg}^{-1}$]) was exposed by a midline abdominal incision. Endothelial damage in mesenteric arterioles was induced by application of a 3 mm^2 filter paper soaked with 20/13% FeCl_3 . Arterioles were visualized using a Zeiss Axiovert 200 inverted microscope equipped with a 100-W HBO fluorescent lamp source and a CoolSNAP-EZ camera (Visitron). Digital images were recorded and analyzed using the Metavue software. Adhesion and aggregation of fluorescently labeled platelets (Dylight-488-conjugated anti-GPIX derivative) was monitored until complete occlusion occurred (blood flow stopped for > 2 min). Experiments were performed by Ina Thielmann (Hic-5) or Martina Morowski (RhoA/Rac1 KO) in our laboratory.

2.2.5.3 Mechanical injury of the abdominal aorta

The abdominal cavity of 8-12-weeks-old anesthetized mice was opened by a longitudinal incision. An ultrasonic flow probe (Transonic Flowprobe 0.5, Transonic Systems) was placed around the exposed abdominal aorta. Thrombosis was induced by a single firm compression using forceps. Blood flow was monitored until complete blood vessel occlusion occurred for a minimum of 5 min. Otherwise the experiment was stopped after 30 min. When indicated, ASA [$1 \mu\text{g g}^{-1}$ bodyweight] was administered to the animals prior to the experiment. Aorta injury experiments were performed and evaluated by Martina Morowski (RhoA/Rac1 KO) or Karen Wolf (BIN2 KO) in our research group.

2.2.5.4 Determination of platelet life span

The clearance of platelets from the circulation was determined by the retro-orbital injection of $5 \mu\text{g}$ DyLight 488-labeled anti-GPIX derivative in PBS into mice. The percentage of labeled platelets was determined by daily blood withdrawal ($50 \mu\text{L}$) and subsequent analysis by flow cytometry.

2.2.5.5 Macrophage depletion with Clodronate

Anesthetized mice were retroorbitally injected with clodronate-encapsulated or PBS-encapsulated liposomes [$2 \mu\text{L g}^{-1}$ body weight].

2.2.5.6 Transient middle cerebral artery occlusion (tMCAO) model

Experiments were conducted by Dr. Michael Schuhmann from the Department of Neurology, University Hospital of Würzburg, Würzburg, Germany, according to the recommendations for research in mechanism-driven basic stroke studies.¹⁵³ tMCAO was induced in 8-12-weeks-old mice under inhalation anesthesia using the intraluminal filament technique.¹⁵⁴ Briefly, a midline neck incision was made and a standardized silicon rubber-coated 6.0 nylon monofilament (6021PK10, Docol, Redlands, CA, USA) was inserted into the right common carotid artery and advanced via the internal carotid artery to occlude the origin of the middle cerebral artery. After 60 min, the filament was removed to allow reperfusion. 24 h after tMCAO the global neurological status was assessed using the Bederson score.¹⁵⁵ Motor function and coordination were evaluated using the grip test.¹⁵⁶ For determination of the ischemic brain infarct volume, mice were euthanized 24 h after induction of tMCAO and brain sections were stained with 2% 2,3,5-triphenyltetrazolium chloride (TTC). Planimetric measurements were performed using ImageJ software to calculate lesion volumes, which were corrected for brain edema as described.¹⁵⁷

2.2.5.7 Whole-body *in vivo* imaging of mice

Mice were injected with $8 \mu\text{g}$ anti-GPIX- Alexa Fluor 750-conjugated antibody to label circulating platelets. After 4 hours, the mice were anesthetized with medetomidine [$0.5 \mu\text{g g}^{-1}$],

midazolam [$5 \mu\text{g g}^{-1}$] and fentanyl [$0.05 \mu\text{g g}^{-1}$ body weight] and the abdominal and thoracic region was shaved with an electric clipper. Subsequently, JAQ1 [$2 \mu\text{g g}^{-1}$] or MWReg30 [$0.8 \mu\text{g g}^{-1}$] was injected and *in vivo* imaging was performed using an *in vivo* imaging system (IVIS Spectrum, Perking Elmer) at 800 nm (emission filter).

2.2.6 Histology

2.2.6.1 Immunohistochemistry (IHC) and immunofluorescence (IF) staining on liver cryosections

Liver samples were embedded in Tissue-Tek (Sakura Finetek) and snap-frozen in liquid nitrogen. Samples were stored at -80°C until further processing. (CM1900, Leica) and immobilized on glass slides. $5 \mu\text{m}$ thick cryosections were prepared using a cryostat (CM1900, Leica) and immobilized on glass slides. The sections were fixed with ice cold acetone (-20°C) for 20 min, air dried, washed three times (5 min) in PBS.

For IHC stainings, endogenous peroxidase was blocked by incubation for 20 min with 0.03% H_2O_2 in PBS. Thereafter, the sections were incubated for 1 h at RT with blocking buffer and stained for 2 h at RT with a 1:1 mixture of HRP-labeled 15E2 and 3G6 anti-GPIb antibodies (1:750 in blocking buffer). After three washing steps in PBS (each 5 min) detection was carried out using AEC as substrate. Staining intensity was controlled by observing the slides through a light microscope. When the desired intensity was reached, the slides were washed with PBS for 5 min to stop the staining and counterstaining with hematoxylin and blueing in tap water (appr. 10 min) was carried out. Analysis was performed with an inverted Leica DMI 4000 B microscope.

For IF stainings, unspecific binding was blocked by preincubation with 3% BSA/PBS for 1 h at RT. For staining of endothelium and platelets, sections were incubated with anti-CD105-Alexa Fluor 647-conjugated antibody (Biolegend) and anti-GPIb-Alexa Fluor 488-conjugated antibody, respectively. Nuclei were stained with DAPI. Samples were visualized with confocal microscopy (Leica TCS-SP5). Images were further processed using Image J software (National Institute of Health, USA).

2.2.7 Microscopy

2.2.7.1 Confocal microscopy

Subsequent to the spreading assays on fibrinogen, platelets were fixed and permeabilized in PHEM complete buffer for 20 min at RT and blocked for 2 h at 37°C with 5% BSA in PBS. The platelets were further incubated for at least 1 h with respective antibodies and Atto647N-conjugated phalloidin to stain for F-actin. After intense washing unlabeled primary antibodies were detected with the respective fluorophore-conjugated secondary antibodies. Samples were mounted with Fluoroshield. Visualization was performed with a Leica TCS SP5 confocal

microscope (Leica Microsystems). To visualize the cytoskeleton of resting platelets, 50 μL washed platelets [$5 \times 10^5 \mu\text{L}^{-1}$] were mixed with 50 μL PHEM complete buffer and allowed to adhere to poly-L-lysine-coated coverslips and processed as described above. Images were further processed using Image J software (National Institute of Health, USA).

2.2.7.2 TEM of platelets

Platelets ultrastructure was investigated by TEM. PRP was prepared and mixed in a 1:2 ratio with 5% glutaraldehyde in PBS for 10 min at 37°C and for 1 h at RT. Platelets were spun down at 1,500 g for 5 min, washed three times with cacodylate buffer and incubated for 1 h at RT with 1% OsO_4 in cacodylate buffer. Afterwards, the samples were washed twice with cacodylate buffer and $\text{H}_2\text{O}_{\text{bidest}}$ and 2% uranyl acetate (in H_2O) was added for 1 h at 4°C. Then, platelets were dehydrated by a graded ethanol series (3x 70%, 5 min; 3x 95%, 15 min; 3x 100%, 15 min), incubated twice for 10 min with propylenoxide and afterwards transferred in a 1:1 mixture of propylenoxide and epon for 1 h under rotation. After this step, epon was added and samples were incubated overnight at RT. Epon was allowed to harden for 48 h at 60°C. Ultrathin sections were prepared, stained with 2% uranyl acetate (in ethanol) and lead citrate (in H_2O) and examined at 80 kV under a EM900 (Zeiss).

2.2.8 Data analysis

Results are shown as mean \pm standard deviation (SD) from three independent experiments per group, unless indicated otherwise. Statistical analysis was conducted using the Student's t-test, apart from the Fischer's exact test which was applied to assess variance between non-occluded vessels in models of arterial thrombosis or in tail bleeding assays and the Mann-Whitney U test which was used for analysis of Bederson score and grip test after tMCAO. Differences between more than two groups were analyzed with one-way ANOVA with Dunnett's T3 as post-hoc test, with SPSS 21. P-values < 0.05 were considered statistically significant.

3 Results

3.1 Bridging integrator 2 (BIN2) controls store-operated calcium entry in platelets and thrombotic and thrombo-inflammatory activity in mice

3.1.1 BIN2 interacts with STIM1 in platelets

To study the molecular mechanisms controlling SOCE in platelets, a screen for STIM1 binding partners in human platelets was performed. Resting human platelets were isolated from healthy donors and lysed under native conditions. For each interaction experiment, platelet lysates of two different donors were pooled and incubated with purified recombinant STIM1-C-tail protein bound to the Affi-Gel 10 affinity matrix (STIM1-C-tail affinity column, SC). Incubation of equal volumes of pooled platelet lysates with uncoupled affinity column served as control (Ctrl). Bound platelet proteins were finally eluted by applying a stepwise pH gradient ranging from pH 6.0 to 2.0. Unspecific protein binding was efficiently reduced by washing with 10 column volumes (CV) PBS and by application of 3 CV glycine/ HCl pH 6.0 (i.e. the first elution step). Specifically bound proteins were finally released from the affinity supports by addition of 3 CV glycine/ HCl pH 2.0. The eluted fractions of both affinity columns were differentially analyzed by SDS-PAGE and subsequent silver staining (Figure 8 A). Comparing the pH 2.0 fractions of three independent biological replicates, differential protein bands were reproducibly detected in the SC versus the Ctrl samples. For identification of these putative STIM1-C-tail interaction partners in resting human platelets, the respective protein bands were excised, tryptically digested and nano-scale liquid chromatographic electrospray ionization tandem mass spectrometry (nano-LC-ESI-MS/MS) was performed. The data obtained by nano-LC-ESI-MS/MS analyses of all differential protein bands of SC versus Ctrl human platelet samples (i.e. three biological replicates) were searched against the UniProtKB/ Swiss-Prot human subset. BIN2 (UniProtKB/ Swiss-Prot accession number: Q9UBW5-1) was identified with a Mascot score of 179 (Figure 8 A). These studies identified BIN2 as a direct or indirect STIM1 interaction partner and were further substantiated by confocal microscopy analysis demonstrating substantial co-localization between STIM1 and BIN2 in resting platelets (Figure 8 B, C) of two healthy donors, with a Pearson's R value of 0.62 ± 0.04 (N = 250).

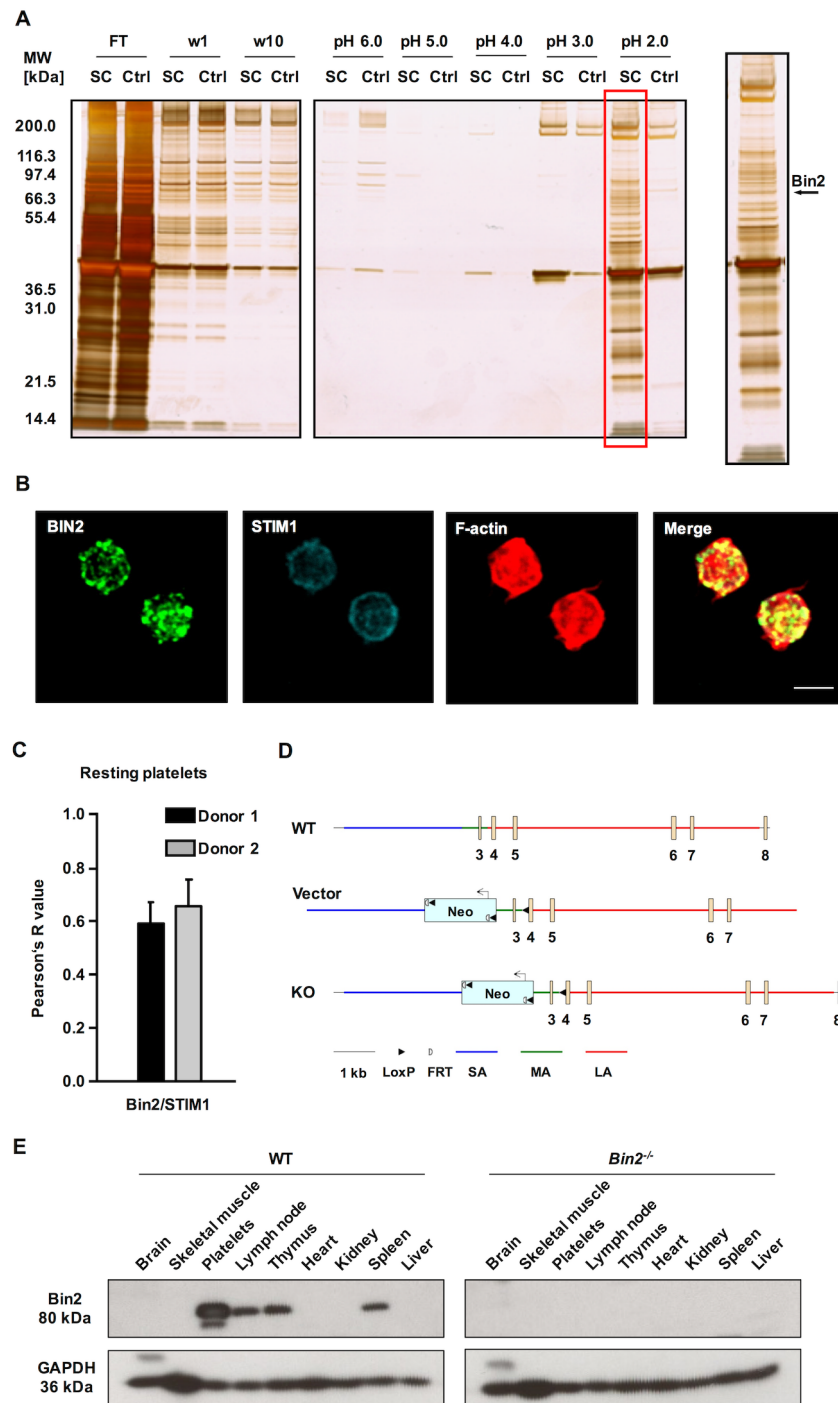


Figure 8: Interaction of native lysates of resting human platelets with the STIM1-C-tail affinity column (SC) vs control column (Ctrl). (A) Control by differential SDS-PAGE (10% Bis-Tris gels, silver staining). FT: column flow through (5 μ L); w1, w10: first and last wash fractions (20 μ L); pH 6.0 - pH 2.0: pooled glycine/ HCl elution fractions (20 μ L). Reproducibly detectable, differential protein bands were excised, tryptically digested and nano-LC-ESI-MS/MS was performed. Arrow indicates protein band, where BIN2 was identified (UniProtKB/ Swiss-Prot accession number: Q9UBW5-1) with a Mascot score of 179. Experiments were conducted by Dr. Thomas Premisler from the Institute of Physiology, University of Würzburg, Würzburg, Germany. (B) Washed human platelets were fixed on poly-L-lysine and stained for BIN2 (green), STIM1 (cyan) and F-actin (red). Representative confocal microscopy images of 2 individuals are shown. Scale bar = 2.5 μ m. (C) Co-localization (Pearson's R value) was determined by thresholding the staining of BIN2 and STIM1 of platelets using the same settings for all samples using Fiji¹⁴⁸ (Donor 1: N = 148; Donor 2: N= 102). (D) Targeting of the *Bin2* locus. Exon 3 was flanked by two loxP sites. (E) Western blot analysis of different tissue lysates in WT and *Bin2*^{-/-} mice. GAPDH served as loading control. SA, short homology arm; MA, target region; LA, long homology arm; WT, wild-type; LN, Lymph node.

3.1.2 BIN2 KO mice are viable and fertile, but display a mild macrothrombocytopenia

To study the function of BIN2 *in vivo*, a KO mouse strain was generated by intercrossing *Bin2^{fl/fl}*, in which exon 3 was flanked by loxP sites, with deleter-Cre mice under the control of the human cytomegalovirus (CMV) promoter.¹⁴⁴ Exon 3 was efficiently deleted giving rise to germline *Bin2* knockout mice. Homozygous *Bin2^{-/-}* mice were born at a normal Mendelian ratio, were viable and fertile and appeared overall healthy. Western blot analysis confirmed strong expression of BIN2 in WT platelets, spleen, lymph nodes and thymus and a complete absence of the protein in the respective tissues of *Bin2^{-/-}* mice (Figure 8 E). Although histological analyses of major organs, including bone marrow and spleen showed no obvious alterations in *Bin2^{-/-}* mice, the animals displayed a mild macrothrombocytopenia, and slightly reduced basic blood cell parameters compared to WT controls (Table 1).

Table 1: Basic blood and platelet parameters in BIN2 knockout mice. Platelet count and size and basic blood parameters were analyzed using a blood cell counter (Sysmex KX-21NTM Hematology Analyzer). N = 30, *P<0.05, **P<0.01, ***P<0.001. WT, wild-type; Plt, platelets; MPV, mean platelet volume; WBC, white blood cells; RBC, red blood cells; HCT, hematocrit; n.s., non significant.

| | <i>Bin2^{fl/fl}</i> | <i>Bin2^{fl/fl} Pf4-Cre</i> (P) | <i>Bin2^{-/-}</i> (P) |
|--|-----------------------------|---|-------------------------------|
| Plt [$\times 10^3 \mu\text{L}^{-1}$] | 899.7 \pm 175.1 | 759.6 \pm 149.4 (**) | 556.5 \pm 70.1 (***) |
| MPV [fL] | 5.39 \pm 0.20 | 5.60 \pm 0.32 (**) | 5.64 \pm 0.17 (***) |
| WBC [$\times 10^3 \mu\text{L}^{-1}$] | 11.3 \pm 3.4 | 11.0 \pm 3.1 (n.s.) | 9.7 \pm 2.9 (*) |
| RBC [$\times 10^6 \mu\text{L}^{-1}$] | 8.9 \pm 1.0 | 8.7 \pm 1.3 (n.s.) | 8.3 \pm 0.9 (*) |
| HCT [%] | 46.4 \pm 4.2 | 47.1 \pm 5.1 (n.s.) | 43.7 \pm 4.2 (*) |

These findings were confirmed in megakaryocyte-/platelet-specific BIN2 KO mice which were generated by intercrossing *Bin2^{fl/fl}* mice with Pf4-Cre mice¹⁴⁵ (Figure 8 D and Table 1) and used for all further studies. Despite the mild macrothrombocytopenia, BIN2-deficient platelets displayed an unaltered life span, ultrastructure and expression levels of prominent major surface glycoproteins, except for a slight reduction of CD9 expression (Table 2 and Figure 9). Immunofluorescence confocal microscopy of resting platelets showed an inhomogeneous distribution of BIN2 in the cytoplasm (Figure 9 C top) of WT platelets, whereas no staining was detectable in *Bin2^{fl/fl} Pf4-Cre* platelets. In spread WT platelets, BIN2 mainly located to the cell center (Figure 9 C bottom).

These data showed that BIN2 is dispensable for embryonic development, but indicated a role of the adapter protein in platelet homeostasis.

Table 2: Surface expression levels of platelet glycoproteins in WT and *Bin2^{fl/fl Pf4-Cre}* mice. Expression of glycoproteins on the platelet surface was determined by flow cytometry. Diluted whole blood was incubated with FITC-labeled antibodies at saturating concentrations for 15 minutes at room temperature, and platelets were analyzed immediately. Data are expressed as mean fluorescence intensity (MFI) \pm SD of 3 independent experiments, $N \geq 4$. * $P < 0.05$; WT, wild-type; CLEC-2, C-type lectin-like receptor 2; n.s., non significant.

| | WT | <i>Bin2^{fl/fl Pf4-Cre}</i> | P |
|------------------------|--------------|-------------------------------------|------|
| GPV | 220 \pm 12 | 209 \pm 14 | n.s. |
| GPIb | 264 \pm 20 | 254 \pm 15 | n.s. |
| GPIX | 338 \pm 13 | 320 \pm 20 | n.s. |
| CD9 | 760 \pm 74 | 657 \pm 25 | * |
| GPVI | 40 \pm 5 | 39 \pm 2 | n.s. |
| CLEC-2 | 100 \pm 4 | 93 \pm 5 | n.s. |
| α IIb β 3 | 423 \pm 26 | 392 \pm 17 | n.s. |
| α 2 | 43 \pm 4 | 41 \pm 2 | n.s. |
| β 1 | 113 \pm 3 | 107 \pm 5 | n.s. |

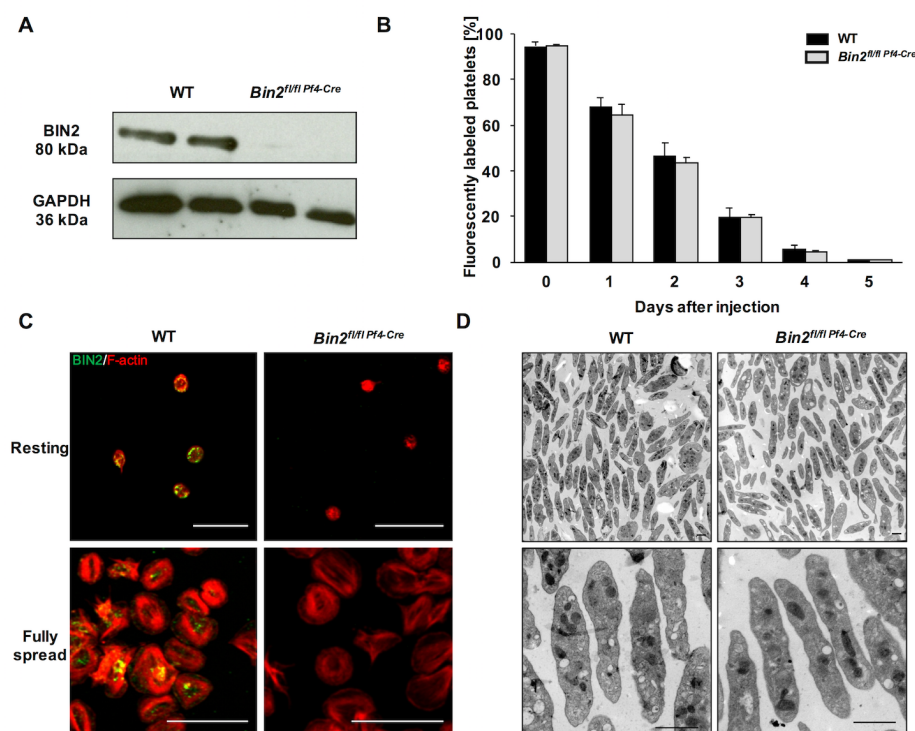


Figure 9: BIN2 is expressed in murine platelets. (A) BIN2 expression in murine platelets was assessed by Western blot analysis. GAPDH served as loading control. (B) Platelet life span was determined by flow cytometric assessment of the percentage of fluorescently labeled platelets in WT and *Bin2^{fl/fl Pf4-Cre}* mice during a 5-day period after intravenous injection of a Dylight-488 anti-GPIX immunoglobulin derivative [0.5 mg kg^{-1} ; $N = 5$] (C) Washed WT and *Bin2^{fl/fl Pf4-Cre}* platelets were fixed on poly-L-lysine (top) or allowed to spread on fibrinogen after stimulation with 0.01 U mL^{-1} thrombin for 30 minutes (bottom). Platelets were stained for BIN2 (green) and F-actin (red). Representative confocal microscopy images are shown. Scale bar = $10 \mu\text{m}$. (D) Representative transmission electron microscopy (TEM) pictures of resting WT and *Bin2^{fl/fl Pf4-Cre}* platelets. Scale bar = $1 \mu\text{m}$. WT, wild-type.

3.1.3 Defective SOCE in BIN2-deficient platelets

To study the role of BIN2 in platelet Ca^{2+} homeostasis, intracellular calcium measurements in *Bin2^{fl/fl} Pf4-Cre* and WT platelets were performed. Ca^{2+} store release evoked by the sarcoplasmic/ER Ca^{2+} ATPase (SERCA) pump inhibitor thapsigargin (TG, [0.1 μM]) was indistinguishable between WT and mutant platelets (WT: 51 ± 14 nM; *Bin2^{fl/fl} Pf4-Cre*: 42 ± 9 nM; $P = 0.14$; $N = 9$) (Figure 10 A). Remarkably, the subsequent SOCE was significantly diminished in the absence of BIN2 (WT: 1157 ± 358 nM; *Bin2^{fl/fl} Pf4-Cre*: 717 ± 215 nM; $P = 0.006$; $N = 9$) (Figure 10 B, C). Next, agonist-evoked Ca^{2+} responses were studied. In the presence of extracellular Ca^{2+} , a pronounced Ca^{2+} influx was detectable in WT platelets, which was markedly reduced by in *Bin2^{fl/fl} Pf4-Cre* platelets in all tested conditions (Figure 10 D, E). Together, these results demonstrated that BIN2 is essential for efficient SOCE in platelets, indicating that it might modulate STIM1-dependent activation of the platelet SOC channel, Orai1. Of note, expression of STIM1 was unaltered in *Bin2^{fl/fl} Pf4-Cre* platelets compared to WT controls (Figure 10 F, G).

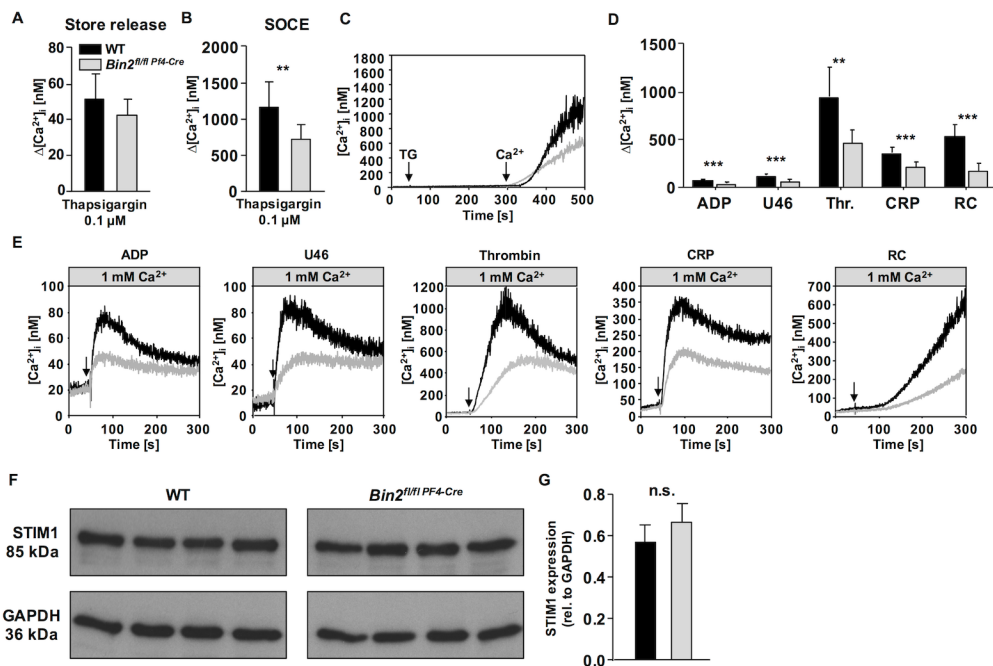


Figure 10: Reduced (hem)ITAM induced Ca^{2+} mobilization in *Bin2^{fl/fl} Pf4-Cre* platelets. (A-C) Statistical evaluation of store release (A) and SOCE (B) and representative curves (C) after treatment with thapsigargin ($N = 9$). (D, E) Time course of intracellular Ca^{2+} mobilization in response to ADP [5 μM], U46 (U46619, [3 μM]), thrombin [0.1 U mL^{-1}], collagen-related peptide (CRP, [1 $\mu\text{g mL}^{-1}$]), and rhodocytin (RC, [0.25 $\mu\text{g mL}^{-1}$]). Addition of agonists is indicated by an arrow. The experiments were performed in the presence of extracellular Ca^{2+} to measure Ca^{2+} influx. Statistical evaluation (D) and representative curves (E) ($N \geq 7$) are shown. (F, G) Expression levels of STIM1 in WT and *Bin2^{fl/fl} Pf4-Cre* mice. (F) Western blot analysis of STIM1 and GAPDH expression and (G) statistical evaluation of STIM1 expression relative to GAPDH expression are shown. Bars represent mean \pm SD. * $P < 0.05$; ** $P < 0.01$; *** $P < 0.001$. WT, wild-type; n.s., non significant.

3.1.4 Defective (hem)ITAM-mediated activation of *Bin2^{fl/fl} Pfl4-Cre* platelets

To investigate functional consequences of the defective SOCE in *Bin2^{fl/fl} Pfl4-Cre* platelets, flow cytometric analysis of agonist induced integrin α IIb β 3 activation using the JON/A-PE antibody¹⁴² and P-selectin surface exposure as a marker of α -granule release (Figure 11 A, B) was performed. Activation of *Bin2^{fl/fl} Pfl4-Cre* platelets was normal in response to the G-protein-coupled receptor agonists ADP, thrombin and the stable TxA₂ analog U46619. In sharp contrast, the response of *Bin2^{fl/fl} Pfl4-Cre* platelets to GPVI-specific agonists (CRP, convulxin) was markedly decreased compared to WT controls. Similar observations were made upon stimulation with the snake venom toxin rhodocytin which signals via the (hem)ITAM receptor C-type lectin-like receptor 2 (CLEC-2).

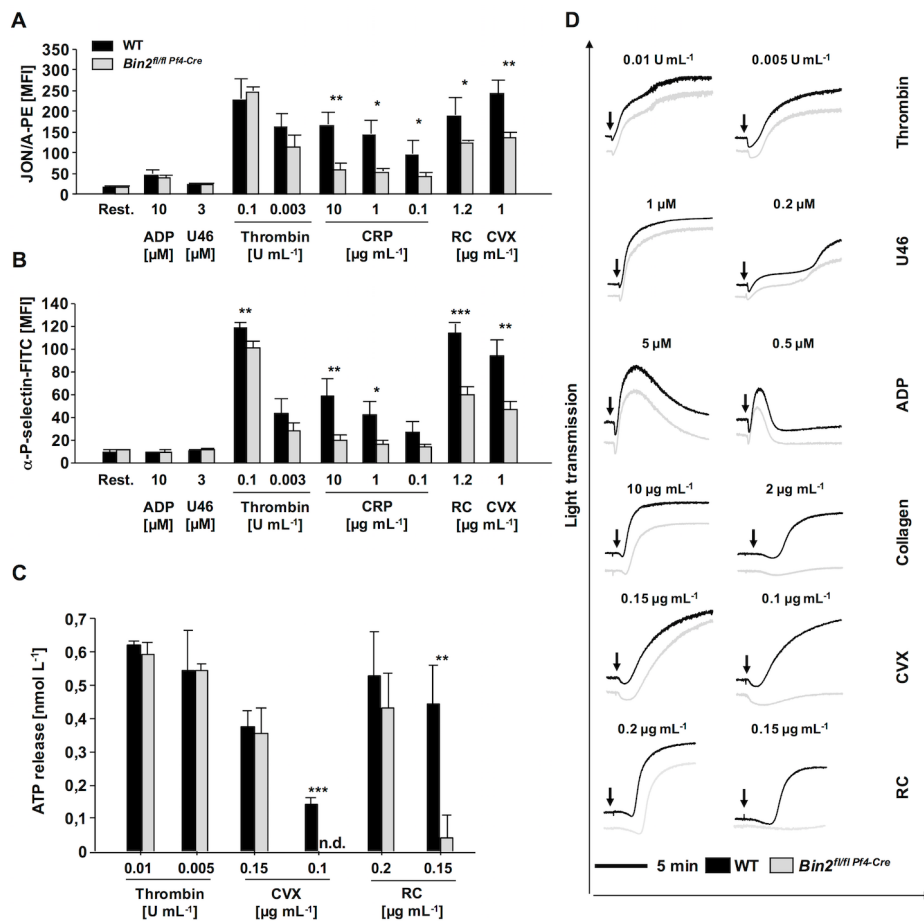


Figure 11: Reduced integrin activation, aggregation and degranulation in *Bin2^{fl/fl} Pfl4-Cre* platelets upon (hem)ITAM stimulation. (A,B) Flow cytometric analysis of (A) integrin α IIb β 3 activation (binding of JON/A-PE) and (B) degranulation-dependent P-selectin exposure in WT and *Bin2^{fl/fl} Pfl4-Cre* platelets in response to the indicated agonists. Results are presented as MFI \pm SD of 3 independent experiments, N \geq 4. (C) Washed platelets were incubated with luciferase-luciferin reagent followed by agonist addition. ATP release was measured on a lumi-aggregometer. The concentration of released ATP is given as mean \pm SD and is representative of 2 independent experiments, N = 4. (D) Washed platelets were stimulated with the indicated agonists, and light transmission was recorded using a four channel aggregometer. Representative aggregation curves of 3 independent experiments are shown, N = 4. WT, wild-type; CRP, Collagen-related peptide; RC, Rhodocytin; CVX, Convulxin; n.d., not detectable *P<0.05; **P<0.01; ***P<0.001.

In line with the decreased integrin activation following (hem)ITAM stimulation, aggregation and dense granule release of *Bin2^{fl/fl} Pfl4-Cre* platelets in response to stimulation with (hem)ITAM-specific agonists was reduced, which was best evident at low agonist concentrations (Figure 11 C, D).

To assess if the reduced (hem)ITAM-mediated activation was a consequence of defective SOCE or caused by defects in different platelet signaling pathways, changes in tyrosine phosphorylation patterns in response to thrombin [0.1 U mL^{-1}], convulxin [$0.5 \text{ } \mu\text{g mL}^{-1}$] and rhodocytin [$2 \text{ } \mu\text{g mL}^{-1}$] were analyzed by Western blotting. The general tyrosine phosphorylation pattern (Figure 12 A) and the changes in tyrosine phosphorylation of the key signaling molecules Syk, linker for activation of T cells (LAT) and PLC γ 2 upon stimulation with convulxin [$0.5 \text{ } \mu\text{g mL}^{-1}$] were indistinguishable between WT and *Bin2^{fl/fl} Pfl4-Cre* platelets (Figure 12 B). Likewise, PLC activity, as assessed by an IP $_3$ ELISA, was similar in WT and *Bin2^{fl/fl} Pfl4-Cre* platelets which together with the unaltered Ca $^{2+}$ store release upon TG stimulation (Figure 10) demonstrated that the (hem)ITAM activation defect was not caused by impaired signaling upstream of PLC γ 2 (Figure 12 C).

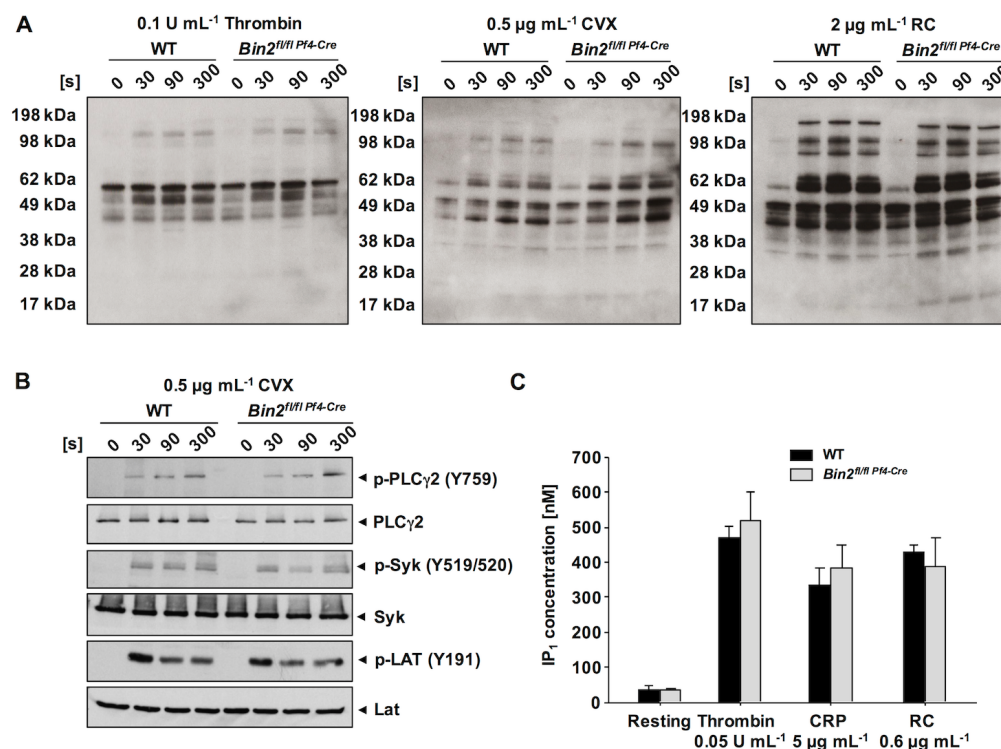


Figure 12: Unaltered tyrosine phosphorylation and PLC γ 2-activity in *Bin2^{fl/fl} Pfl4-Cre* platelets. (A) Washed platelets [$7 \times 10^5 \text{ } \mu\text{L}^{-1}$] were stimulated with 0.1 U mL^{-1} thrombin, $0.5 \text{ } \mu\text{g mL}^{-1}$ convulxin (CVX), or $2 \text{ } \mu\text{g mL}^{-1}$ rhodocytin (RC) for the indicated time points and subsequently lysed with IGEPAL[®] CA-630. Whole-cell lysates were Western blotted and probed with the anti-phosphotyrosine antibody 4G10. (B) Washed platelets [$7 \times 10^5 \text{ } \mu\text{L}^{-1}$] were stimulated with $0.5 \text{ } \mu\text{g mL}^{-1}$ convulxin (CVX) for the indicated time points and subsequently lysed with IGEPAL[®] CA-630. Whole-cell lysates were Western blotted and probed with the respective antibodies. (C) Quantification of inositol-1-phosphate (IP $_1$) produced upon platelet activation. Washed platelets were stimulated with the indicated agonists for 5 minutes at 37°C. Platelets were lysed, and IP $_1$, a specific stable metabolite of inositol-1,4,5-trisphosphate (IP $_3$), was quantified using an ELISA assay. Results are presented as mean \pm SD, N = 4. WT, wild-type.

3.1.5 Defective aggregate formation on collagen under flow and reduced coagulant activity of BIN2-deficient platelets

Thrombus formation at sites of vascular injury requires stable shear-resistant platelet adhesion to the extracellular matrix and auto- and paracrine platelet activation by locally released secondary mediators.¹⁵⁸ When whole blood was perfused over immobilized collagen at a shear rate of 1700 s^{-1} , WT platelets rapidly adhered to the collagen-coated surface and recruited additional platelets, resulting in the formation of stable three-dimensional aggregates. In sharp contrast, adhesion and aggregate formation of *Bin2^{fl/fl Pfl4-Cre}* platelets was severely impaired, which resulted in a reduction of surface coverage and thrombus volume by ~ 72% and 78%, respectively, for *Bin2^{fl/fl Pfl4-Cre}* platelets compared to the WT (Figure 13 A-D). Highly activated platelets expose negatively charged PS, thereby providing high-affinity binding sites for key coagulation factors that promote thrombin generation. In line with the observations that PS exposure is strongly dependent on intact SOCE,¹⁵⁹ collagen-adherent *Bin2^{fl/fl Pfl4-Cre}* platelets exposed significantly less PS on their surface compared to WT controls (Figure 13 E, F). Similarly, BIN2-deficient platelets displayed markedly reduced PS exposure upon stimulation with a combination of CRP and thrombin or rhodocytin, as assessed by flow cytometric analysis of annexin A5 binding (Figure 13 G). Furthermore, in an *in vitro* thrombin generation assay the maximal amount of newly generated thrombin (peak height) in *Bin2^{fl/fl Pfl4-Cre}* platelets was reduced by ~30% after CRP stimulation (Figure 13 H, I) and also the overall amount of produced thrombin (ETP, endogenous thrombin potential) was reduced by ~15% (Figure 13 H, J). Of note, thrombin generation was indistinguishable between WT and *Bin2^{fl/fl Pfl4-Cre}* platelets following stimulation with the Ca^{2+} ionophore ionomycin, demonstrating that the mutant platelets can become fully procoagulant when intracellular Ca^{2+} levels are sufficiently high.

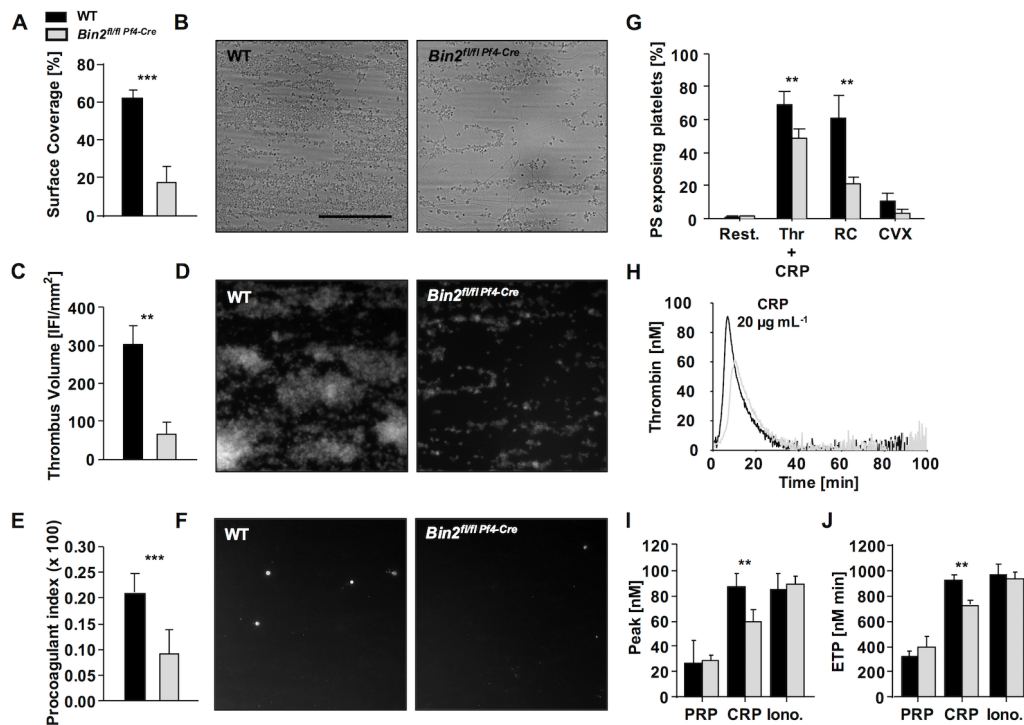


Figure 13: Impaired adhesion and defective aggregate formation of *Bin2*^{fl/fl Pf4-Cre} platelets on collagen under flow and defective procoagulant activity. (A-D) Adhesion (A, B) and thrombus formation (C, D) of platelets on collagen was assessed in a flow adhesion assay at a wall shear rate of 1700 s⁻¹. (A, C) Statistical evaluation and (B, D) representative images of 3 independent experiments are shown, N = 5. (E, F) PS exposure of *Bin2*^{fl/fl Pf4-Cre} and WT platelets, as demonstrated by annexin A5-DyLight 488 binding to platelets. Procoagulant index indicates the ratio of surface coverage of PS-exposing platelets (annexin A5-DyLight 488 staining of platelets) to the total surface covered by platelets. (E) Statistical evaluation and (F) representative images of 2 independent experiments are shown, N = 6. Scale bar = 50 µm. (G) Flow cytometric analysis of phosphatidylserine (PS) exposure in response to the indicated agonists in WT and *Bin2*^{fl/fl Pf4-Cre} platelets. Washed platelets were stained with annexin A5-DyLight-488 in the presence of Tyrode's buffer containing 2 mM Ca²⁺. Agonist concentrations: Thrombin, 0.1 U mL⁻¹; collagen-related peptide (CRP), 20 µg mL⁻¹; RC (rhodocytin), 1 µg mL⁻¹; CVX (convulxin), 1.2 µg mL⁻¹. Results are percentage of annexin A5-positive platelets ± SD and are representative of 3 independent experiments, N = 4. (H-I) Citrate-anticoagulated PRP was left unstimulated, or platelets were activated by incubation with CRP [20 mg mL⁻¹] or the Ca²⁺ ionophore Ionomycin [20 µM] for 10 minutes at 37°C. Thrombin generation was triggered with tissue factor/CaCl₂. Representative curves (H), quantification of thrombin peak height (I), and endogenous thrombin potential (ETP) (J) of 2 independent experiments, N = 4. PRP, platelet-rich plasma; *P<0.05; **P<0.01; ***P<0.001.

3.1.6 Lack of BIN2 has no influence on platelet spreading on fibrinogen and platelet integrin outside-in signaling *in vitro*

Ligand-occupied integrin α IIb β 3 mediates outside-in signaling, leading to cytoskeletal reorganization and platelet spreading.⁸⁹ BAR domain proteins are involved in membrane deformations, as required during filopodia and lamellipodia formation.¹¹⁷ To test a possible involvement of BIN2 in integrin outside-in signaling, *Bin2*^{fl/fl Pf4-Cre} and WT platelets were allowed to spread on a fibrinogen-coated surface in the presence of low concentrations of thrombin. *Bin2*^{fl/fl Pf4-Cre} and WT platelets formed filopodia and lamellipodia with similar kinetics, and after

30 minutes, the number of fully spread platelets was comparable between the two groups (Figure 14 A, B) indicating that BIN2 is not required for these processes. Immunofluorescence staining of the α -granular protein vWF in spread platelets showed the typical localization in the center of both $Bin2^{fl/fl Pf4-Cre}$ and WT platelets (Figure 14 C). Similarly, clot retraction was indistinguishable between WT and $Bin2^{fl/fl Pf4-Cre}$ mice (Figure 14 D, E), excluding a major role of BIN2 in this integrin $\alpha IIb\beta 3$ -integrin-dependent process.¹⁶⁰

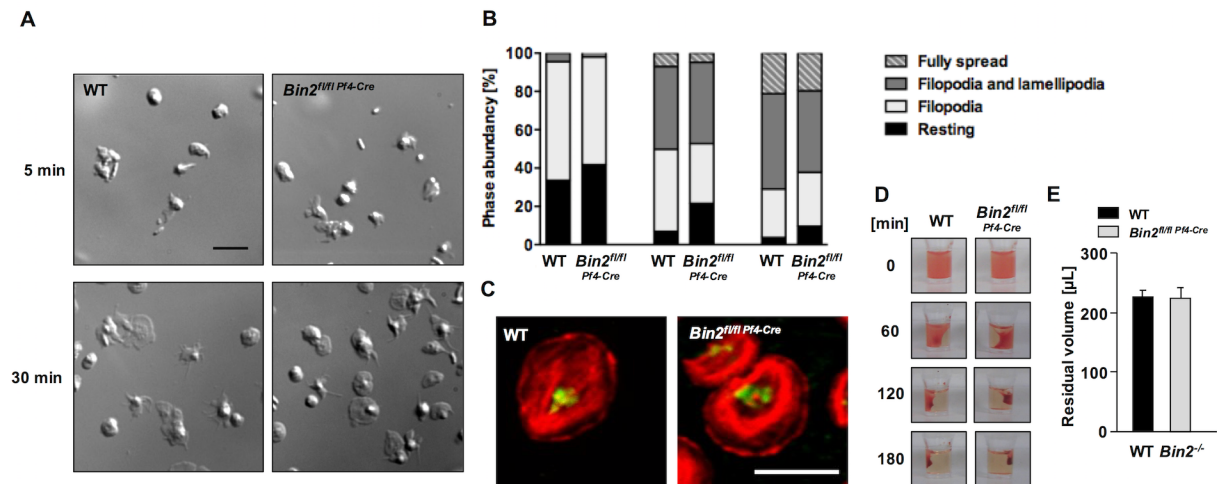


Figure 14: Lack of BIN2 has no influence on spreading on fibrinogen and platelet integrin outside-in signaling *in vitro*. (A-C) Washed platelets of WT and $Bin2^{fl/fl Pf4-Cre}$ mice were allowed to spread on fibrinogen for up to 30 minutes after stimulation with 0.01 U mL^{-1} thrombin. (A) representative images and (B) statistical evaluation of the percentage of spread platelets at different spreading stages of 3 independent experiments are shown, $N = 3$. Scale bar = $5 \mu\text{m}$. (C) Spread platelets were fixed and permeabilized and stained with phalloidin Atto647N (red) and vWF antibody (green). Scale bar = $5 \mu\text{m}$. (D, E) Clot formation in platelet-rich plasma was induced by the addition of thrombin [5 U mL^{-1}] and 20 mM CaCl_2 and clot retraction was monitored over time (D). (E) Residual volume of serum after clot retraction was measured. Representative of 2 independent experiments, $N \geq 5$. WT, wild-type.

3.1.7 Impaired hemostasis and defective arterial thrombus formation in $Bin2^{fl/fl Pf4-Cre}$ mice

To examine to which extent the *in vitro* observed defects of $Bin2^{fl/fl Pf4-Cre}$ platelets were influenced, their thrombotic activity was analyzed *in vivo*, in a model of occlusive thrombus formation in the mechanically injured abdominal aorta (Figure 15 A) was analyzed. The time to vessel occlusion was significantly prolonged in $Bin2^{fl/fl Pf4-Cre}$ compared to WT mice and 3 out of 14 vessels did not occlude at all, whereas all WT vessels occluded (mean occlusion time: WT: $230 \pm 85 \text{ s}$; KO: $323 \pm 90 \text{ s}$; $P = 0.008$). To investigate whether the defective GPVI signaling was partially compensated through TxA_2 -induced signaling pathways *in vivo*,¹⁶¹ TxA_2 synthesis was inhibited in WT and $Bin2^{fl/fl Pf4-Cre}$ mice by i.v. administration of a low dose of acetylsalicylic acid (ASA) [$1 \mu\text{g g}^{-1} \text{ i.v.}$] 15 min prior to assessment of tail bleeding times and thrombus formation in the injured aorta. In vehicle treated mice, tail bleeding times were found to be comparable for $Bin2^{fl/fl Pf4-Cre}$ and WT mice (Figure 15 B).

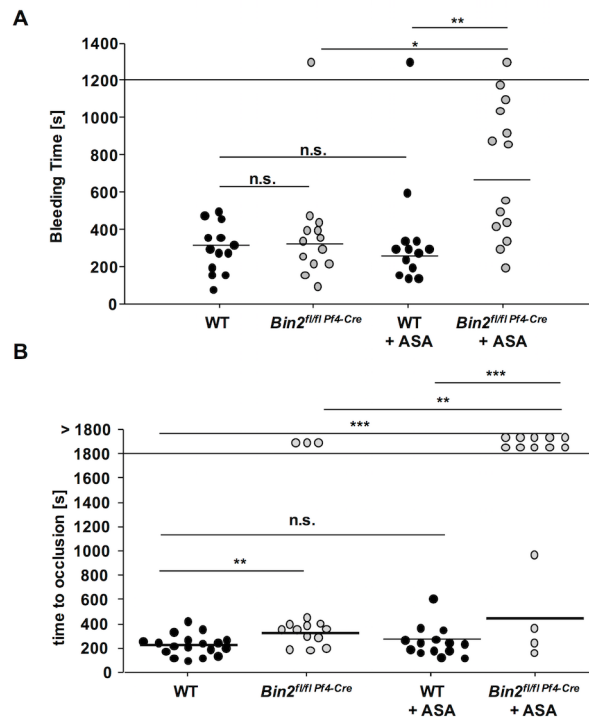


Figure 15: Impaired hemostasis and partially defective thrombus formation in *Bin2^{fl/fl} Pf4-Cre* mice. (A) Tail bleeding times of WT and *Bin2^{fl/fl} Pf4-Cre* mice without or with acetylsalicylic acid (ASA) treatment [$1 \mu\text{g g}^{-1}$ i.v.] 15 minutes before the start of the experiment. Each symbol represents 1 animal. (B) Time to stable vessel occlusion of WT and *Bin2^{fl/fl} Pf4-Cre* mice without or with ASA treatment [$1 \mu\text{g g}^{-1}$ i.v.] 15 minutes before the start of the experiment. The abdominal aorta was injured by firm compression with forceps, and blood flow was monitored for 30 minutes. Each symbol represents 1 animal. Aorta model was performed by Karen Wolf. * $P < 0.05$, ** $P < 0.01$, *** $P < 0.001$.

In sharp contrast, ASA treatment resulted in significantly prolonged tail bleeding times in *Bin2^{fl/fl} Pf4-Cre* mice, but had no major effect in WT mice (Figure 15 B). Similarly, ASA treatment did not affect occlusion times in the mechanically injured aorta of WT mice, but resulted in a profound protection of *Bin2^{fl/fl} Pf4-Cre* mice from occlusive arterial thrombosis (10 out of 14 ASA-treated BIN2 KO mice did not form occlusive thrombi, $P = 0.0002$, Figure 15 A). Together, these data confirmed that the ITAM-mediated activation defects in *Bin2^{fl/fl} Pf4-Cre* are at least partially compensated by TxA_2 -induced signaling pathways *in vivo* which is in line with previous observations.^{161,162}

3.1.8 BIN2 plays an important role in the progression of ischemic stroke

Ischemic stroke is among the leading causes of death and morbidity worldwide. Rapid restoration of blood flow by thrombolysis and/or mechanical thrombectomy is the mainstay of acute stroke treatment, but does not guarantee a favorable outcome.¹⁶³ This so-called reperfusion injury denotes the acute, paradoxically harmful aspect of restoring blood flow in the ischemic brain which triggers thrombo-inflammatory infarct progression.⁹¹ Although the exact pathomechanisms underlying this thrombo-inflammatory process remain elusive, platelet SOCE^{78,81} and GPVI/ITAM signaling^{164,165} are critical determinants of the neurological outcome. To test an involvement of BIN2 in this process, *Bin2^{fl/fl} Pf4-Cre* mice were subjected to transient middle cerebral artery occlusion (tMCAO) for 1 h as described¹⁶⁴ and infarct outcome was assessed after a 24 h reperfusion period. Strikingly, infarct volumes in *Bin2^{fl/fl} Pf4-Cre* mice were reduced by >30% compared to control mice (WT: $90 \pm 6 \text{ mm}^3$, KO: $59 \pm 7 \text{ mm}^3$; $P = 0.003$)

(Figure 16 A-C). In summary, these results demonstrated that BIN2 is a critical regulator of platelet reactivity in the setting of thrombo-inflammatory brain infarction.

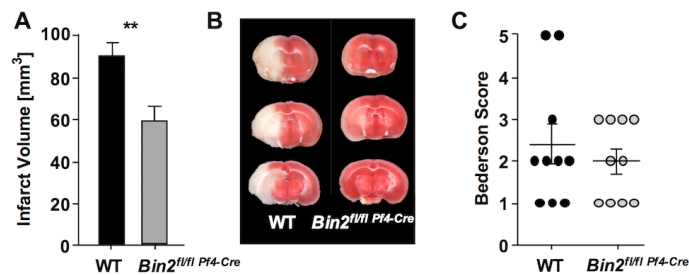


Figure 16: Smaller infarct size in *Bin2*^{fl/fl} *Pf4-Cre* mice upon ischemic brain infarction. (A-C) Infarct volumes and functional outcome (24 h after focal cerebral ischemia in WT and *Bin2*^{fl/fl} *Pf4-Cre* mice were investigated in a murine model of ischemic stroke. Mice were subjected to 60 minutes of transient middle cerebral artery occlusion (tMCAO). (A) Brain infarct volumes in WT (N = 10) and *Bin2*^{fl/fl} *Pf4-Cre* (N = 10) mice were measured by planimetry. Results represent mean ± SEM. (B) Representative images of 3 coronal brain sections stained with 2,3,5-triphenyltetrazolium chloride for 24 h after 60 minutes of tMCAO. (C) Bederson score was determined 24 h after tMCAO. Each symbol represents 1 animal. Experiments were conducted by Dr. Michael Schuhmann from the Department of Neurology, University Hospital of Würzburg, Würzburg, Germany **P<0.01.

3.1.9 Calpain-mediated degradation of BIN2

Platelet activation is controlled by various mechanisms, including proteolytic degradation of intracellular proteins. Calpain, the major Ca²⁺-dependent protease in platelets, undergoes activation upon increase in [Ca²⁺]_i. Analysis of the amino acid sequence (www.calpain.org) of BIN2 predicted several highly conserved cleavage sites and an area lacking any cleavage sites at the N-terminus of BIN2, corresponding to the BAR domain (Figure 18).

To study calpain-mediated degradation of BIN2, wild-type platelets were stimulated in the presence of extracellular Ca²⁺ with TG (Figure 17 A) or the Ca²⁺ ionophore ionomycin (Figure 17 C) and a rapid degradation of BIN2 was detected, which could be prevented in the presence of the calpain inhibitor calpeptin. However, stimulation with high doses of the physiological agonists thrombin and CRP did not lead to the degradation of BIN2 (Figure 17 B). Using an antibody directed against the N-terminus of BIN2, a smaller fragment with a size of approximately 32 kDa was detected upon stimulation with TG and ionomycin (Figure 17 D, F), which was hardly detectable using thrombin and CRP (Figure 17 E). These results demonstrated that BIN2 can be degraded by calpain, however, further studies are required, to decipher the molecular function of this cleavage mechanism in platelet physiology.

Taken together, these data showed that BIN2 is a critical regulator of SOCE in platelets and that its absence results in defective platelet activation and aggregation *in vitro* and protects mice from occlusive arterial thrombus formation and ischemic stroke.

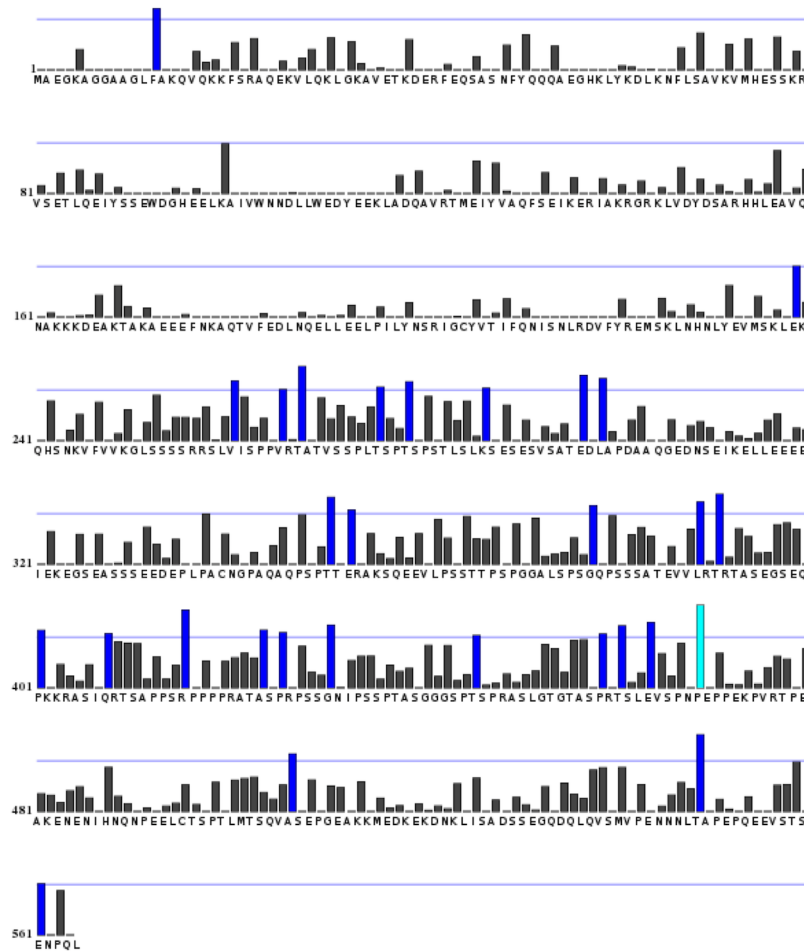


Figure 18: Predicted calpain-cleavage sites of BIN2 from www.calpain.org. Predicted cleavage sites are marked in blue. Light blue indicated most relevant cleavage site.

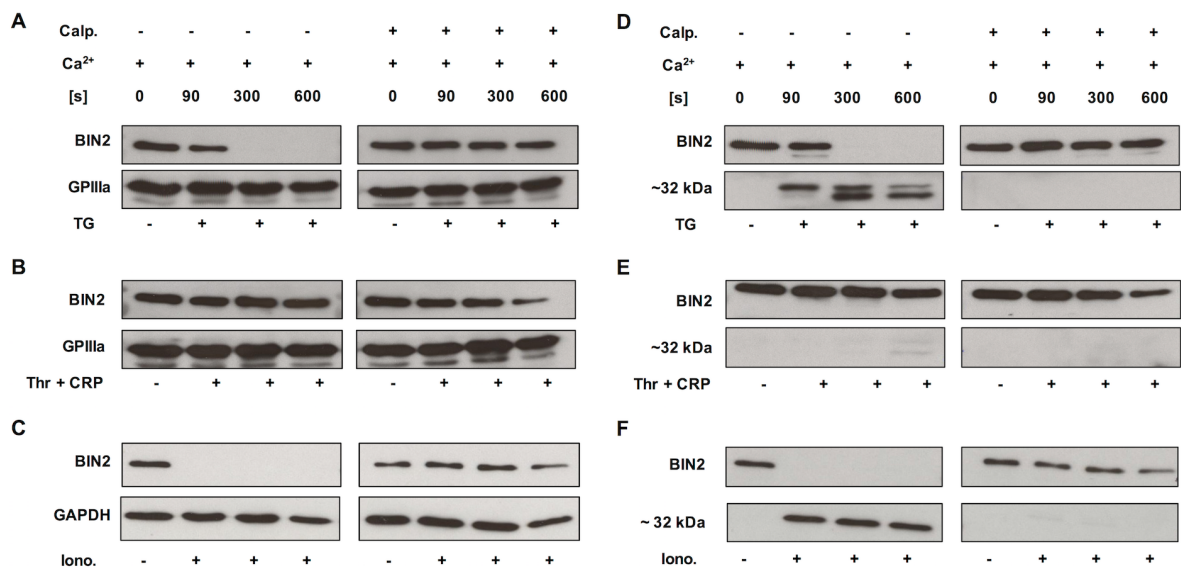


Figure 17: BIN2 is partially degraded during platelet activation. (A-F) Platelets were stimulated with TG ($0.1 \mu\text{M}$; A, D), thrombin and CRP ($0.1 \text{ U mL}^{-1}/10 \mu\text{g mL}^{-1}$; B, E) or ionomycin ($20 \mu\text{M}$; C, F) and lysed at the indicated time points in the presence and absence of the calpain inhibitor calpeptin. GAPDH served as loading control. (D, E, F) Appearance of a $\sim 32 \text{ kDa}$ -sized fragment upon platelet stimulation. TG, thapsigargin; Thr, thrombin; Iono, ionomycin; Calp, calpeptin.

3.2 Normal platelet function in mice lacking hydrogen peroxide-induced clone-5 (Hic-5)

3.2.1 Hic-5 is dispensable for hematopoiesis and platelet morphology

Embryonic stem cells (clone EPD0817_1_D04), provided by CSD, with a knockout first approach targeting exon 1 of the *Tgfb1i1* gene were used, leading to the generation of *Tgfb1i1*^{+/-} mice. *Tgfb1i1*^{+/-} mice were intercrossed to obtain *Tgfb1i1*^{-/-} mice (further referred to as Hic-5-null mice) and the respective control mice. Hic-5-null mice were born at normal Mendelian ratio, were viable and fertile and appeared overall healthy. The absence of Hic-5 in platelets was confirmed by Western blot analysis and RT-PCR (Figure 19 A, B). Expression levels of the other paxillin family members, leupaxin and paxillin, were unaltered in Hic-5-null platelets compared to wild-type platelets (Figure 19 A).

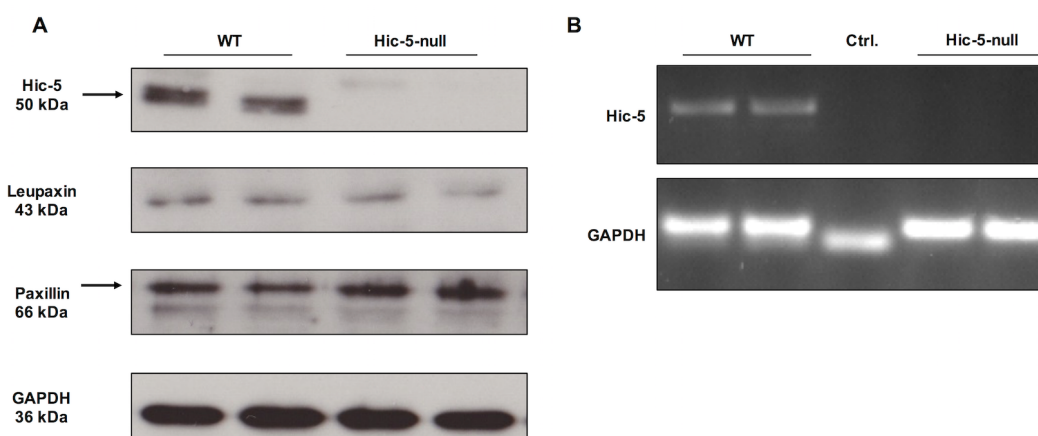


Figure 19. Efficient deletion of Hic-5, but unaltered expression of Leupaxin and Paxillin. (A) Hic-5, leupaxin and paxillin expression was assessed by Western blot analysis. GAPDH served as loading control. (B) Analysis of the presence of *Tgfb1i1* mRNA in platelets by RT-PCR. GAPDH mRNA served as positive control. Popp *et al.*, 2015.¹¹²

The loss of Hic-5 did not alter platelet count or size and red and white blood cell counts were also indistinguishable from controls (Table 3). Flow cytometric measurements of major platelet surface proteins did not show significant alterations in expression levels in Hic-5-null platelets compared to wild-type platelets (Table 4). The unaltered basic blood and platelet parameters in the mutant mice indicate that Hic-5 plays no role in hematopoiesis or platelet morphology.

Table 3. Basic blood and platelet parameters. Platelet count and size, as well as white blood cell count and red blood cell count were analyzed using a blood cell counter. Representative of 3 independent experiments, N = 4. P_≥0.05, n.s. WT, wild-type; n.s., non significant.

| | WT | Hic-5-null | P |
|--|------------------|------------------|------|
| Platelets μL^{-1} [$\times 10^6$] | 0.94 \pm 0.13 | 0.93 \pm 0.14 | n.s. |
| Platelet volume [fL] | 5.48 \pm 0.15 | 5.63 \pm 0.05 | n.s. |
| White blood cells μL^{-1} [$\times 10^3$] | 11.52 \pm 2.44 | 11.20 \pm 1.26 | n.s. |
| Red blood cells μL^{-1} [$\times 10^6$] | 7.23 \pm 0.12 | 7.52 \pm 0.48 | n.s. |

3.2.2 Hic-5 is dispensable for inside-out signaling and thrombus formation *in vitro*

To clarify the role of Hic-5-deficiency on integrin activation and platelet degranulation, activation of the major platelet integrin α IIb β 3 and surface exposure of α -granular P-selectin in response to different agonists was analyzed by flow cytometry. Stimulation of GPCRs with ADP, U46619, a combination of both, or thrombin resulted in comparable results for wild-type and Hic-5-null platelets. Similarly, Hic-5-null platelets reacted normally upon activation of GPVI by CRP and in response to stimulation of the hemITAM receptor CLEC-2 by rhodocytin (Figure 20 A, B). β 1-integrin activation was also assessed by flow cytometry using the 9EG7-antibody which selectively binds to the activated conformation of β 1-integrins,¹⁶⁶ and found to be indistinguishable between Hic-5-null and wild-type platelets (Figure 20 C). In addition, aggregation responses of Hic-5-deficient platelets were tested by aggregometry, but no effects of the Hic-5-deficiency could be observed upon stimulation with any of the tested agonists (Figure 20 D). A flow adhesion assay was used to test adhesion and aggregate formation on collagen. These processes are strongly dependent on functional GPVI and α 2 β 1 integrins.^{96,98} No differences in aggregate formation were detectable between wild-type and Hic-5-null platelets. These results demonstrate that Hic-5 is dispensable for platelet integrin inside-out activation downstream of both GPCRs and for (hem)ITAM receptors (Figure 20 E, F).

Table 4: Surface expression levels of platelet glycoproteins in wild-type and Hic-5-null platelets.

Expression of glycoproteins on the platelet surface was determined by flow cytometry. Diluted whole blood from the indicated mice was incubated with FITC-labeled antibodies at saturating concentrations for 15 minutes at room temperature, and platelets were analyzed directly. Data are expressed as mean fluorescence intensity \pm SD and are representative of 3 independent experiments, N = 4. P \geq 0.05, n.s. WT, wild-type; CLEC-2, C-type lectin-like receptor 2; n.s., non significant.

| | WT | Hic-5-null | P |
|------------------------|--------------|--------------|------|
| GPV | 215 \pm 6 | 218 \pm 3 | n.s. |
| GPIb | 184 \pm 4 | 192 \pm 6 | n.s. |
| GPIX | 351 \pm 16 | 354 \pm 8 | n.s. |
| GPVI | 38 \pm 2 | 37 \pm 1 | n.s. |
| α IIb β 3 | 420 \pm 23 | 434 \pm 17 | n.s. |
| α 2 | 44 \pm 2 | 47 \pm 7 | n.s. |
| β 1 | 117 \pm 4 | 118 \pm 3 | n.s. |
| CD9 | 810 \pm 14 | 781 \pm 42 | n.s. |
| CLEC-2 | 105 \pm 3 | 106 \pm 4 | n.s. |

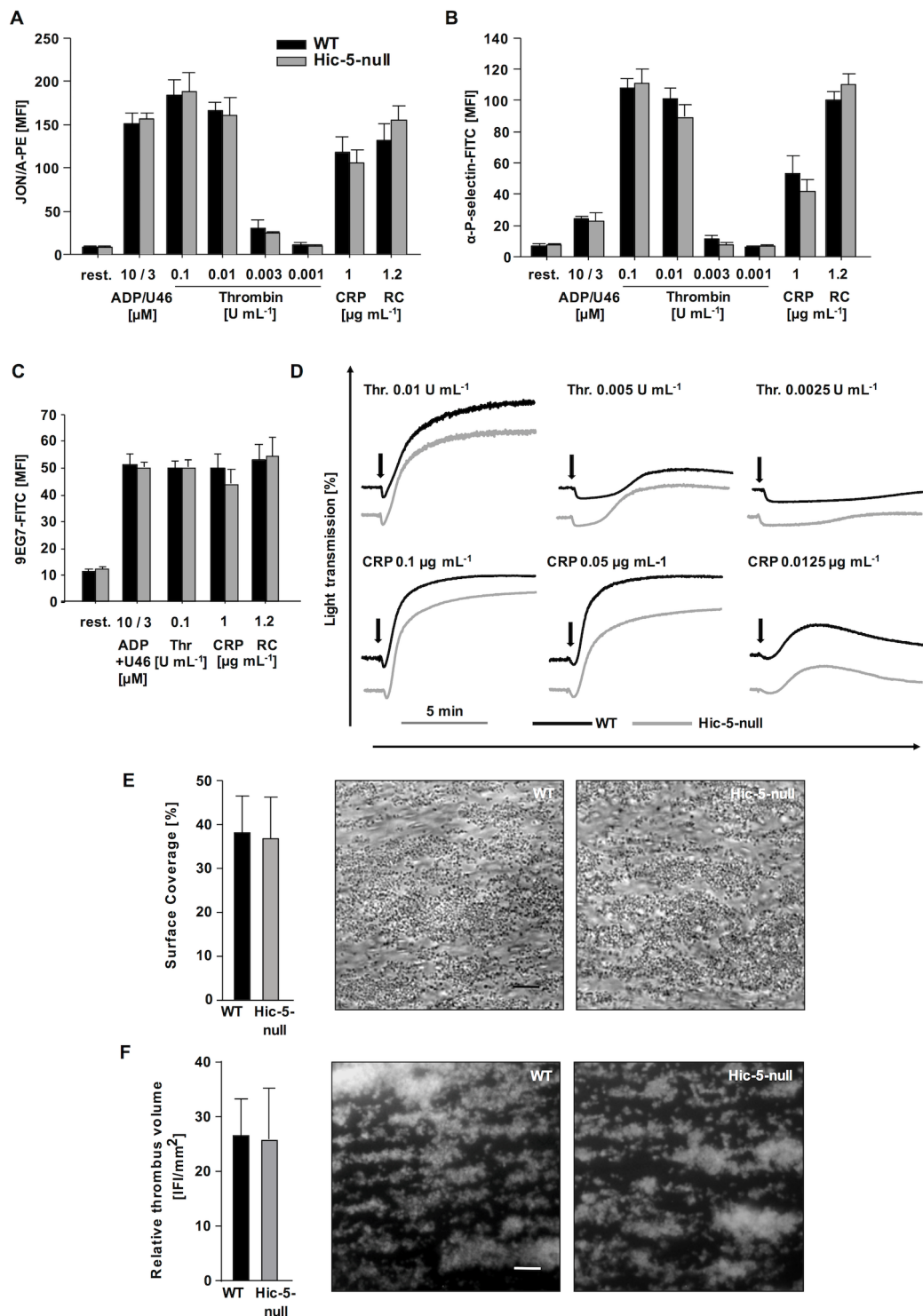


Figure 20: Hic-5 deficiency has no effects on inside-out activation of platelet integrins, degranulation, platelet aggregation and adhesion to collagen. (A, B) Flow cytometric analyses of (A) $\alpha\text{IIb}\beta 3$ integrin activation and (B) degranulation-dependent P-selectin exposure in response to the indicated agonists. (C) Flow cytometric analysis of $\beta 1$ integrin activation. Results are mean fluorescence intensity (MFI) \pm standard deviation (SD) and are representative of 3 independent experiments, N = 4. (D) Washed platelets were stimulated with the indicated agonists, and light transmission was recorded using a four channel aggregometer. Representative aggregation curves of three independent experiments are shown, N = 4. (E, F) Adhesion (E) and thrombus formation (F) of platelets on collagen was assessed in a flow adhesion assay at a wall shear rate of 1000 s^{-1} . Representative of 2 independent experiments, N = 5. Scale bar = 25 μm . CRP, collagen-related peptide, FITC, fluorescein isothiocyanate; Thr., Thrombin; RC, rhodocytin; U46, U46619; WT, wild-type. Popp *et al.*, 2015.¹¹²

3.2.3 Lack of Hic-5 has no influence on platelet spreading on fibrinogen and platelet integrin outside-in signaling *in vitro*

Ligand-occupied integrin $\alpha\text{IIb}\beta\text{3}$ mediates outside-in signaling, leading to cytoskeletal reorganization and platelet spreading.⁸⁹ To assess these processes, Hic-5-null and wild-type platelets were allowed to spread on a fibrinogen-coated surface in the presence of low concentrations of thrombin and found to form filopodia and lamellipodia with similar kinetics, and after 30 minutes, the number of fully spread platelets was comparable between both groups (Figure 21 A, B, C). Moreover, no differences in filopodia length were observed. To further assess integrin outside-in signaling, clot retraction¹⁶⁰ was analyzed and no differences in the kinetics and extent of this process were found between wild-type and Hic-5-null platelets (Figure 21 D, E). Together, these data exclude a major role of Hic-5 for integrin $\alpha\text{IIb}\beta\text{3}$ outside-in signaling in mouse platelets.

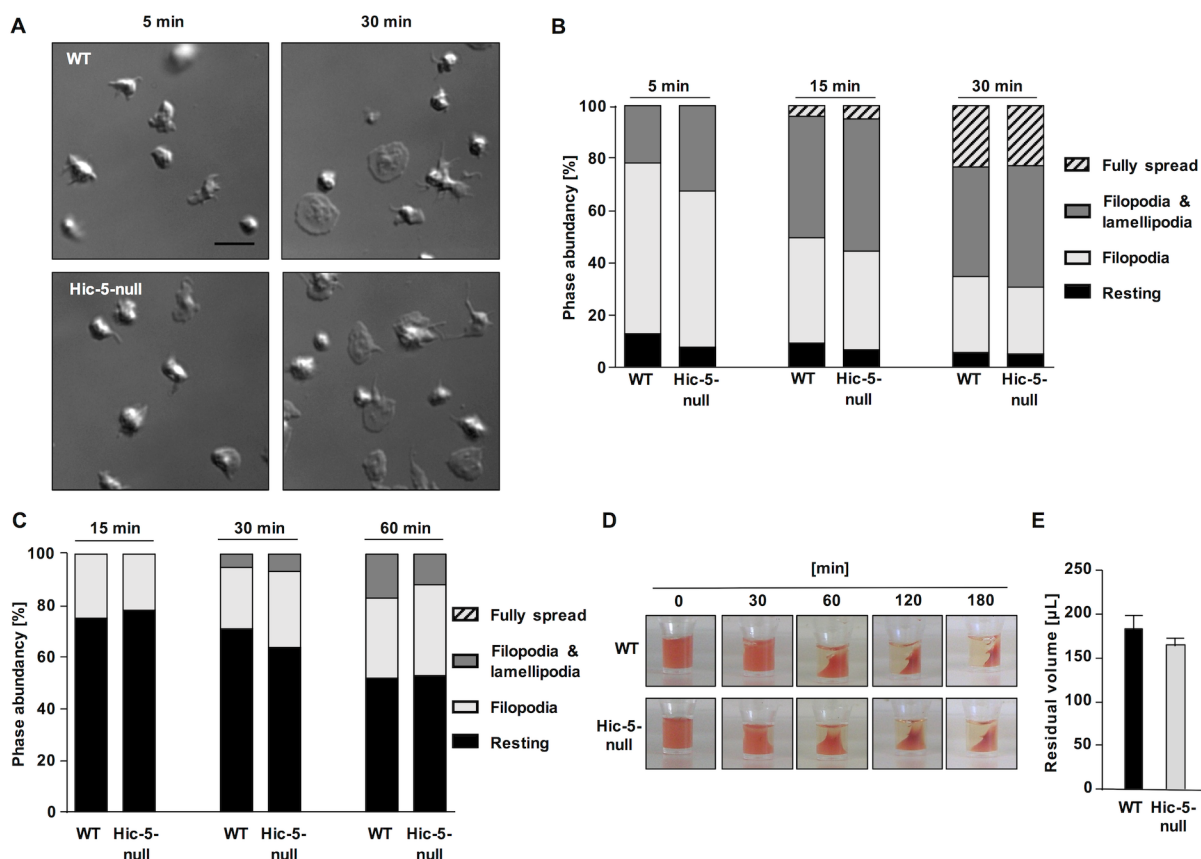


Figure 21. Lack of Hic-5 has no influence on platelet spreading on fibrinogen and platelet integrin outside-in signaling *in vitro*. (A, B) Washed platelets of WT and Hic-5-null mice were allowed to spread on fibrinogen for up to 30 minutes after stimulation with 0.01 U mL^{-1} thrombin. (A) Representative images and (B) statistical evaluation of the percentage of spread platelets at different spreading stages of 2 independent experiments (N = 3) are shown. Scale bar = $5 \mu\text{m}$. (C) WT and Hic-5-deficient platelets were allowed to spread on fibrinogen for up to 60 minutes in the presence of apyrase [2 U mL^{-1}] and indomethacin [$1.4 \mu\text{M}$]. Representative of 2 independent experiments, N = 3. (D, F) Clot formation in platelet-rich plasma was induced by the addition of thrombin [5 U mL^{-1}] and 20 mmol L^{-1} CaCl_2 and clot retraction was monitored over time (D). (E) Residual volume of serum after clot retraction was measured. Representative of 2 independent experiments, N = 4. Popp *et al.*, 2015.¹¹²

3.2.4 *Hic-5*-deficient platelets have unaltered GPIb function

At sites of vascular injury, vWF, bound to collagen, is exposed on the subendothelial ECM. The interaction between the platelet GPIb-V-IX receptor complex and vWF is important for platelet tethering, the initial step in the formation of a hemostatic plug. The potential role of *Hic-5* in GPIb-mediated processes was assessed by monitoring the adhesion of platelets on immobilized vWF under high shear conditions. *Hic-5*-null and wild-type platelets attached to the immobilized vWF and in part firmly adhered to the surface to comparable extent and with similar kinetics (Figure 22 A). In addition, platelet spreading on a vWF-coated matrix under conditions of α IIb β 3 integrin-blockade was analyzed. The stimulation of platelets by a GPIb specific signal results in a shape change, which is limited to contraction of the cell body and filopodia formation.⁵⁹ Both, *Hic-5*-null and wild-type platelets extended comparable numbers of filopodia (Figure 22 B). Together, these results indicate that GPIb function is intact in *Hic-5*-deficient platelets.

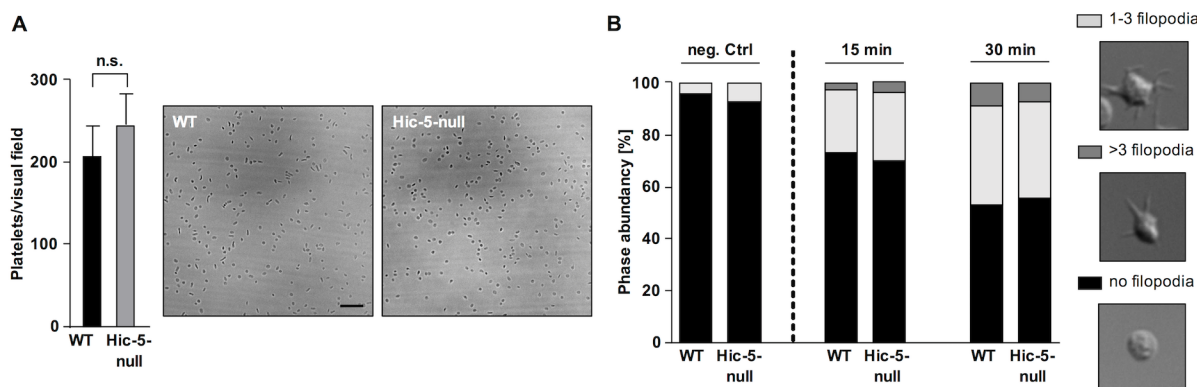


Figure 22: Unaltered GPIb function in *Hic-5*-deficient mice. (A) Whole blood of wild-type and *Hic-5*-null mice was perfused over a vWF-coated surface at a wall shear rate of 1,700 sec⁻¹ and the number of adherent platelets was quantified. Representative of 2 independent experiments, N = 5 (B) Washed platelets were treated with integrilin [40 μ g mL⁻¹] and botrocetin [2 μ g mL⁻¹] and allowed to adhere to vWF-coated coverslips. Filopodia formation was quantified according to the number of extensions per platelet at indicated the time points. Representative of 2 independent experiments, N = 3. Popp *et al.*, 2015.¹¹²

3.2.5 Unaltered *in vivo* thrombus formation in *Hic-5*-deficient mice.

To investigate the role of *Hic-5* in platelet function *in vivo*, two widely used tail bleeding time assays (filter paper and warm saline) were used and comparable bleeding times for control and *Hic-5*-null mice were found (Figure 23 A, B).

Consistent with the *in vitro* results, pathological thrombus formation, as assessed by intravital microscopy of FeCl₃-injured mesenteric arterioles, was indistinguishable between wild-type and *Hic-5*-null mice, resulting in similar occlusion times for both groups (Figure 23 C, D). These data indicate a dispensable role for *Hic-5* in thrombus formation *in vivo*.

In summary, these results show that *Hic-5* is dispensable for integrin inside-out and outside-in signaling in platelets and consequently for hemostasis and arterial thrombosis in mice.

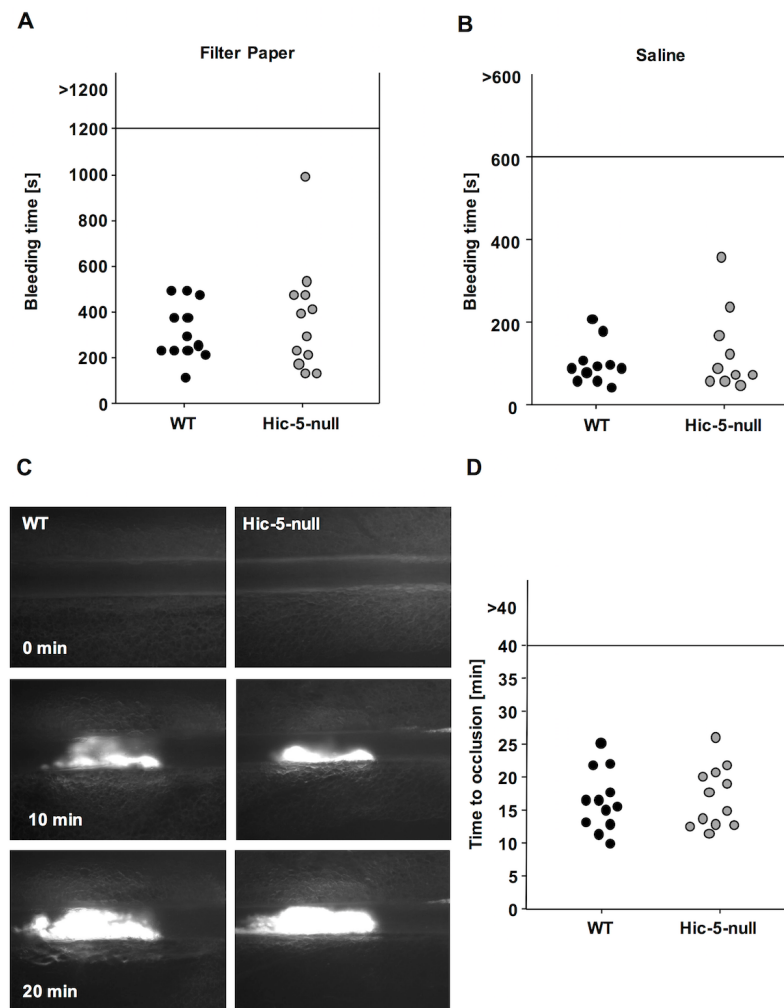


Figure 23. Unaltered *in vivo* thrombus formation in Hic-5-deficient mice. (A, B) Tail bleeding times of wild-type and Hic-5-null mice, using (A) the filter paper method and (B) the saline model. Each symbol represents 1 animal. (C, D) Thrombus formation in small mesenteric arterioles was induced by topical application of 20% FeCl₃. For monitoring of thrombus formation by intravital microscopy, platelets were labeled fluorescently. Representative pictures (C) and time to stable occlusion (D) of wild-type and Hic-5-null mice are shown. Each symbol represents one arteriole. FeCl₃ model was performed by Ina Thielmann. Popp *et al.*, 2015.¹¹²

3.3 Non-redundant functions of small Rho GTPases RhoA and Rac1 in murine platelets

Rho GTPases, such as RhoA, Rac1, and Cdc42, are key regulators of cytoskeletal rearrangements in platelets.⁵⁵ However, constitutive deficiency of RhoA, Cdc42 and Rac1 in mice resulted in early embryonic lethality which hampered studies in primary knockout cells.¹⁸²⁻¹⁸⁴ The availability of tissue- and lineage-specific deletion of the three ubiquitously expressed Rho GTPases without potential off-target effects by the use of inhibitors, overexpression or knockdown approaches made it possible to analyze the specific role of each GTPase in platelet biogenesis and platelet function.⁵⁷⁻⁵⁹

The understanding of functional redundancies in these processes is only at the beginning. Recently, a redundant function of Rac1 and Cdc42 has been demonstrated in the regulation of microtubule dynamics and (pro-)platelet formation, and concomitant deficiency of both GTPases led to severe macrothrombocytopenia.⁶⁹ In addition, double-deficiency of RhoA and Cdc42 causes abnormal megakaryocyte development, severe macrothrombocytopenia and defective tubulin organization (Cherpokova *et al.*, unpublished).

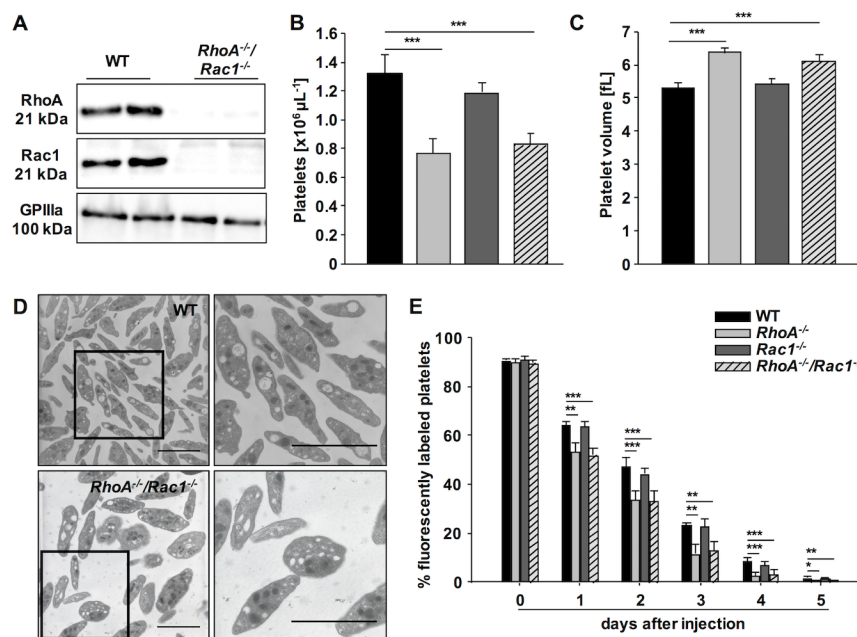


Figure 24: $RhoA^{-/-}/Rac1^{-/-}$ mice display a distinct macrothrombocytopenia, increased platelet size and moderately reduced platelet life span. (A) Analysis of RhoA and Rac1 expression in wild-type (WT) and $RhoA^{-/-}/Rac1^{-/-}$ platelets by Western blot. GPIIIa served as loading control. Peripheral platelet counts (B) and platelet volume (C) of WT and $RhoA^{-/-}/Rac1^{-/-}$ mice measured using a blood cell counter respectively. Data are presented as mean \pm SD of 5 mice per group. (D) Representative transmission electron microscopy pictures of resting $RhoA^{-/-}/Rac1^{-/-}$ platelets in comparison to WT, $RhoA^{-/-}$ and $Rac1^{-/-}$ platelets. (E) Determination of platelet life span of WT, $RhoA^{-/-}$, $Rac1^{-/-}$ and $RhoA^{-/-}/Rac1^{-/-}$ mice. Mice were injected with a DyLight 488-conjugated anti-GPIX Ig derivate [$0.5 \mu\text{g g}^{-1}$ body weight] to label platelets *in vivo*. Results are percentage of fluorescently labeled platelets at the indicated days after injection as determined by flow cytometry. Values are mean \pm SD of 5 mice per group. * $P < 0.05$; ** $P < 0.01$; *** $P < 0.001$.

3.3.1 Non-redundant functions of RhoA and Rac1 for basic platelet parameters

To study the consequences of combined loss of RhoA and Rac1 specifically in the MK-/platelet-lineage, mice carrying both the *RhoA*¹⁷⁰ and the *Rac1*¹⁷¹ genes flanked by loxP sites - *RhoA*^{fl/fl}/*Rac1*^{fl/fl} - were intercrossed with transgenic mice carrying the Cre-recombinase under the control of the MK-/platelet-specific Pf4 promoter.¹⁴⁵ Resulting double-deficient *RhoA*^{fl/fl}/*Rac1*^{fl/fl Pf4-Cre} mice (further referred to as *RhoA*^{-/-}/*Rac1*^{-/-}) and littermate control mice *RhoA*^{fl/fl}/*Rac1*^{fl/fl} (further referred to as WT) were used in all studies. In some experiments, conditional single-deficient mice - *RhoA*^{fl/fl Pf4-Cre} (*RhoA*^{-/-}) and *Rac1*^{fl/fl Pf4-Cre} (*Rac1*^{-/-}) - were used in parallel in order to better discriminate between redundant and non-redundant functions of both GTPases. Loss of RhoA and Rac1 in *RhoA*^{-/-}/*Rac1*^{-/-} platelets was confirmed by Western blot analysis (Figure 24 A). In agreement with previous studies, *RhoA*^{-/-} mice displayed a mild macrothrombocytopenia, whereas platelet count and size from *Rac1*^{-/-} mice were indistinguishable from wild-type controls (Figure 24 B, C).^{57,58} Double-deficiency of RhoA and Rac1 did not induce further alterations, but resulted in platelet count and size comparable to that seen in *RhoA*^{-/-} mice. Transmission electron microscopy (TEM) analyses revealed only a moderately increased size of *RhoA*^{-/-}/*Rac1*^{-/-} platelets and a roundish shape similar to *RhoA*^{-/-} platelets. Subcellular morphology and granule distribution were largely unaltered in the double-deficient platelets (Figure 24 D). These data indicate that the functions of RhoA and Rac1 are non-redundant in platelet production. Rac1 seems to have only a minor role in platelet production in *RhoA*^{-/-}/*Rac1*^{-/-} mice compared to RhoA, but on the other hand, Rac1 is important in *Rac1*^{-/-}/*Cdc42*^{-/-} mice, which display a severe macrothrombocytopenia with highly altered platelet morphology.⁶⁹

Table 5: Analysis of surface expression of glycoproteins in WT, *RhoA*^{-/-}, *Rac1*^{-/-} and *RhoA*^{-/-}/*Rac1*^{-/-} platelets. Diluted whole blood was stained with saturating amounts of fluorophore-labeled antibodies and platelets were analyzed by flow cytometry. Results express MFI ± SD of 3 independent experiments (N = 5 mice per group). Statistical analyses represent comparison to WT platelets. *P<0.05; **P<0.01; ***P<0.001.

| | WT | <i>RhoA</i> ^{-/-} | <i>Rac1</i> ^{-/-} | <i>RhoA</i> ^{-/-} / <i>Rac1</i> ^{-/-} |
|---------------|--------|----------------------------|----------------------------|---|
| GPIb | 296±26 | 302±6 | 285±10 | 272±7 |
| GPV | 256±9 | 294±3 (***) | 254±24 | 270±5 (*) |
| GPIX | 484±34 | 491±21 | 442±8 | 443±6 |
| CD9 | 927±15 | 919±24 | 906±45 | 937±27 |
| GPVI | 64±3 | 75±7 (*) | 68±2 | 72±3 (**) |
| CLEC-2 | 128±4 | 159±3 (***) | 130±7 | 137±7 |
| α2 | 51±2 | 58±5 | 53±4 | 50±2 |
| β1 | 117±4 | 154±10 (**) | 117±6 | 133±3 (*) |
| αIIbβ3 | 558±41 | 664±8 (**) | 526±14 | 641±28 (**) |

Flow cytometric analysis of *RhoA*^{-/-}/*Rac1*^{-/-} platelets revealed a significant increase in mean fluorescence intensities for several major platelet surface receptors like α IIb β 3 and GPVI. This increase was also found in *RhoA*^{-/-} platelets and is probably caused by the increased size of the platelets (Table 5). In accordance with *RhoA*^{-/-} platelets, *RhoA*^{-/-}/*Rac1*^{-/-} platelets displayed a reduced life span, which is partially contributing to the reduced platelet counts in both *RhoA*- and *RhoA/Rac1*-deficient animals (Figure 24 E).

3.3.2 Non-redundant functions of RhoA and Rac1 for integrin inside-out signaling

Flow cytometric analysis of *RhoA*^{-/-}/*Rac1*^{-/-} platelets revealed combined defects of RhoA- and Rac1-single-deficiency without further alteration, leading to activation defects upon stimulation of GPCRs as well as of the hem(ITAM) receptors GPVI and CLEC-2 (Figure 25 A). Similar to integrin activation, release of α -granules, measured by P-selectin exposure, in *RhoA*^{-/-}/*Rac1*^{-/-} platelets was reduced comparable to both *RhoA*^{-/-} and *Rac1*^{-/-} single-deficient platelets, except for a slightly stronger reduction upon stimulation with thrombin (Figure 25 B).

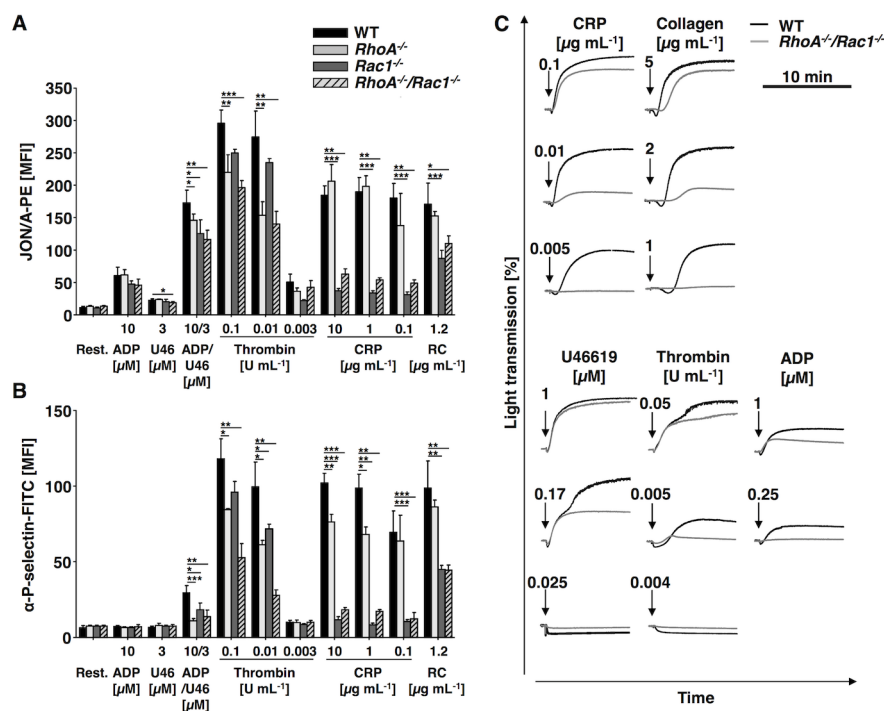


Figure 25: Reduced integrin α IIb β 3 activation and P-selectin exposure upon $G_{q/13}$ and (hem)ITAM stimulation and limited platelet aggregation in *RhoA*^{-/-}/*Rac1*^{-/-} platelets. (A) Flow cytometric analysis of α IIb β 3 activation (binding of JON/A-PE) and (B) degranulation-dependent P-selectin exposure in response to the indicated agonists in WT, *RhoA*^{-/-}, *Rac1*^{-/-} and *RhoA*^{-/-}/*Rac1*^{-/-} platelets. Data are mean fluorescence intensities (MFI) \pm SD of 4 mice per group and representative of 2 independent experiments. (C) Washed platelets were stimulated with the indicated agonists, and light transmission was recorded using a four-channel aggregometer. ADP measurements were performed in PRP (platelet rich plasma). Representative aggregation curves of 3 independent experiments are shown, N = 4. *P<0.05; **P<0.01; ***P<0.001. CVX, convulxin; RC, rhodocytin.

In aggregation studies, *RhoA*^{-/-}/*Rac1*^{-/-} platelets showed like *RhoA*^{-/-} platelets defective shape change after G₁₃ stimulation and partially reduced aggregation and strongly impaired aggregation responses to GPVI agonists like *Rac1*^{-/-} platelets, but no further impairments were detectable (Figure 25 C). Taken together, these findings show that in *RhoA*^{-/-}/*Rac1*^{-/-} platelets defects upon G_{q/13} stimulation and upon stimulation of (hem)ITAM receptors are present, as in *RhoA*^{-/-} and *Rac1*^{-/-} single-deficient mice, respectively. As no worsening was detectable, these data indicate that functions of RhoA and Rac1 in platelet activation are largely non-redundant.

3.3.3 Non-redundant functions of RhoA and Rac1 for platelet spreading on fibrinogen and clot retraction *in vitro*

To investigate the effects of RhoA/Rac1-deficiency on platelet spreading, thrombin-activated WT and *RhoA*^{-/-}/*Rac1*^{-/-} platelets were allowed to spread on fibrinogen - a process dependent on integrin α IIb β 3 induced outside-in signaling for adhesion and cytoskeletal remodeling.

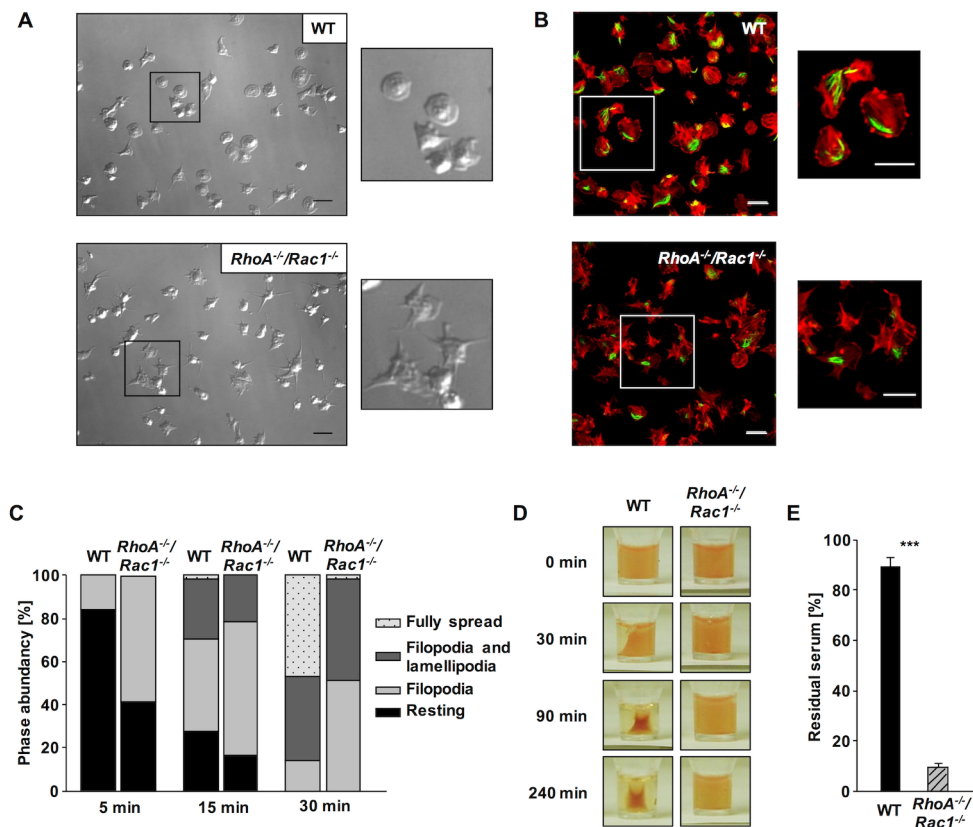


Figure 26: *RhoA*^{-/-}/*Rac1*^{-/-} platelets fail to fully spread and show completely abolished clot retraction. (A,B) Washed platelets of WT and *RhoA*^{-/-}/*Rac1*^{-/-} mice were allowed to spread for up to 30 minutes on fibrinogen [200 μ g mL⁻¹] after stimulation with 0.01 U mL⁻¹ thrombin. (A) Representative differential interference contrast (DIC) images of 3 independent experiments (N = 2) after 30 minutes. Black squares indicate magnified areas. Scale bar = 5 μ m. (B) Analysis of filamentous actin (red) and tubulin (green) structure in spread (30 minutes) WT and *RhoA*^{-/-}/*Rac1*^{-/-} platelets by confocal microscopy. Scale bar = 5 μ m. White squares indicate magnified area. (C) Statistical evaluation of the percentage of spread platelets at different spreading stages. (D) Clot retraction of PRP (platelet rich plasma) upon activation with 3 U mL⁻¹ thrombin in the presence of 20 mM CaCl₂. Representative images of 3 independent experiments are depicted (N = 4). (E) Residual serum after 4 h of clot retraction in %. ***P<0.001.

RhoA^{-/-}/*Rac1*^{-/-} platelets spread slower and were not able to fully spread, similar to *Rac1*^{-/-} platelets (Figure 26 A, C). Immunofluorescent imaging of spread platelets confirmed the spreading defect, but did not show major alterations of the actin and tubulin cytoskeleton (Figure 26 B). Integrin α IIb β 3 outside-in signaling also regulates clot retraction. After induction with thrombin, clot retraction started already after 30 min in wild-type PRP and proceeded to the maximum after 4 h, the process was virtually abolished in *RhoA*^{-/-}/*Rac1*^{-/-} PRP similar to clot retraction defect in *RhoA*^{-/-} mice (Figure 26 D, E). These data confirm that *Rac1* is important for the formation of lamellipodia, whereas *RhoA* is dispensable for spreading of platelets on fibrinogen but is indispensable for integrin-mediated clot retraction. In both experiments, no further alterations were detectable by the lack of the respective other GTPase indicating independent functions of *RhoA* and *Rac1* in α IIb β 3-dependent outside-in signaling.

3.3.4 Combined deficiency of *RhoA* and *Rac1* results in defective hemostasis and defective thrombus formation *in vivo*

To assess the impact of *RhoA/Rac1*-deficiency on hemostasis, tail bleeding times were determined (Figure 27 A). *RhoA*^{-/-}/*Rac1*^{-/-} mice displayed a severe hemostatic defect characterized by the inability to arrest bleeding within an observation period of 20 min, comparable to *RhoA*^{-/-} mice. Double-deficiency of *RhoA* and *Rac1* led in addition to protection in models of arterial thrombosis (Figure 27 B, C). In both models, either after injury of small mesenteric arterioles by FeCl₃ or after mechanical injury of the abdominal aorta, no formation of stable thrombi was observed in *RhoA*^{-/-}/*Rac1*^{-/-} mice, similarly to single-deficient animals. Together, these data show that the functions of the *Rho* GTPases *RhoA* and *Rac1* are non-redundant for platelet activation *in vitro* and *in vivo*.

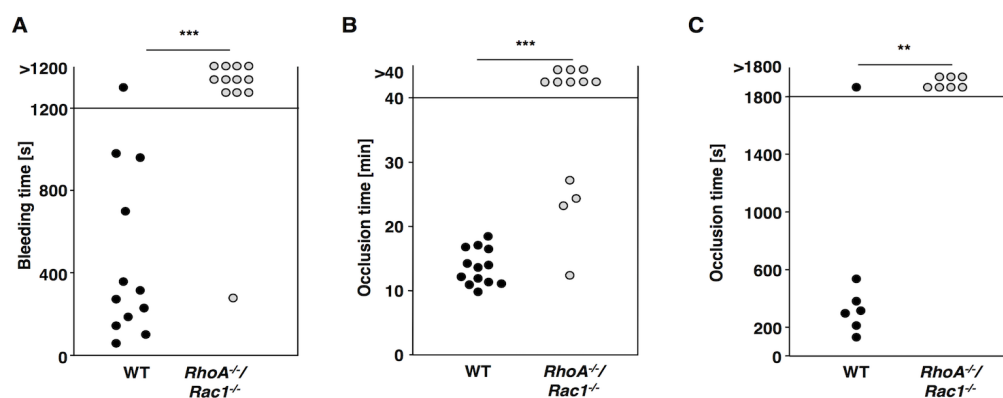


Figure 27: Impaired hemostasis and defective thrombus formation and in *RhoA*^{-/-}/*Rac1*^{-/-} mice. (A) Tail bleeding times of WT and *RhoA*^{-/-}/*Rac1*^{-/-} mice. Each symbol represents 1 animal. (B, C) Time to stable vessel occlusion of WT and *RhoA*^{-/-}/*Rac1*^{-/-} mice. (B) Injury of mesenteric arterioles was induced by topical application of 20% FeCl₃. Adhesion and aggregation of fluorescently labeled platelets in arterioles was monitored for 40 minutes or until complete occlusion occurred (blood flow stopped for > 2 minutes). (C) The abdominal aorta was injured by firm compression with forceps, and blood flow was monitored for 30 minutes. FeCl₃ and aorta model were performed by Martina Morowski. **P<0.01, ***P<0.001.

3.4 Liver sinusoidal endothelial cells process antibody opsonized platelets through the inhibitory Fc γ receptor IIB in mice

3.4.1 Fc γ Rs are required for anti-GPVI-induced transient thrombocytopenia and the generation of sGPVI

The two most common antigens of anti-platelet antibodies in patients suffering from immune thrombocytopenia (ITP) are the von Willebrand factor receptor GPIb, and the major platelet integrin α IIb β 3 (GPIIb/IIIa).^{129–131} Anti-GPIb antibodies induce Fc-independent platelet destruction, while anti-GPIIb/IIIa antibodies efficiently trigger Fc-dependent platelet clearance. In some ITP patients, anti-GPVI auto-antibodies have been reported to cause GPVI immunodepletion,^{172,173} but the underlying mechanism remained ill-defined. To assess whether anti-GPVI mAbs induced thrombocytopenia is a Fc-dependent process, WT mice were challenged with intravenous injection of the IgG or F(ab')₂ fragments of the anti-GPVI mAb, JAQ1. JAQ1-IgG induced a rapid loss of surface GPVI and the appearance of soluble GPVI (sGPVI) in the plasma and this was accompanied by a transient thrombocytopenia. In sharp contrast, JAQ1-F(ab')₂ fragments did not cause thrombocytopenia (Figure 28 A) and only induced a delayed downregulation of GPVI from the platelet surface (Figure 28 B) with no detectable sGPVI in the plasma (Figure 28 C). Thus, while GPVI dimerization is sufficient to trigger GPVI internalization without affecting platelet counts, the Fc part of the anti-GPVI antibodies is required for the induction of a transient thrombocytopenia and, remarkably, GPVI ectodomain shedding. These results suggest that anti-GPVI-F(ab')₂ antibody fragments might be a promising therapeutic agent to provide long-term anti-thrombotic protection without the undesired transient thrombocytopenia induced by intact IgGs.

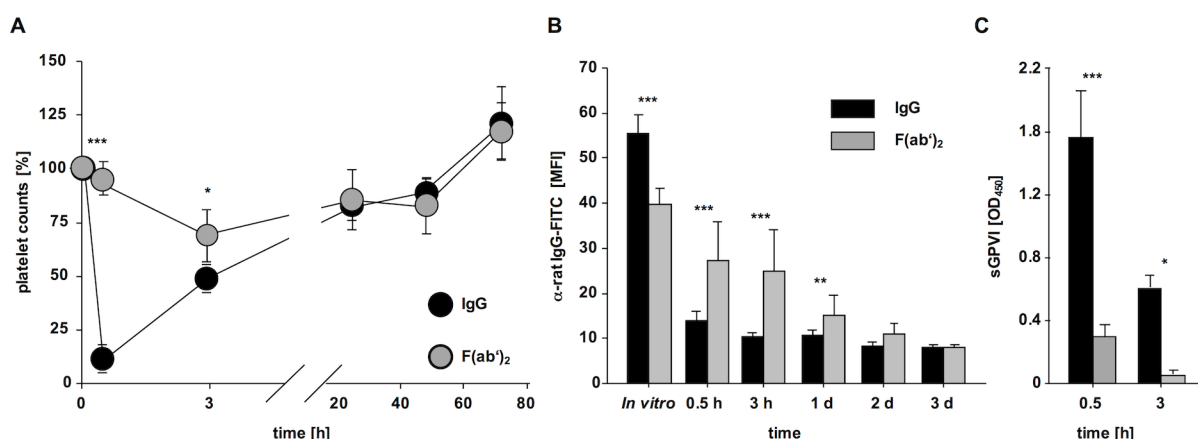


Figure 28: JAQ1-IgG, but not JAQ1-F(ab')₂ fragments induces a transient thrombocytopenia. (A) Platelet counts of WT mice were monitored upon injection of JAQ1-IgG or JAQ1-F(ab')₂ fragments. (B) Expression of GPVI on the platelet surface was determined by flow cytometry using an anti-rat IgG-FITC antibody. (C) The plasma levels of soluble GPVI (sGPVI) were determined using an ELISA system. Data are expressed as mean \pm SD ($n \geq 4$) and are representative of 3 independent experiments. * $P < 0.05$, ** $P < 0.01$, *** $P < 0.001$. Experiments were conducted together with D. Stegner.

To test if Fc γ R-dependent mechanisms caused the anti-GPVI-IgG induced thrombocytopenia, mice were treated with 2.4G2 mAbs, which block Fc γ Rs III and IIB,¹⁷⁴ or vehicle 24 h before receiving anti-GPIb α , anti-GPVI or anti-GPIIb/IIIa antibodies. While this Fc γ R blockade had no effect on the severe thrombocytopenia induced by anti-GPIb α IgGs (Figure 29 A), it significantly ameliorated the drop in platelet counts in anti-GPIIb/IIIa treated mice confirming that these antibodies cause Fc-independent and Fc-dependent thrombocytopenia, respectively (Figure 29 B).^{129–131}

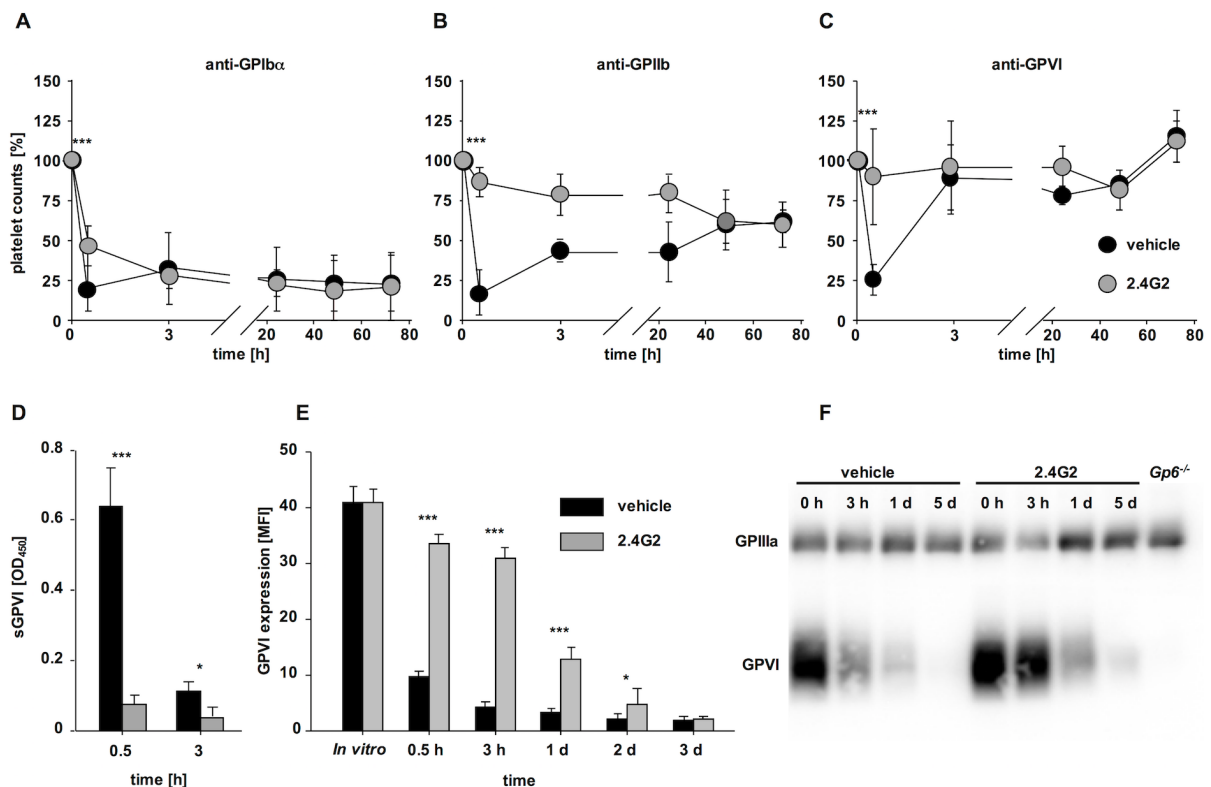


Figure 29: 2.4G2 treatment prevents anti-GPIIb/IIIa and anti-GPVI-induced thrombocytopenia and the generation of soluble GPVI. (A-C) Platelet counts of 2.4G2 (grey) or vehicle-treated (black) mice were monitored upon injection of the anti-GPIb α antibody p0p/B (A), the anti-GPIIb/IIIa antibody MWRReg30 (B) or the anti-GPVI antibody JAQ1^{biotin} by flow cytometry (C). (D) The plasma levels of soluble GPVI (sGPVI) were determined using an ELISA system. (E) Expression of GPVI on the platelet surface was determined by flow cytometry using an anti-rat IgG-FITC antibody. (A-E) Data are expressed as mean \pm SD (N = 4) and are representative of 3 independent experiments. (F) Total GPVI levels were determined by Western blotting, GPIIIa served as loading control. The Western blot is representative of 3 independent experiments. *P<0.05, ***P<0.001. Experiments were conducted together with D. Stegner.

Importantly, 2.4G2 pretreatment also completely prevented anti-GPVI induced thrombocytopenia, demonstrating that Fc γ Rs are critical in this process (Figure 29 C). Of note, while anti-GPIb or anti-GPIIb/IIIa antibodies induced sustained thrombocytopenia which was only overcome by the production of new platelets (Figure 29 A-C), the anti-GPVI induced thrombocytopenia was transient with a return of sequestered platelets to the circulation within a few hours, suggesting different processing of the opsonized cells. In support of this notion, 2.4G2-pretreatment also completely prevented the antibody-induced generation of sGPVI

(Figure 29 D) and down-regulation of the receptor in circulating platelets was markedly delayed (Figure 29 E,F), similar to the effect induced by JAQ1-F(ab')₂ fragments in control mice (Figure 28 B). These results demonstrated that anti-GPVI antibodies induce transient thrombocytopenia and GPVI ectodomain shedding through Fc γ R-dependent mechanisms. If this pathway is not functional, GPVI dimerization by the antibody (or F(ab')₂ fragments thereof) still causes internalization and degradation of the receptor in circulating platelets.

3.4.2 Fc γ RIIB, but not Fc γ RIII, is necessary to promote anti-GPVI-induced transient thrombocytopenia and the generation of sGPVI

2.4G2 blocks the activatory Fc γ RIII as well as the inhibitory Fc γ RIIB.¹⁷⁴ To test which of these Fc γ Rs was required for the anti-GPVI-induced thrombocytopenia and GPVI ectodomain shedding, mice lacking Fc γ RIII (*Fcgr3*^{-/-})¹⁴⁷ or Fc γ RIIB (*Fcgr2b*^{-/-})¹⁴⁶ were challenged with biotinylated anti-GPVI antibody (JAQ1^{biotin}). Surprisingly, absence of the activating Fc γ RIII had no effect on the anti-GPVI-induced transient drop in platelet counts (Figure 30 A) and surface GPVI was down-regulated with similar kinetics as in control mice (Figure 30 B). In line with the fast loss of platelet GPVI, sGPVI was detectable in similar concentrations in *Fcgr3*^{-/-} mice compared to WT mice (Figure 30 C). In sharp contrast, the lack of Fc γ RIIB prevented JAQ1-induced thrombocytopenia (Figure 30 A) and the same effect was seen when the mice were challenged with another anti-GPVI antibody which binds to a different epitope on the receptor.¹⁴¹ Furthermore, GPVI downregulation was delayed in *Fcgr2b*^{-/-} mice compared to WT controls (Figure 30 B) and, most notably, no sGPVI could be detected in the plasma of JAQ1^{biotin}-treated *Fcgr2b*^{-/-} mice (Figure 30 C).

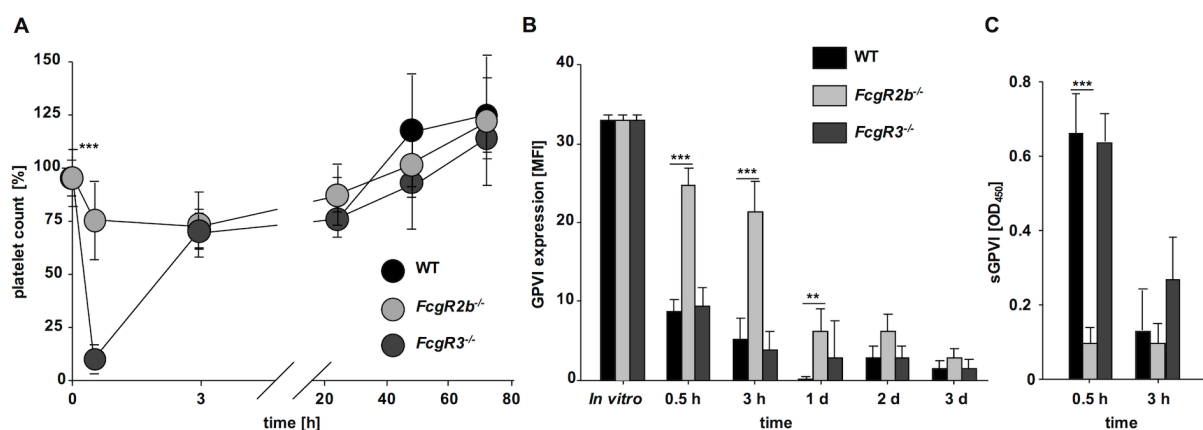


Figure 30: Fc γ RIIB, but not Fc γ RIII, mediates the anti-GPVI-induced thrombocytopenia and the generation of sGPVI. (A) Platelet counts of mice lacking Fc γ RIII (*Fcgr3*^{-/-}), Fc γ RIIB (*Fcgr2b*^{-/-}) or control mice (WT) were monitored upon injection of the anti-GPVI antibody JAQ1^{biotin} by flow cytometry. (B) Expression of GPVI on the platelet surface was determined by flow cytometry using an anti-rat IgG-FITC antibody. (C) The plasma levels of soluble GPVI (sGPVI) were determined using an ELISA system. Data are expressed as mean \pm SD (N = 4) and are representative of 3 independent experiments. **P<0.01, ***P<0.001. Experiments were conducted together with D. Stegner.

3.4.3 JAQ1-opsionized platelets are retained primarily in the liver by Fc γ RIIB-expressing liver sinusoidal endothelial cells

To test in which organ(s) anti-GPVI-opsionized platelets are trapped by Fc γ RIIB-bearing cells, platelets were fluorescently labeled *in vivo* and the fluorescent signal was monitored over time after anti-GPVI mAb injection using an intravital imaging system (IVIS Spectrum, Perking Elmer). In anti-GPVI-treated, but not vehicle-treated mice, a rapid increase of the fluorescence signal was detectable in the liver, indicating sequestration of the antibody-opsionized platelets in this organ (Figure 31 A). This was confirmed by immunohistochemical analysis of cryosections showing massive platelet accumulation in the liver sinusoids of anti-GPVI-treated, but not control mice already a few minutes after injection which peaked within the first 30 min (Figure 31 B). In sharp contrast, anti-GPVI-treatment did not induce platelet accumulation in the liver of *Fcgr2b*^{-/-} mice (Figure 31 B), revealing an essential role of this Fc γ R in this process.

Western blot analysis of isolated LSECs from WT and Fc γ RIIB-deficient mice using 2.4G2 mAb demonstrated strong expression of Fc γ RIIB in WT, but not in *Fcgr2b*^{-/-} cells (Figure 32 A). This result is in line with previous reports showing that LSECs account for the majority of total Fc γ RIIB and lack other Fc γ Rs.¹³⁷

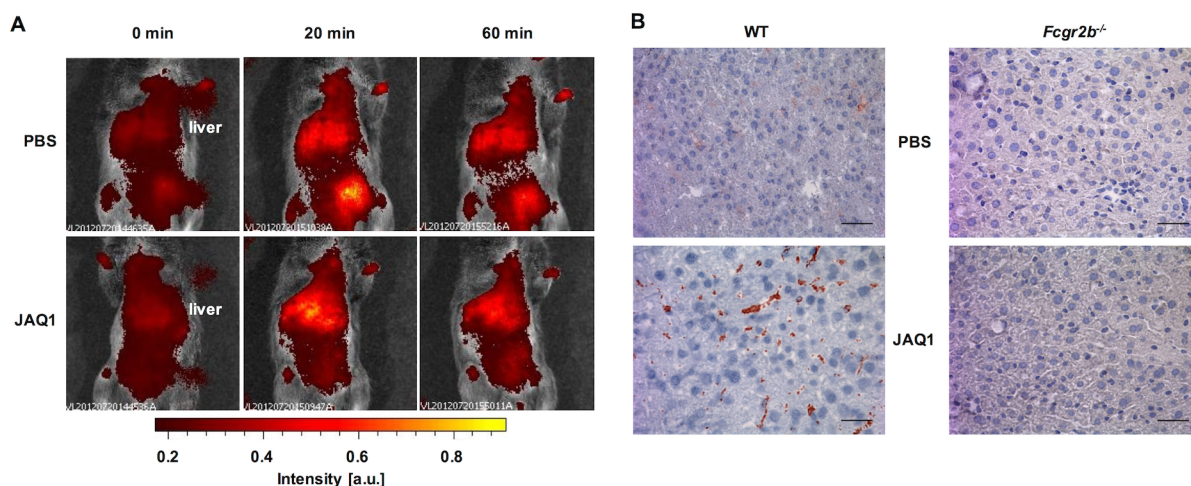


Figure 31: JAQ1-opsionized platelets are sequestered primarily to the liver of WT, but not Fc γ RIIB-deficient mice. (A) Sequestration of fluorescently labeled platelets was monitored in live mice upon injection of JAQ1 or vehicle using an *in vivo* imaging system. (B) Sections of snap-frozen liver samples of WT mice and mice lacking Fc γ RIIB (*Fcgr2b*^{-/-}) were probed with HRP-conjugated anti-GPIb antibodies. Detection was performed using 3-Amino-9-Ethylcarbazole. Sections were counterstained with hematoxylin. Scale bar = 20 μ m. Experiments were conducted together with D. Stegner.

To test a possible role of Kupffer cells (hepatic macrophages), which also express Fc γ RIIB, in anti-GPVI induced thrombocytopenia and GPVI shedding, these cells were depleted by injections of clodronate liposomes before anti-GPVI treatment.¹⁷⁵ While the clodronate efficiently depleted Kupffer cells (Figure 32 B), it had no effect on anti-GPVI-induced thrombocytopenia, the kinetics of GPVI downregulation or the appearance of plasma sGPVI in the plasma (Figure 32 C-F), clearly demonstrating that indeed LSECs mediate anti-GPVI triggered thrombocytopenia and GPVI shedding through Fc γ RIIB *in vivo*.

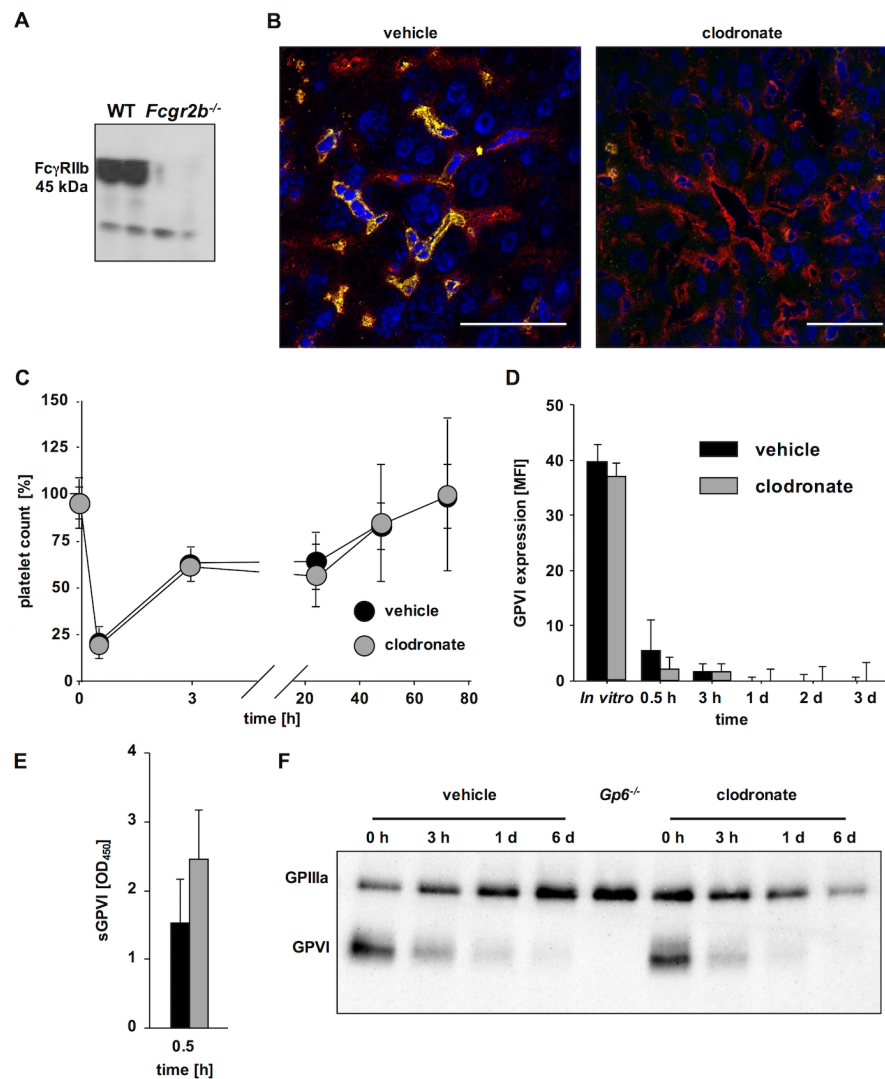


Figure 32: Kupffer cell depletion using clodronate liposomes has no effect on JAQ1-induced thrombocytopenia and the generation of sGPVI. (A) LSEC express Fc γ RIIB. Western blotting with 2.4G2 revealed a strong band in WT LSECs at approx. 45 kDa which was absent in mice lacking Fc γ RIIB (*Fcgr2b*^{-/-}). (B) Sections of snap-frozen liver samples of vehicle and clodronate-treated WT mice were probed with F4/80 (Kupffer cells; green); anti-CD105 antibodies (LSEC; red) and counterstained with DAPI (blue). Scale bar = 50 μ m. (C) Platelet counts of mice which received clodronate liposomes (clodronate) or PBS liposomes (vehicle) 48 h before the experiment were monitored upon injection of the anti-GPVI antibody JAQ1^{biotin} by flow cytometry. (D) Expression of GPVI on the platelet surface was determined by flow cytometry using an anti-rat IgG-FITC antibody. (E) The plasma levels of soluble GPVI (sGPVI) were determined using an ELISA system. (C-E) Data are expressed as mean \pm SD (N = 4) and are representative of 3 independent experiments. (F) Total GPVI levels were determined by Western blotting, GPIIIa served as loading control. The Western blot is representative of 3 independent experiments. Experiments were conducted together with D. Stegner.

3.4.4 Absence of endothelial ADAM10 does not prevent the generation of sGPVI

The above described data had shown that Fc γ RIIB on LSEC is responsible for the sequestration of JAQ1-opsonized platelets. It might be that GPVI is shed *in trans* by endothelial metalloproteases, a phenomenon which has been described for ADAM10-mediated ephrin-A5 shedding.¹⁷⁶ Our group has previously shown that global deficiency of ADAM17 did not affect GPVI shedding *in vivo*,³⁹ making ADAM10 the most likely candidate. To test this, mice lacking ADAM10 in endothelial cells (*Adam10*^{-/-}) using the Tie2-Cre system¹⁷⁷ were generated, resulting in ADAM10 deficiency in LSECs. *Adam10*^{-/-} mice developed a transient thrombocytopenia upon JAQ1-injection (Figure 33 A). Strikingly, loss of surface expression and sGPVI levels in plasma following GPVI depletion were not affected by the absence of endothelial ADAM10 (Figure 33 B,C), ruling out a central role of this protease.

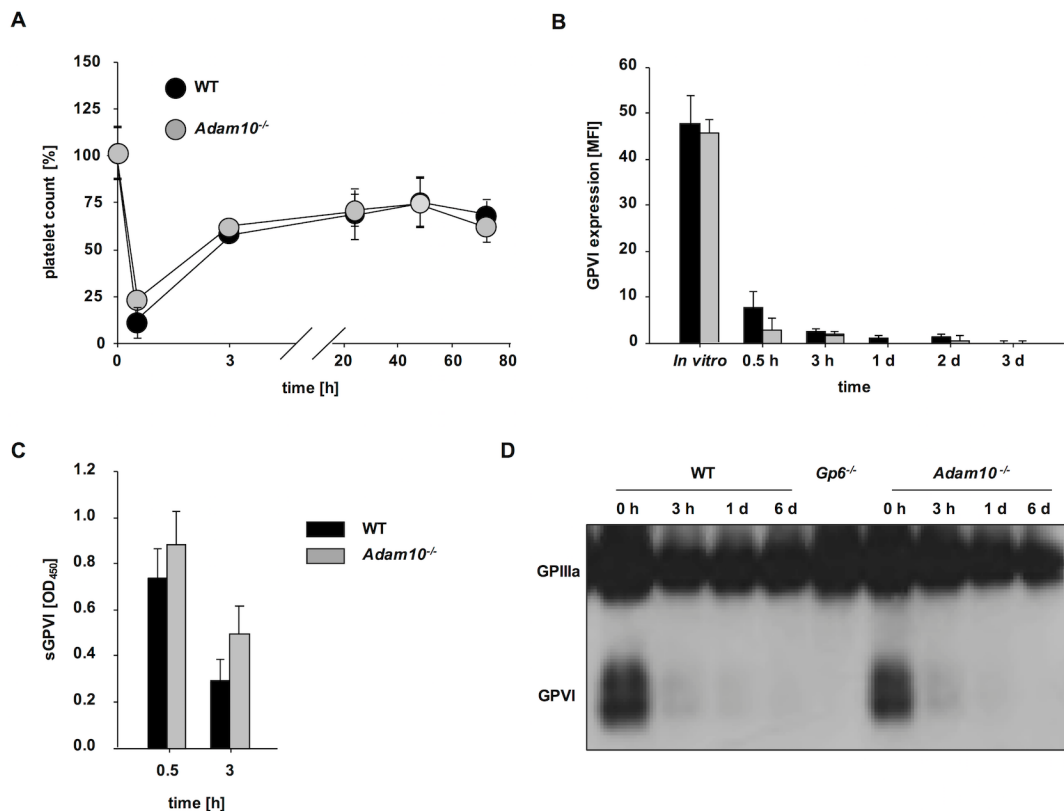


Figure 33: Endothelial ADAM10 is not required for the generation of sGPVI. (A) Platelet counts of mice with an endothelial-specific ADAM10 deficiency (*Adam10*^{-/-}) were monitored upon injection of the anti-GPVI antibody JAQ1^{biotin} by flow cytometry. (B) Expression of GPVI on the platelet surface was determined by flow cytometry using an anti-rat IgG-FITC antibody. (C) The plasma levels of soluble GPVI (sGPVI) were determined using an ELISA system. (A-C) Data are expressed as mean \pm SD (N = 4) and are representative of 3 independent experiments. (D) Total GPVI levels were determined by Western blotting, GPIIIa served as loading control. The Western blot are representative of 3 independent experiments. Experiments were conducted together with D. Stegner.

3.4.5 Fc γ RIIB mediates the sequestration of anti-GPIIb/IIIa-opsionized platelets in the liver and contributes to the early phase of thrombocytopenia

The critical role of Fc γ RIIB in anti-GPVI induced platelet sequestration prompted us to assess a potential role of this receptor in the Fc-dependent clearing of platelets opsonized with other antibodies, most notably the clinically relevant anti-GPIIb/IIIa-IgGs. Thus, *Fcgr2b*^{-/-} mice were challenged in a passive ITP model with a bolus of anti-GPIIb/IIIa antibodies. Surprisingly, lack of Fc γ RIIB ameliorated the initial drop in platelet counts after anti-GPIIb/IIIa challenge (Figure 34 A), showing for the first time that this receptor also actively contributes to platelet clearing in a model of ITP. However, in line with its established role as an inhibitory Fc γ R in phagocytic cells, *Fcgr2b*^{-/-} mice developed a more severe and prolonged thrombocytopenia compared to control mice at later time points (Figure 34 A), confirming previous studies.^{178,179} Comparable to anti-GPVI antibodies, anti-GPIIb/IIIa antibodies induced immediate, but only transient platelet sequestration in the liver (Figure 34 B). This transient ‘trapping’ of platelets was entirely Fc γ RIIB-dependent (Figure 34 B), revealing an essential role of this FcR in the initial phase of anti-platelet IgG-mediated platelet sequestration.

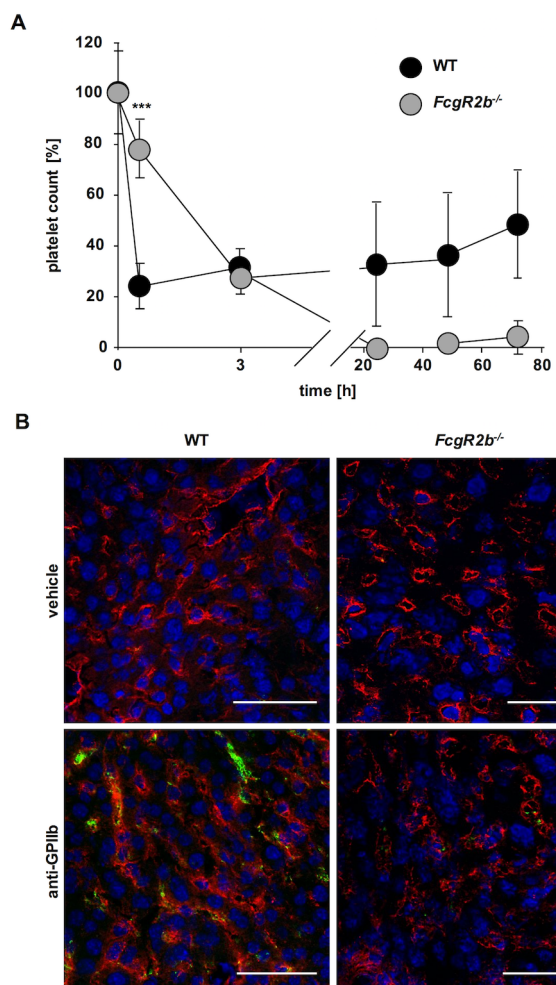


Figure 34: MWReg30-opsonized platelets are initially sequestered to the liver of WT, but not Fc γ RIIB-deficient mice. (A) Platelet counts of mice lacking Fc γ RIIB (*Fcgr2b*^{-/-}) or control mice (WT) were monitored upon injection of the anti-GPIIb/IIIa antibody MWReg30 by flow cytometry. (B) Sections of snap-frozen liver samples of vehicle and MWReg30-treated (30 min) *Fcgr2b*^{-/-} and WT mice were probed with anti-GPIX (platelets; green); anti-CD105 antibodies (endoglin on LSEC; red) and counterstained with DAPI (blue). Scale bar = 50 μ m. ***P<0.001. Experiments were conducted together with D. Stegner.

4 Discussion

In this thesis, the roles of the BAR protein BIN2 and the paxillin family member Hic-5 in platelets was investigated using the respective knockout mice. The results presented reveal important functions of BIN2 for thrombosis and hemostasis *in vitro* and *in vivo*, whereas Hic-5 is dispensable for normal platelet function in mice. Furthermore, in the course of this thesis, it could be shown that the Rho GTPase family members RhoA and Rac1 play major roles in platelet activation at sites of vascular injury but that their functions are non-redundant. Finally, a novel and unexpected function of the hepatic Fc γ RIIB in processing of antibody-opsonized platelets has been shown.

4.1 Bridging integrator 2 (BIN2) controls store operated calcium entry in platelets and thrombotic and thrombo-inflammatory activity in mice

The measurements of Ca²⁺ influx in platelets have shown that the adapter protein BIN2 is critically required for SOCE in murine platelets and that its absence impairs platelet reactivity and results in profound protection from arterial thrombosis and thrombo-inflammatory brain infarction. The presented data indicate that BIN2 directly or indirectly interacts with STIM1 in platelets (Figure 8 A-C) and thereby presumably contributes to the proper assembly and/or function of the SOCE complex in these cells (Figure 10). The exact molecular mechanisms underlying this regulation are not clear, but similar to other BAR domain proteins,^{117,120,121} BIN2 may control ion flux and homeostasis by facilitating specific membrane geometries that enable redistribution of proteins critical for intact SOCE. BIN1, another member of the BIN protein family, has recently been identified as a T-tubule anchoring protein in cardiomyocytes that regulates the microtubule-mediated transport and surface expression of the voltage-dependent L-type calcium channel Cav1.2.¹²⁰ Cardiomyocyte-specific loss of BIN1 resulted in a decreased amount of protective membrane folds of T-tubules and alters cation diffusion within the T-tubules, thus increasing the duration of action potentials.¹²¹ The ultrastructural analysis of BIN2-deficient resting platelets did not reveal any morphological alterations. The analysis of platelets, stimulated with TG to induce the relocalization of the STIM1/Orai1 complex, could provide further insight into a potential mechanism, how BIN2 regulates SOCE. Furthermore, altered expression of SOCE complex component could account for the observed defects. However, Western blot analysis revealed unaltered expression levels of STIM1 (Figure 10). This was not possible for the expression levels of Orai1 in *Bin2^{fl/fl} Pf4-Cre* platelets since the available antibodies against the murine channel protein consistently yielded insufficient specific signals. qPCR analysis of Orai1 mRNA from *Bin2^{fl/fl} Pf4-Cre* platelets and WT platelets might answer this question.

As previously described for mice lacking STIM1⁷⁸ or Orai1,⁸¹ the severe SOCE defect in *Bin2*^{fl/fl Pfl4-Cre} platelets hardly affected their functional responses to GPCR-coupled stimulation, but markedly impaired cellular activation through the (hem)ITAM/PLC γ 2 axis, which is of particular importance for thrombus formation and stabilization under flow, procoagulant activity and occlusive arterial thrombosis *in vivo* (Figure 13, Figure 15). The difference in SOCE dependence between these two major activation pathways is not fully understood. One possible explanation could be that G $_q$ -PLC β -dependent Ca²⁺ store release sufficiently increases [Ca²⁺]_i, enabling cellular responses such as integrin activation or granule secretion independently of Ca²⁺ influx, whereas ITAM-PLC γ 2-induced Ca²⁺ store release might be slightly less effective and thus not sufficient to elicit these cellular responses by itself.

BIN2 is mainly expressed in hematopoietic cells (Figure 8 E). *Bin2*^{-/-} mice are healthy and fertile, indicating that BIN2 is non-essential for embryonic development. This finding is similar to a constitutive knockout for another BAR domain family member, BIN3¹²², whereas deletion of BIN1 leads to perinatal lethality due to a critical role for BIN1 in cardiac muscle development.¹⁸⁰ Only little is known about the function of BIN2 in other cell types. Sánchez-Barrena and colleagues¹²⁴ could show that siRNA knockdown of BIN2 led to reduced cell movement in monocytes and mast cells, but also to enhanced phagocytosis in macrophages. In the presented studies on platelets, processes which require a remodeling of the cytoskeleton, such as platelet spreading and clot retraction were also not affected by BIN2-deficiency. These data indicate that BIN2 plays no obvious role on these actin-dependent processes in platelets and further suggest that the defects from the knockdown experiments might be consequences of reduced [Ca²⁺]_i.¹⁷⁵⁻¹⁷⁷ Further studies are required to analyze whether the knockdown experiments are reproducible in *Bin2*^{-/-} mice and if BIN2 controls SOCE in other cell types as well. It has already been shown that STIM1 controls SOCE in T cells¹⁸⁴ and macrophages.¹⁸⁵ A function of Orai1 in SOCE has been shown for B cells¹⁸⁶ and mast cells,¹⁸⁷ whereas its function in T cells is controversial.^{186,187} Vig *et al.* found normal SOCE in Orai1-deficient murine T cells, which stands in contrast to Orai1-deficient human patients,¹⁸⁸ probably due to species-specific use of CRACM homologs.¹⁸⁷ Unpublished data from our laboratory (Chakarova, Chen, *et al.*, unpublished) indicate that BIN1 and BIN3 are expressed in platelets, but deficiency for BIN1 and BIN3 did not alter platelet function, pointing out that BIN2 is the main isoform in platelets. Nevertheless, it would be interesting to analyze if BIN1 and BIN3 are upregulated in BIN2-deficient platelets and immune cells and provide some compensatory mechanism. If it is like that, the analysis of a double-deficient mouse strain would be interesting.

Remarkably, platelet-specific BIN2 deficiency significantly reduced cerebral infarct growth in a model of acute ischemic stroke without increasing the risk of intracranial hemorrhage (Figure 16). This underpins the critical role of GPVI-ITAM-dependent platelet activation^{164,165} and the

SOCE machinery^{78,81} in the progression of thrombo-inflammatory brain infarction. These findings further corroborate the notion that molecules regulating Ca^{2+} homeostasis in platelets may become promising novel targets in the prevention and/or treatment of thrombotic and thrombo-inflammatory diseases. *Bin2*^{fl/fl Pf4-Cre} mice displayed a ~30% reduction in infarct size, albeit this reduction did not translate into an improved outcome in neurological tests. It is possible that the benefit of the reduced infarct size in *Bin2*^{fl/fl Pf4-Cre} mice can not be revealed in this experimental setup.

Besides the BAR domain, BIN2 contains no further functional domains, which makes it difficult to predict regulatory mechanisms. A potential regulatory mechanism was identified by the observed activation-dependent degradation of BIN2. Analysis of the amino acid sequence (www.calpain.org) predicted several highly conserved cleavage sites and an area lacking any cleavage sites at the N-terminus of BIN2, corresponding to the BAR domain (Figure 18). Upon stimulation of platelets, indeed a fragment with a size corresponding to the BAR domain could be detected when using an antibody directed against the N-terminus of BIN2. Since no cleavage of BIN2 was detectable under physiological conditions and since other BAR protein family members, such as BIN3, mainly consist of the BAR domain, it is possible that the cleavage of BIN2 has no physiological role or that the cleaved form of BIN2 is sufficient to maintain its physiological function. Further experiments measuring SOCE while inhibiting cleavage of the protein and using truncated BIN2 proteins will help to address this question.

In summary, the findings presented here BIN2 as a critical modulator of SOCE in platelets and clearly reveal that BIN2 is required for efficient activation responses of platelets in hemostasis, arterial thrombosis and thrombo-inflammatory brain infarction.

4.2 Normal platelet function in mice lacking hydrogen peroxide-induced clone-5 (Hic-5)

In this study, constitutive knockout mice for Hic-5 were used to assess the role of this focal adhesion protein in platelet function *in vitro* and *in vivo*. No alterations in integrin inside-out or outside-in signaling in the absence of Hic-5 were detectable, arguing against an essential role of this adaptor protein in these processes. Consequently, hemostasis and experimental thrombus formation were not affected by the lack of Hic-5.

These findings stand in contrast to the findings by Kim-Kaneyama and colleagues,¹⁸⁹ who proposed Hic-5 as a novel regulatory factor for integrin $\alpha\text{IIb}\beta\text{3}$ activation and platelet aggregation in mice. They found limited activation of $\alpha\text{IIb}\beta\text{3}$ upon thrombin treatment resulting in weaker thrombin-induced aggregation in Hic-5-null platelets. This activation defect translated into a hemostatic defect and resistance to thromboembolism.

It is difficult to explain the discrepancy between this study and that of Kim-Kaneyama et al.,¹⁸⁹ but differences in the genetic background might contribute, as previously proposed as a possible explanation for differences observed in the phenotype of GPVI-deficient mice.¹⁹⁰ However, it is possible that Hic-5 plays only a minor role in platelet integrin signaling *in vitro* and *in vivo*. Presumably, Hic-5-deficiency can be compensated by the other paxillin family members, paxillin and leupaxin, which are both expressed in murine platelets.¹⁹¹ This is supported by a study from Rathore and colleagues.¹⁹¹ They could show that in aggregating human platelets, Hic-5 was tyrosine phosphorylated and recruited Csk (C-terminal Src kinase) via its SH2 domains to regulate SFK (Src family kinases) activity. However, in aggregating mouse platelets, Csk bound preferentially to paxillin instead of Hic-5, although both are abundantly expressed. It is possible that Hic-5 and the other paxillin family members share some tissue specific functions and that Hic-5 could play important roles in cells or tissues other than platelets. As an example, Hic-5 has been shown to have a role in the development of abdominal aortic aneurysms.¹⁹² Notably, however, in contrast to mouse platelets human platelets express Hic-5 as the only paxillin family member.¹⁹¹ Under these conditions, loss of Hic-5 could exert effects on human platelet function in thrombosis and hemostasis. To investigate this in mice, a mouse strain lacking all three paxillin members would be required.

4.3 Non-redundant functions of small Rho GTPases RhoA and Rac1 in murine platelets

The crucial role of the Rho GTPases RhoA, Rac1 and Cdc42 in platelet function is well-established. RhoA and Cdc42 are important regulators of platelet formation, as deficiency for RhoA or Cdc42 in MKs leads to a significant macrothrombocytopenia, whereas lack of Rac1 has no influence on platelet count and size.

It could be shown in this thesis that RhoA/Rac1 double-deficient mice displayed only a mild macrothrombocytopenia, similar to the phenotype observed in RhoA single-deficient mice. With regard to thrombopoiesis, the lack of Rac1 is negligible in *Rac1*^{-/-} and *RhoA*^{-/-}/*Rac1*^{-/-} mice. It has been recently shown that phosphorylation of RhoA leads to the activation of Rac1 in vascular smooth muscle cells,¹⁹³ which could be a possible explanation for the minor role of Rac1 in platelet production in contrast to RhoA. Although deficiency of Rac1 is of minor importance for platelet biogenesis in *RhoA*^{-/-}/*Rac1*^{-/-} mice, it has a high impact in *Rac1*^{-/-}/*Cdc42*^{-/-} mice,⁶⁹ leading to a more severe macrothrombocytopenia than in *Cdc42*^{-/-} mice and highly altered platelet morphology.

RhoA, Rac1 and Cdc42 also regulate distinct aspects of platelet function. Double-deficiency of RhoA and Cdc42, as well as Rac1 and Cdc42, strongly impairs activation of platelets (Cherpokova *et al.*, unpublished and ⁶⁹). Studies on these mice have shown that the loss of

one Rho GTPase can be, at least partially, compensated by the other, still present, GTPases in the respective single-deficient mice. When both Rho GTPases (*RhoA*^{-/-}/*Cdc42*^{-/-} and *Rac1*^{-/-}/*Cdc42*^{-/-}) are missing, the activation of platelets is severely impaired. In contrast to this, *RhoA*^{-/-}/*Rac1*^{-/-} mice showed the combined defect of each Rho GTPase knockout without an additional effect, both *in vitro* and *in vivo*.

This indicates, that lack of Rac1 has different effects in *RhoA*^{-/-}/*Rac1*^{-/-} and *Rac1*^{-/-}/*Cdc42*^{-/-} double-deficient mice. One possible explanation could be the different shared signaling pathways and effector molecules of Rho GTPases in platelets.¹⁹⁴ RhoA is mainly activated upon stimulation of G₁₃, leading to the activation of the RhoA–ROCK–MLC axis,¹⁹⁵ but also the formin mammalian diaphanous 1 (mDia1), which is also a downstream effector of Cdc42.¹⁹⁶ Unlike RhoA, Rac1 is activated by G_q through PLCβ, but also through integrin- and GPVI-coupled SFKs.^{22,62} This leads to the activation of several downstream effectors, including Arp2/3 and PAK, which are effectors of Cdc42 as well.⁶³ Due to these shared downstream effectors of RhoA and Cdc42 as well as of Rac1 and Cdc42, the deficiency of one Rho GTPase could be easily compensated, but if both GTPases are missing, the effect is severe. Common downstream effectors of RhoA and Rac1 are less obvious, providing a possible explanation, why the functions of RhoA and Rac1 are non-redundant in platelet function. More studies on these signaling pathways in platelets would provide deeper insight into the question why the lack of Rac1 results in the different effects observed in *RhoA*^{-/-}/*Rac1*^{-/-} and *Rac1*^{-/-}/*Cdc42*^{-/-} double deficient mice.

Taken together, the obtained results indicate that the functions of RhoA and Rac1 are very distinct and non-redundant in platelet biogenesis and function. These findings may assist in further understanding of the signaling crosstalks of Rho GTPases.

4.4 Liver sinusoidal endothelial cells process antibody opsonized platelets through the inhibitory Fcγ receptor IIB in mice

These presented results reveal a novel role of the inhibitory FcγRIIB in processing antibody-opsonized platelets and show that LSECs are the critical cell type to execute these functions. The thrombocytopenia promoting effect of FcγRIIB was entirely unexpected, as this receptor is best known for its inhibitory action on either activating FcγRs or BCRs via a Lyn-SHIP1-dependent ITIM phosphorylation cascade.¹³⁶ Moreover, FcγRIIB has been shown to dampen complement-triggered inflammatory reactions¹⁹⁷ and its deficiency results in enhanced immune responses^{146,198} and an increased risk of autoimmunity, in particular systemic lupus erythematosus (SLE).^{199,200} On the other hand, more recent studies have also shown that the engagement of FcγRIIB is critical for immune activation by agonistic anti-CD40 and death receptor antibodies²⁰¹ and contributes to β-amyloid triggered neurotoxicity in Alzheimer's

disease.²⁰² These observations indicate that Fc γ RIIB can have activatory roles in certain settings and that its cross-linking may be sufficient to trigger such activities, as recently discussed.²⁰³

These data show for the first time that LSECs are major effector cells mediating anti-platelet IgG-triggered responses. LSECs have been recognized as the major Fc γ RIIB-expressing cell pool and reported to represent about three-quarters of the total Fc γ RIIB in the body, despite the absence of activating Fc γ Rs or BCR.¹³⁷ Interestingly, Fc γ RIIB has been implicated in mediating the protective effects of intravenous immunoglobulin (IVIG),¹⁷⁸ but the underlying mechanisms are still incompletely understood and several models are controversially discussed. To date, a possible role of LSEC-expressed Fc γ RIIB as a mediator of the protective/therapeutic effects of IVIG in ITP has not been assessed.^{204,205} In light of these data and the prominent role of LSECs in clearing sIC,¹³⁷ it might be worth considering future studies on a potential involvement of these cells in auto-immune diseases.

Like myeloid cells, LSECs express predominantly the b2 isoform of Fc γ RIIB shown to form clustered structures for efficient elimination of sICs. In contrast, the b1 isoform alternatively expressed by B cells, prevents association with clathrin-coated pits and internalization when co-ligated with the BCR.²⁰⁶ It is unclear at present how the interaction between Fc γ RIIB and antibody-opsonized platelets would result in the quantitative loss of platelet GPVI. The high abundance of Fc γ RIIBb2 on LSEC and its capacity to cluster anti-GPVI-antibodies may however provide a sufficient cross-linking array necessary for platelet binding, activation and potent GPVI signaling that in turn results in the generation of sGPVI.

It was previously shown by our group that combined loss of ADAM17 and ADAM10 in platelets prevents GPVI shedding *in vitro* but not *in vivo*.³⁹ In light of the data of the sequestration of platelets to the liver (Figure 31), shedding *in trans* might be a possible mechanism. Trans-shedding has first been described for ADAM10-mediated processing of ephrin-5a¹⁷⁶ and has more recently been proposed to contribute to T cell transmigration via VE-cadherin shedding by ADAM10. However, mice constitutively lacking ADAM17³⁹ or ADAM10 in endothelial cells (Figure 33) did not display any alterations in the production of sGPVI. Thus, the protease responsible for the generation of sGPVI *in vivo* remains elusive. Of note, GPVI clustering appears to be required for GPVI down-regulation to occur, as Fab fragments of anti-GPVI antibodies do not affect GPVI surface expression on murine platelets.²⁰⁷ This seemingly contradicts the first report of the *in vivo* effects of JAQ1, where it was reported that JAQ1-Fab fragments do cause a very mild but significant transient thrombocytopenia.³⁶ A possible explanation for this discrepancy could be very low concentrations of undigested IgG or other contaminants, such as trace amounts of endotoxin, might have been present in the Fab preparations and induced the small drop in platelet counts. Thus, it appears that efficient *in*

in vivo GPVI down-regulation requires a bivalent binding moiety at least in mice. However, Newman and colleagues³⁷ elegantly demonstrated that anti-GPVI-Fab fragments are able to immuno-deplete GPVI from human platelets in a NOD/SCID mouse model. One explanation might be that human platelets are more 'reactive' in terms of GPVI shedding than their murine counterparts, as agonist-induced platelet activation results in GPVI shedding of human, but not of murine platelets.^{33,39,208} The primary route of antibody-induced GPVI ectodomain shedding *in vivo* depends on the interaction between the anti-GPVI IgG and endothelial Fc γ RIIB (Figure 31), as well as on intact GPVI signaling. In the absence of either, GPVI is downregulated by internalization/degradation, which appears to be a slower process compared to shedding (Figure 29, Figure 31).³⁸

Taken together, these data demonstrate for the first time that LSECs are critically involved in the processing of antibody opsonized platelets and that this is strictly dependent on Fc γ RIIB in these cells. This novel pathway not only contributed to anti-platelet antibody induced thrombocytopenia but was also essential for targeted GPVI ectodomain shedding *in vivo* which is the first report of a platelet function modulating regimen acting *in trans*. These results may contribute to a better understanding of the pathomechanisms underlying platelet processing in ITP, but also be important for the development of antibody-based anti-platelet therapies.

4.5 Outlook and concluding remarks

The findings summarized in this thesis shed new light on the mechanisms of platelet activation and receptor regulation. BIN2 and Hic-5 deficient mice were characterized. In addition, redundant functions of the Rho GTPases RhoA and Rac1 in double-deficient mice were analyzed. Further, the function of hepatic Fc γ RIIB in the processing of antibody-opsonized platelets was analyzed.

Studies on BIN2-deficient mice identified BIN2 as a critical regulator of platelet SOCE in thrombosis and thrombo-inflammatory disease. However, the question remains, whether BIN2 regulates SOCE in other cell types as well or exclusively in platelets. Further experiments on these cell types using constitutive *Bin2*^{-/-} will help to answer this question. It has already been reported, that siRNA knockdown of BIN2 alters the function of immune cells *in vitro*. If this can be confirmed in immune cells obtained from *Bin2*^{-/-} mice, the effect of BIN2-deficiency on immune cells could also be analyzed using respective *in vivo* models. The consequences of BIN2 deficiency in platelets were analyzed in detail. At this point, the mechanism of BIN2 function is not completely understood. There are several approaches that help to further understand BIN2 function. The analysis of platelet store content and agonist induced store release, as well as the use of different inhibitors and modulators of the calcium signaling pathway in platelets, like LOE 908²⁰⁹ to inhibit TRPC6, 2APB²¹⁰ an IP₃ receptor antagonist or the CRAC channel inhibitor BTP2²¹¹ may help to further understand how BIN2 regulates

SOCE. The small size of murine platelets limits studies on the localization of BIN2. The establishment of a heterologous cell system, where the phenotype of BIN2-deficiency can be reproduced, could help to analyze localization of BIN2 in resting cells and after stimulation. With regard to the calpain-dependent cleavage of BIN2 upon stimulation with TG and ionomycin, a physiological role of this process is unclear. Still, the identification of calpain cleavage sites after *in vitro* digestion of BIN2 would be of high interest for the understanding of calpain activity. Interestingly, it was shown for other BAR domain family members, like BIN1 and BIN3 that the deletion of respective proteins increases susceptibility to lung cancer and lymphoma respectively during aging supporting a role for these BAR domain proteins as tumor suppressors.^{118,122} Further studies are required to analyze if BIN2 acts as a tumor suppressor as well.

Studies on Hic-5-deficient mice did not show any role of Hic-5 in integrin α IIb β 3 activation and consequently does not play a role in thrombosis and hemostasis. In contrast to human platelets mouse platelets express besides Hic-5 also the other paxillin family member paxillin and leupaxin. Although no alterations of the expression of paxillin and leupaxin were detectable in Hic-5-deficient mice compared to WT-mice, a mouse strain lacking all three paxillin members would be required, to assess possible compensatory effects.

Rho GTPases have been established as critical regulators of cytoskeletal rearrangements. The data summarized in this thesis demonstrate that the Rho GTPases RhoA and Rac1 have non-redundant functions in the control of platelet production and function. However, Rho GTPases have been increasingly recognized as important modulators of the final steps of megakaryopoiesis, as well. A current model of thrombopoiesis suggests that mature MKs are localized in the vicinity of vascular sinusoids in which they extend and release proplatelets.²¹² What remains elusive are the mechanisms responsible for the final localization of the MKs close to the blood vessels in the BM and how interactions between differentiated MKs and sinusoidal endothelial cells are regulated. Data from our laboratory have only recently led to the hypothesis that RhoA may act as a negative regulator of MK migration and directed proplatelet formation *in vivo*. The effects of double-deficiency of RhoA/Rac1 on the final steps of megakaryopoiesis are the current subject of intensive research.

Anti-platelet therapy is the first line treatment for cardio- and cerebrovascular diseases. Limitations of current therapies include weak inhibition of platelet function and the inability to separate the desired anti-thrombotic function from an increase in bleeding events. Therefore, novel anti-thrombotic targets are needed to overcome these restraints. The absence or functional inhibition of GPVI provides protection from pathological thrombus formation without causing major bleeding complications. While different anti-GPVI antibodies of the IgG class efficiently deplete the receptor *in vivo* they do not affect GPVI surface expression in platelets

in vitro, indicating the involvement of a non-platelet compartment. LSECS, bearing the inhibitory Fc γ RIIB showed an important role in processing antibody-opsonized platelets. Deficiency of Fc γ RIIB inhibited GPVI immunodepletion, but also prevented thrombocytopenia in mice treated with antibodies against GPIIb/IIIa, the major target antigen in human ITP. The identification of hepatic Fc γ RIIB in the processing of antibody-opsonized platelets could help to establish a functional *in vitro* system of GPVI immunodepletion to get deeper insights in the mechanism of how this platelet function modulating regimen is acting *in trans*. Although the inhibitory Fc γ RIIB, but not the activatory Fc γ RIII, abolished sequestration of anti-GPVI opsonized platelets, studies on Fc γ RIII could reveal regulatory mechanisms of other platelet surface receptors.

5 References

1. Grozovsky R, Hoffmeister KM, Falet H. Novel clearance mechanisms of platelets. *Curr. Opin. Hematol.* 2010;17(6):585–589.
2. G. Fox J, W. Barthold S, Davisson MT, et al. The Mouse in Biomedical Research. *Acad. Press.* 2007;
3. Daly ME. Determinants of platelet count in humans. *Haematologica.* 2011;96(1):10–13.
4. Patel SR, Hartwig JH, Jr JEI. Review series The biogenesis of platelets from megakaryocyte proplatelets. 2005;115(12.):
5. Italiano JE, Patel-Hett S, Hartwig JH. Mechanics of proplatelet elaboration. *J. Thromb. Haemost.* 2007;5(SUPPL. 1):18–23.
6. Stasi R. Pathophysiology and therapeutic options in primary immune thrombocytopenia. *Blood Transfus.* 2011;9(3):262–273.
7. Hadjadj J, Michel M, Chauveheid MP, et al. Immune thrombocytopenia in chronic myelomonocytic leukemia. *Eur J Haematol.* 2014;93:521–526.
8. Ochs H, Thrasher A. The Wiskott-Aldrich syndrome. *J. Allergy Clin. Immunol.* 2006;117(4):725–738.
9. Peck-Radosavljevic M. Hypersplenism. *Eur. J. Gastroenterol. Hepatol.* 2001;13(4):317–23.
10. Machlus KR, Thon JN, Italiano JE. Interpreting the developmental dance of the megakaryocyte: A review of the cellular and molecular processes mediating platelet formation. *Br. J. Haematol.* 2014;165(2):227–236.
11. Thon J, Italiano J. Platelets: Production, Morphology and Ultrastructure. *Antiplatelet Agents SE - 1.* 2012;210:3–22.
12. Ruggeri ZM. Platelets in atherothrombosis. *Nat. Med.* 2002;8(11):1227–1234.
13. Lozano R, Naghavi M, Foreman K, et al. Global and regional mortality from 235 causes of death for 20 age groups in 1990 and 2010: a systematic analysis for the Global Burden of Disease Study 2010. *Lancet.* 2016;380(9859):2095–2128.
14. Varga-Szabo D, Pleines I, Nieswandt B. Cell adhesion mechanisms in platelets. *Arterioscler. Thromb. Vasc. Biol.* 2008;28(3):403–413.
15. Savage B, Almus-Jacobs F, Ruggeri ZM. Specific synergy of multiple substrate-receptor interactions in platelet thrombus formation under flow. *Cell.* 1998;94(5):657–666.
16. Nieswandt B, Watson SP. Platelet-collagen interaction: Is GPVI the central receptor? *Blood.* 2003;102(2):449–61.
17. Nieswandt B, Brakebusch C, Bergmeier W, et al. Glycoprotein VI but not $\alpha 2\beta 1$ integrin is essential for platelet interaction with collagen. *EMBO J.* 2001;20(9):2120–2130.
18. Heemskerk J, Mattheij N, Cosemans J. Platelet-based coagulation: different populations, different functions. *J. Thromb. Haemost.* 2013;11(1):2–16.
19. De Witt SM, Verdoold R, Cosemans JMEM, Heemskerk JWM. Insights into platelet-based control of coagulation. *Thromb. Res.* 2014;133(SUPPL. 2):S139–S148.
20. Offermanns S. Activation of platelet function through G protein-coupled receptors. *Circ. Res.* 2006;99(12):1293–304.
21. Watson SP, Auger JM, McCarty OJT, Pearce AC. GPVI and integrin $\alpha \text{IIb} \beta 3$ signaling in platelets. *J. Thromb. Haemost.* 2005;3(8):1752–1762.

22. Offermanns S, Toombs CF, Hu YH, Simon MI. Defective platelet activation in G alpha(q)-deficient mice. *Nature*. 1997;389(6647):183–186.
23. Hart MJ, Jiang X, Kozasa T, et al. Direct stimulation of the guanine nucleotide exchange activity of p115 RhoGEF by G alpha13. *Science*. 1998;280(5372):2112–2114.
24. Cantley LC. The phosphoinositide 3-kinase pathway. *Science*. 2002;296(5573):1655–1657.
25. Reth M. Antigen receptor tail clue. *Nature*. 1989;338(6214):383–384.
26. Isakov N. Immunoreceptor tyrosine-based activation motif (ITAM), a unique module linking antigen and Fc receptors to their signaling cascades. *J. Leukoc. Biol.* 1997;61(1):6–16.
27. Stegner D, Haining EJ, Nieswandt B. Targeting glycoprotein VI and the immunoreceptor tyrosine-based activation motif signaling pathway. *Arterioscler. Thromb. Vasc. Biol.* 2014;34(8):1615–1620.
28. Sims PJ, Wiedmer T, Esmon CT, Weiss HJ, Shattil SJ. Assembly of the platelet prothrombinase complex is linked to vesiculation of the platelet plasma membrane. Studies in Scott syndrome: An isolated defect in platelet procoagulant activity. *J. Biol. Chem.* 1989;264(29):17049–17057.
29. Berlanga O, Tulasne D, Bori T, et al. The Fc receptor gamma-chain is necessary and sufficient to initiate signalling through glycoprotein VI in transfected cells by the snake C-type lectin, convulxin. *Eur. J. Biochem.* 2002;269(12):2951–2960.
30. Watson S, Herbert J, Pollitt A. GPVI and CLEC-2 in hemostasis and vascular integrity. *J. Thromb. Haemost.* 2010;8(7):1456–1467.
31. Berlanga O, Bori-Sanz T, James JR, et al. Glycoprotein VI oligomerization in cell lines and platelets. *J. Thromb. Haemost.* 2007;5(5):1026–1033.
32. Miura Y, Takahashi T, Jung SM, Moroi M. Analysis of the interaction of platelet collagen receptor glycoprotein VI (GPVI) with collagen: A dimeric form of GPVI, but not the monomeric form, shows affinity to fibrous collagen. *J. Biol. Chem.* 2002;277(48):46197–46204.
33. Arthur JF, Shen Y, Kahn ML, et al. Ligand binding rapidly induces disulfide-dependent dimerization of glycoprotein VI on the platelet plasma membrane. *J. Biol. Chem.* 2007;282(42):30434–30441.
34. Dütting S, Bender M, Nieswandt B. Platelet GPVI: A target for antithrombotic therapy?! *Trends Pharmacol. Sci.* 2012;33(11):583–590.
35. Vögtle T, Cherpokova D, Nieswandt B. Targeting platelet receptors in thrombotic and thrombo-inflammatory disorders. *Haemostaseologie*. 2015;35(3):235–243.
36. Nieswandt B, Schulte V, Bergmeier W, et al. Long-term antithrombotic protection by in vivo depletion of platelet glycoprotein VI in mice. *J. Exp. Med.* 2001;193(4):459–469.
37. Boylan B, Berndt MC, Kahn ML, Newman PJ. Activation-independent, antibody-mediated removal of GPVI from circulating human platelets: development of a novel NOD/SCID mouse model to evaluate the in vivo effectiveness of anti-human platelet agents. *Blood*. 2006;108(3):908–14.
38. Rabie T, Varga-Szabo D, Bender M, et al. Diverging signaling events control the pathway of GPVI down-regulation in vivo. *Blood*. 2007;110(2):529–35.
39. Bender M, Hofmann S, Stegner D, et al. Differentially regulated GPVI ectodomain shedding by multiple platelet-expressed proteinases. *Blood*. 2010;116(17):3347–3355.
40. Suzuki-Inoue K. A novel Syk-dependent mechanism of platelet activation by the C-type

- lectin receptor CLEC-2. *Blood*. 2006;107(2):542–549.
41. Hughes CE, Pollitt AY, Mori J, et al. CLEC-2 activates Syk through dimerization. *Blood*. 2010;115(14):2947–2955.
 42. Bender M, Hagedorn I, Nieswandt B. Genetic and antibody-induced glycoprotein VI deficiency equally protects mice from mechanically and FeCl₃-induced thrombosis. *J. Thromb. Haemost.* 2011;9(7):1423–1426.
 43. May F, Hagedorn I, Pleines I, et al. CLEC-2 is an essential platelet activating receptor in hemostasis and thrombosis. *Blood*. 2009;114(16):3464–3473.
 44. Boulaftali Y, Hess PR, Getz TM, et al. Platelet ITAM signaling is critical for vascular integrity in inflammation. *J. Clin. Invest.* 2013;123(2):908–916.
 45. Bender M, May F, Lorenz V, et al. Combined in vivo depletion of glycoprotein VI and C-type lectin-like receptor 2 severely compromises hemostasis and abrogates arterial thrombosis in mice. *Arterioscler. Thromb. Vasc. Biol.* 2013;33(5):926–934.
 46. Herzog BH, Fu J, Wilson SJ, et al. Podoplanin maintains high endothelial venule integrity by interacting with platelet CLEC-2. *Nature*. 2013;502(1476-4687):105–109.
 47. Bertozzi CC, Schmaier AA, Mericko P, et al. Platelets regulate lymphatic vascular development through CLEC-2-SLP-76 signaling. *Blood*. 2010;116(4):661–670.
 48. Nayar S, Finney BA, Withers DR, et al. CLEC-2 is required for development and maintenance of lymph nodes. 2014;123(20):3200–3207.
 49. Suzuki-Inoue K, Inoue O, Ding G, et al. Essential in vivo roles of the C-type lectin receptor CLEC-2: Embryonic/neonatal lethality of CLEC-2-deficient mice by blood/lymphatic misconnections and impaired thrombus formation of CLEC-2-deficient platelets. *J. Biol. Chem.* 2010;285(32):24494–24507.
 50. Murugappa S, Kunapuli S. The role of ADP receptors in platelet function. *Front. Biosci.* 2006;(11):1977–86.
 51. Thomas DW, Mannon RB, Mannon PJ, et al. Coagulation defects and altered hemodynamic responses in mice lacking receptors for thromboxane A₂. *J. Clin. Invest.* 1998;102(11):1994–2001.
 52. Mackman N. Role of Tissue Factor in Hemostasis, Thrombosis, and Vascular Development. *Arterioscler. Thromb. Vasc. Biol.* 2004;24(6):1015–1022.
 53. Martorell L, Martínez-González J, Rodríguez C, et al. Thrombin and protease-activated receptors (PARs) in atherothrombosis. *Thromb. Haemost.* 2008;99(2):305–315.
 54. Stegner D, Nieswandt B. Platelet receptor signaling in thrombus formation. *J. Mol. Med.* 2011;89(2):109–21.
 55. Heasman SJ, Ridley AJ. Mammalian Rho GTPases: new insights into their functions from in vivo studies. *Nat. Rev. Mol. Cell Biol.* 2008;9(9):690–701.
 56. Jaffe AB, Hall A. Rho GTPases: biochemistry and biology. *Annu. Rev. Cell Dev. Biol.* 2005;21:247–69.
 57. Pleines I, Hagedorn I, Gupta S, et al. Megakaryocyte-specific RhoA deficiency causes macrothrombocytopenia and defective platelet activation in hemostasis and thrombosis. *Blood*. 2012;119(4):1054–63.
 58. Pleines I, Elvers M, Strehl A, et al. Rac1 is essential for phospholipase C-gamma2 activation in platelets. *Pflugers Arch.* 2009;457(5):1173–85.
 59. Pleines I, Eckly A, Elvers M, et al. Multiple alterations of platelet functions dominated by increased secretion in mice lacking Cdc42 in platelets. *Blood*. 2010;115(16):3364–73.

-
60. Wheeler AP, Ridley AJ. Why three Rho proteins? RhoA, RhoB, RhoC, and cell motility. *Exp. Cell Res.* 2004;301(1):43–49.
 61. Klages B, Brandt U, Simon MI, Schultz G, Offermanns S. Activation of G12/G13 results in shape change and Rho/Rho-kinase-mediated myosin light chain phosphorylation in mouse platelets. *J. Cell Biol.* 1999;144(4):745–754.
 62. McCarty OJT, Larson MK, Auger JM, et al. Rac1 is essential for platelet lamellipodia formation and aggregate stability under flow. *J. Biol. Chem.* 2005;280(47):39474–39484.
 63. Stefanini L, Boulaftali Y, Ouellette TD, et al. Rap1-Rac1 Circuits Potentiate Platelet Activation. *Arterioscler. Thromb. Vasc. Biol.* 2012;32(2):434–441.
 64. Gao Y, Dickerson JB, Guo F, Zheng J, Zheng Y. Rational design and characterization of a Rac GTPase-specific small molecule inhibitor. *Proc. Natl. Acad. Sci. U. S. A.* 2004;101(20):7618–23.
 65. Shutes A, Onesto C, Picard V, et al. Specificity and mechanism of action of EHT 1864, a novel small molecule inhibitor of Rac family small GTPases. *J. Biol. Chem.* 2007;282(49):35666–35678.
 66. Dütting S, Heidenreich J, Cherpokova D, et al. Critical off-target effects of the widely used Rac1 inhibitors NSC23766 and EHT1864 in mouse platelets. *J. Thromb. Haemost.* 2015;13(5):827–838.
 67. Akbar H, Shang X, Perveen R, et al. Gene targeting implicates Cdc42 GTPase in GPVI and non-GPVI mediated platelet filopodia formation, secretion and aggregation. *PLoS One.* 2011;6(7):e22117.
 68. Goggs R, Savage JS, Mellor H, Poole AW. The Small GTPase Rif Is Dispensable for Platelet Filopodia Generation in Mice. *PLoS One.* 2013;8(1.):
 69. Pleines I, Dütting S, Cherpokova D, et al. Defective tubulin organization and proplatelet formation in murine megakaryocytes lacking Rac1 and Cdc42. *Blood.* 2013;122(18):3178–87.
 70. Berridge MJ, Bootman MD, Roderick HL. Calcium signalling: dynamics, homeostasis and remodelling. *Nat. Rev. Mol. Cell Biol.* 2003;4(7):517–529.
 71. Hathaway DR, Adelstein RS. Human platelet myosin light chain kinase requires the calcium-binding protein calmodulin for activity. *Proc. Natl. Acad. Sci. U. S. A.* 1979;76(4):1653–1657.
 72. Shattil SJ, Brass LF. Induction of the fibrinogen receptor on human platelets by intracellular mediators. *J. Biol. Chem.* 1987;262(3):992–1000.
 73. Putney JW. A model for receptor-regulated calcium entry. *Cell Calcium.* 1986;7(1):1–12.
 74. Parekh A, Putney Jr J. Store-operated calcium channels. *Physiol. Rev.* 2005;85(2):757–810.
 75. Williams RT, Manji SS, Parker NJ, et al. Identification and characterization of the STIM (stromal interaction molecule) gene family: coding for a novel class of transmembrane proteins. *Biochem. J.* 2001;357(Pt 3):673–685.
 76. Stathopoulos PB, Zheng L, Li G-Y, Plevin MJ, Ikura M. Structural and Mechanistic Insights into STIM1-Mediated Initiation of Store-Operated Calcium Entry. *Cell.* 2008;135(1):110–122.
 77. Grosse J, Braun A, Varga-Szabo D, et al. An EF hand mutation in Stim1 causes premature platelet activation and bleeding in mice. *J. Clin. Invest.* 2007;117(11):3540–50.
-

-
78. Varga-Szabo D, Braun A, Kleinschnitz C, et al. The calcium sensor STIM1 is an essential mediator of arterial thrombosis and ischemic brain infarction. *J. Exp. Med.* 2008;205(7):1583–1591.
 79. Prakriya M, Feske S, Gwack Y, et al. Orai1 is an essential pore subunit of the CRAC channel. *Nature.* 2006;443(7108):230–233.
 80. Vig M, Beck A, Billingsley JM, et al. CRACM1 Multimers Form the Ion-Selective Pore of the CRAC Channel. *Curr. Biol.* 2006;16(20):2073–2079.
 81. Braun A, Varga-Szabo D, Kleinschnitz C, et al. Orai1 (CRACM1) is the platelet SOC channel and essential for pathological thrombus formation. *Blood.* 2009;113(9):2056–2063.
 82. Hassock SR, Zhu MX, Trost C, et al. Expression and role of TRPC proteins in human platelets: Evidence that TRPC6 forms the store-independent calcium entry channel. *Blood.* 2002;100(8):2801–2811.
 83. Ramanathan G, Gupta S, Thielmann I, et al. Defective diacylglycerol-induced Ca²⁺ entry but normal agonist-induced activation responses in TRPC6-deficient mouse platelets. *J. Thromb. Haemost.* 2012;10(3):419–429.
 84. Chen W, Thielmann I, Gupta S, et al. Orai1-induced store-operated Ca²⁺ entry enhances phospholipase activity and modulates canonical transient receptor potential channel 6 function in murine platelets. *J. Thromb. Haemost.* 2014;12(4):528–539.
 85. Mahaut-Smith M, Sage S. Activation of Receptor-operated Cation Channels via P2X1 Not P2T Purinoceptors in Human Platelets. *J. Biol. Chem.* 1996;271(6):2879–2881.
 86. Hechler B, Lenain N, Marchese P, et al. A role of the fast ATP-gated P2X1 cation channel in thrombosis of small arteries in vivo. *J. Exp. Med.* 2003;198(4):661–667.
 87. Nieswandt B, Varga-Szabo D, Elvers M. Integrins in platelet activation. *J. Thromb. Haemost.* 2009;7 Suppl 1:206–9.
 88. Hynes RO. Integrins: Bidirectional, allosteric signaling machines. *Cell.* 2002;110(6):673–687.
 89. Shattil SJ, Newman PJ. Integrins: Dynamic scaffolds for adhesion and signaling in platelets. *Blood.* 2004;104(6):1606–1615.
 90. Bennett JS. Structure and function of the platelet integrin α IIb β 3. *J. Clin. Invest.* 2005;115(12):3363–3369.
 91. Nieswandt B, Pleines I, Bender M. Platelet adhesion and activation mechanisms in arterial thrombosis and ischaemic stroke. *J. Thromb. Haemost.* 2011;9:92–104.
 92. Ginsberg MH, Partridge A, Shattil SJ. Integrin regulation. *Curr. Opin. Cell Biol.* 2005;17(5):509–16.
 93. Legate KR, Fässler R. Mechanisms that regulate adaptor binding to beta-integrin cytoplasmic tails. *J. Cell Sci.* 2009;122(Pt 2):187–198.
 94. Tadokoro S, Shattil SJ, Eto K, et al. Talin binding to integrin beta tails: a final common step in integrin activation. *Science.* 2003;302(5642):103–6.
 95. Petrich BG, Marchese P, Ruggeri ZM, et al. Talin is required for integrin-mediated platelet function in hemostasis and thrombosis. *J. Exp. Med.* 2007;204(13):3103–11.
 96. Nieswandt B, Moser M, Pleines I, et al. Loss of talin1 in platelets abrogates integrin activation, platelet aggregation, and thrombus formation in vitro and in vivo. *J. Exp. Med.* 2007;204(13):3113–3118.
 97. Xu Z, Chen X, Zhi H, et al. Direct Interaction of Kindlin-3 With Integrin α IIb β 3 in Platelets
-

-
- Is Required for Supporting Arterial Thrombosis in Mice. *Arterioscler. Thromb. Vasc. Biol.* 2014;
98. Moser M, Nieswandt B, Ussar S, Pozgajova M, Fässler R. Kindlin-3 is essential for integrin activation and platelet aggregation. *Nat. Med.* 2008;14(3):325–30.
 99. Ma Y-Q, Qin J, Wu C, Plow EF. Kindlin-2 (Mig-2): a co-activator of beta3 integrins. *J. Cell Biol.* 2008;181(3):439–46.
 100. Ginsberg AB and MH. Integrin activation. *Biochem Soc Trans.* 2008;36(Pt 2):229–234.
 101. Chrzanowska-Wodnicka M, Smyth S, Schönwälder S, Fischer T, White G. Rap1b is required for normal platelet function and hemostasis in mice. 2005;115(3):1–8.
 102. Crittenden JR, Bergmeier W, Zhang Y, et al. CalDAG-GEFI integrates signaling for platelet aggregation and thrombus formation. *Nat. Med.* 2004;10(9):982–986.
 103. Cifuni S, Wagner D, Bergmeier W. CalDAG-GEFI and protein kinase C represent alternative pathways leading to activation of integrin alphaIIb beta3 in platelets. 2008;112(5):1696–1703.
 104. Stritt S, Wolf K, Lorenz V, et al. Rap1-GTP – interacting adaptor molecule (RIAM) is dispensable for platelet integrin activation and function in mice. *Blood.* 2015;125(2):219–223.
 105. Shibanuma M, Mashimo J, Kuroki T, Nose K. Characterization of the TGF beta 1-inducible hic-5 gene that encodes a putative novel zinc finger protein and its possible involvement in cellular senescence. *J. Biol. Chem.* 1994;269(43):26767–26774.
 106. Hagmann J, Grob M, Welman A, van Willigen G, Burger MM. Recruitment of the LIM protein hic-5 to focal contacts of human platelets. *J. Cell Sci.* 1998;111:2181–8.
 107. Thomas SM, Hagel M, Turner CE. Characterization of a focal adhesion protein, Hic-5, that shares extensive homology with paxillin. *J. Cell Sci.* 1999;112:181–90.
 108. Bach I. The LIM domain: Regulation by association. *Mech. Dev.* 2000;91(1-2):5–17.
 109. Schmeichel KL, Beckerle MC. The LIM domain is a modular protein-binding interface. *Cell.* 1994;79(2):211–219.
 110. Sakata A, Ohmori T, Nishimura S, et al. Paxillin is an intrinsic negative regulator of platelet activation in mice. *Thromb. J.* 2014;12(1):1.
 111. Kim-Kaneyama J, Takeda N, Sasai A, et al. Hic-5 deficiency enhances mechanosensitive apoptosis and modulates vascular remodeling. *J. Mol. Cell. Cardiol.* 2011;50(1):77–86.
 112. Popp M, Thielmann I, Nieswandt B, Stegner D. Normal Platelet Integrin Function in Mice Lacking Hydrogen Peroxide-Induced Clone-5 (Hic-5). *PLoS One.* 2015;10(7):e0133429.
 113. Sakamuro D, Elliott KJ, Wechsler-Reya R, Prendergast GC. BIN1 is a novel MYC-interacting protein with features of a tumour suppressor. *Nat. Genet.* 1996;14(1):69–77.
 114. David C, Solimena M, De Camilli P. Autoimmunity in Stiff-Man syndrome with breast cancer is targeted to the C-terminal region of human amphiphysin, a protein similar to the yeast proteins, Rvs167 and Rvs161. *FEBS Lett.* 1994;351(1):73–79.
 115. Peter BJ, Kent HM, Mills IG, et al. BAR domains as sensors of membrane curvature: the amphiphysin BAR structure. *Science.* 2004;303(5657):495–9.
 116. Ren G, Vajjhala P, Lee JS, Winsor B, Munn AL. The BAR Domain Proteins : Molding Membranes in Fission , Fusion , and Phagy. *Microbiol Mol Biol Rev.* 2006;70(1):37–120.
-

117. Suetsugu S, Toyooka K, Senju Y. Subcellular membrane curvature mediated by the BAR domain superfamily proteins. *Semin. Cell Dev. Biol.* 2010;21(4):340–9.
118. Chang MY, Boulden J, Katz JB, et al. Bin1 ablation increases susceptibility to cancer during aging, particularly lung cancer. *Cancer Res.* 2007;67(16):7605–12.
119. Prendergast GC, Muller AJ, Ramalingam A, Chang MY. BAR the door: cancer suppression by amphiphysin-like genes. *Biochim. Biophys. Acta.* 2009;1795(1):25–36.
120. Hong TT, Smyth JW, Gao D, et al. BIN1 localizes the L-type calcium channel to cardiac T-tubules. *PLoS Biol.* 2010;8(2.):
121. Hong T, Yang H, Zhang S-S, et al. Cardiac BIN1 folds T-tubule membrane, controlling ion flux and limiting arrhythmia. *Nat. Med.* 2014;20(6):624–32.
122. Ramalingam A, Duhadaway JB, Sutanto-Ward E, et al. Bin3 deletion causes cataracts and increased susceptibility to lymphoma during aging. *Cancer Res.* 2008;68(6):1683–1690.
123. Ge K, Prendergast GC. Bin2, a functionally nonredundant member of the BAR adaptor gene family. *Genomics.* 2000;67(2):210–20.
124. Sánchez-Barrena MJ, Vallis Y, Clatworthy MR, et al. Bin2 is a membrane sculpting N-BAR protein that influences leucocyte podosomes, motility and phagocytosis. *PLoS One.* 2012;7(12):e52401.
125. Neunert C, Lim W, Crowther M, et al. The American Society of Hematology 2011 evidence-based practice guideline for immune thrombocytopenia. *Blood.* 2011;117(16):4190–4207.
126. McKenzie CGJ, Guo L, Freedman J, Semple JW. Cellular immune dysfunction in immune thrombocytopenia (ITP). *Br. J. Haematol.* 2013;163(1):10–23.
127. Cines DB, Bussel JB, Liebman H a, Luning Prak ET. The ITP syndrome: pathogenic and clinical diversity. *Blood.* 2009;113(26):6511–21.
128. McMillan R. Antiplatelet antibodies in chronic adult immune thrombocytopenic purpura: assays and epitopes. *J. Pediatr. Hematol. Off. J. Am. Soc. Pediatr. Hematol.* 2003;25 Suppl 1(December):S57–S61.
129. Nieswandt B, Bergmeier W, Rackebrandt K, et al. Identification of critical antigen-specific mechanisms in the development of immune thrombocytopenic purpura in mice Identification of critical antigen-specific mechanisms in the development of immune thrombocytopenic purpura in mice. 2000;96(7):2520–2527.
130. Webster ML, Sayeh E, Crow M, et al. Relative efficacy of intravenous immunoglobulin G in ameliorating thrombocytopenia induced by antiplatelet GPIIb/IIIa versus GPIb/alpha antibodies. *Blood.* 2006;108(3):943–6.
131. Li J, van der Wal DE, Zhu G, et al. Desialylation is a mechanism of Fc-independent platelet clearance and a therapeutic target in immune thrombocytopenia. *Nat. Commun.* 2015;6:7737.
132. Chang M, Nakagawa P a., Williams S a., et al. Immune thrombocytopenic purpura (ITP) plasma and purified ITP monoclonal autoantibodies inhibit megakaryocytopoiesis in vitro. *Blood.* 2003;102(3):887–895.
133. Olsson B, Andersson P-O, Jernås M, et al. T-cell-mediated cytotoxicity toward platelets in chronic idiopathic thrombocytopenic purpura. *Nat. Med.* 2003;9(9):1123–1124.
134. Kuwana M, Okazaki Y, Ikeda Y. Splenic macrophages maintain the anti-platelet autoimmune response via uptake of opsonized platelets in patients with immune thrombocytopenic purpura. *J. Thromb. Haemost.* 2009;7(2):322–329.

135. Nimmerjahn F, Ravetch J V. Fcγ receptors as regulators of immune responses. *Nat. Rev. Immunol.* 2008;8(1):34–47.
136. Smith KGC, Clatworthy MR. FcγRIIB in autoimmunity and infection: evolutionary and therapeutic implications. *Nat. Rev. Immunol.* 2010;10(5):328–343.
137. Ganesan LP, Kim J, Wu Y, et al. Fc RIIb on Liver Sinusoidal Endothelium Clears Small Immune Complexes. *J. Immunol.* 2012;189(10):4981–4988.
138. Ganesan LP, Mohanty S, Kim J, et al. Rapid and efficient clearance of blood-borne virus by liver sinusoidal endothelium. *PLoS Pathog.* 2011;7(9):
139. Bergmeier W, Rackebrandt K, Schröder W, Zirngibl H, Nieswandt B. Structural and functional characterization of the mouse von Willebrand factor receptor GPIb-IX with novel monoclonal antibodies. *Blood.* 2000;95(3):886–893.
140. Nieswandt B, Bergmeier W, Schulte V, et al. Expression and function of the mouse collagen receptor glycoprotein VI is strictly dependent on its association with the FcRγ chain. *J. Biol. Chem.* 2000;275(31):23998–24002.
141. Schulte V, Rabie T, Prostredna M, et al. Targeting of the collagen-binding site on glycoprotein VI is not essential for in vivo depletion of the receptor. *Blood.* 2003;101(10):3948–3952.
142. Bergmeier W, Schulte V, Brockhoff G, et al. Flow cytometric detection of activated mouse integrin αIIbβ3 with a novel monoclonal antibody. *Cytometry.* 2002;48(2):80–86.
143. Nieswandt B, Echtenacher B, Wachs FP, et al. Acute systemic reaction and lung alterations induced by an antiplatelet integrin gpIIb/IIIa antibody in mice. *Blood.* 1999;94(2):684–93.
144. Schwenk F, Baron U, Rajewsky K. A cre-transgenic mouse strain for the ubiquitous deletion of loxP-flanked gene segments including deletion in germ cells. *Nucleic Acids Res.* 1995;23(24):5080–5081.
145. Tiedt R, Schomber T, Hao-Shen H, Skoda RC. Pf4-Cre transgenic mice allow the generation of lineage-restricted gene knockouts for studying megakaryocyte and platelet function in vivo. *Blood.* 2007;109(4):1503–6.
146. Takai T, Ono M, Hikida M, Ohmori H, Ravetch J V. Augmented humoral and anaphylactic responses in Fc γ RII-deficient mice. *Nature.* 1996;379(6563):346–349.
147. Hazenbos WLW, Gessner JE, Hofhuis FMA, et al. Impaired IgG-dependent anaphylaxis and Arthus reaction in Fc γ RIII (CD16) deficient mice.pdf. 1996;5:181–188.
148. Schindelin J, Arganda-Carreras I, Frise E, et al. Fiji: an open-source platform for biological-image analysis. *Nat. Methods.* 2012;9(7):676–82.
149. Vanschoonbeek K, Feijge M a H, Van Kampen RJW, et al. Initiating and potentiating role of platelets in tissue factor-induced thrombin generation in the presence of plasma: Subject-dependent variation in thrombogram characteristics. *J. Thromb. Haemost.* 2004;2(3):476–484.
150. Hemker HC, Giesen P, Al Dieri R, et al. Calibrated automated thrombin generation measurement in clotting plasma. *Pathophysiol. Haemost. Thromb.* 2003;33(1):4–15.
151. Winkler C, Denker K, Wortelkamp S, Sickmann A. Silver- and Coomassie-staining protocols: Detection limits and compatibility with ESI MS. *Electrophoresis.* 2007;28(12):2095–2099.
152. Premisler T, Lewandrowski U, Sickmann A, Zahedi RP. Serum/Plasma Proteomics: Methods and Protocols. 2011;279–290.

153. Dirnagl U. Bench to bedside: the quest for quality in experimental stroke research. *J. Cereb. Blood Flow Metab.* 2006;26(12):1465–1478.
154. Clark WM, Lessov NS, Dixon MP, Eckenstein F. Monofilament intraluminal middle cerebral artery occlusion in the mouse. *Neurol. Res.* 1997;19(6):641–648.
155. Bederson JB, Pitts LH, Tsuji M, et al. Rat middle cerebral artery occlusion: evaluation of the model and development of a neurologic examination. *Stroke.* 2015;17(3):472–476.
156. Moran PM, Higgins LS, Cordell B, Moser PC. Age-related learning deficits in transgenic mice expressing the 751-amino acid isoform of human beta-amyloid precursor protein. *Proc. Natl. Acad. Sci. U. S. A.* 1995;92(12):5341–5345.
157. Swanson R a, Morton MT, Tsao-Wu G, et al. A semiautomated method for measuring brain infarct volume. *J. Cereb. Blood Flow Metab.* 1990;10(2):290–3.
158. Jackson SP. Arterial thrombosis-insidious, unpredictable and deadly. *Nat. Med.* 2011;17(11):1423–36.
159. Gilio K, van Kruchten R, Braun A, et al. Roles of platelet STIM1 and Orai1 in glycoprotein VI- and thrombin-dependent procoagulant activity and thrombus formation. *J. Biol. Chem.* 2010;285(31):23629–38.
160. Morgenstern E, Ruf A, Patscheke H. Ultrastructure of the interaction between human platelets and polymerizing fibrin within the first minutes of clot formation. *Blood Coagul. Fibrinolysis.* 1990;1:547–549.
161. Grüner S, Prostedna M, Aktas B, et al. Anti-glycoprotein VI treatment severely compromises hemostasis in mice with reduced $\alpha 2\beta 1$ levels or concomitant aspirin therapy. *Circulation.* 2004;110(18):2946–2951.
162. Dütting S, Vögtle T, Morowski M, et al. Growth factor receptor-bound protein 2 contributes to (hem)immunoreceptor tyrosine-based activation motif-mediated signaling in platelets. *Circ. Res.* 2014;114(3):444–53.
163. Berkhemer O, Fransen P, Beumer D, et al. A Randomized Trial of Intraarterial Treatment for Acute Ischemic Stroke. *New Engl. J. Med.* 2014;372(1):11–20.
164. Kleinschnitz C, Pozgajova M, Pham M, et al. Targeting platelets in acute experimental stroke: impact of glycoprotein Ib, VI, and IIb/IIIa blockade on infarct size, functional outcome, and intracranial bleeding. *Circulation.* 2007;115(17):2323–30.
165. Cherpokova D, Bender M, Morowski M, et al. SLAP / SLAP2 prevent excessive platelet (hem) ITAM signaling in thrombosis and ischemic stroke in mice. 2015;125(1):185–195.
166. Lenter M, Uhlig H, Hamannt ALF, et al. A monoclonal antibody against an activation epitope on mouse integrin chain beta 1 blocks adhesion of lymphocytes to the endothelial integrin alpha 6 beta 1. *Proc. Natl. Acad. Sci. U. S. A.* 2000;90(October 1993):9051–9055.
167. Pedersen E, Brakebusch C. Rho GTPase function in development: how in vivo models change our view. *Exp. Cell Res.* 2012;318(14):1779–87.
168. Chen F, Ma L, Parrini MC, et al. Cdc42 is required for PIP(2)-induced actin polymerization and early development but not for cell viability. *Curr. Biol.* 2000;10(13):758–765.
169. Sugihara K, Nakatsuji N, Nakamura K, et al. Rac1 is required for the formation of three germ layers during gastrulation. *Oncogene.* 1998;17(26):3427–3433.
170. Jackson B, Peyrollier K, Pedersen E, et al. RhoA is dispensable for skin development, but crucial for contraction and directed migration of keratinocytes. *Mol. Biol. Cell.*

- 2011;22(5):593–605.
171. Chrostek A, Wu X, Quondamatteo F, et al. Rac1 Is Crucial for Hair Follicle Integrity but Is Not Essential for Maintenance of the Epidermis. *Mol. Cell. Biol.* 2006;26(18):6957–6970.
 172. Boylan B, Chen H, Rathore V, et al. Anti-GPVI-associated ITP: An acquired platelet disorder caused by autoantibody-mediated clearance of the GPVI/FcRgamma-chain complex from the human platelet surface. *Blood.* 2004;104(5):1350–1355.
 173. Takahashi H, Moroi M. Antibody against platelet membrane glycoprotein VI in a patient with systemic lupus erythematosus. *Am. J. Hematol.* 2001;67(4):262–7.
 174. Unkeless J. Characterization of a monoclonal antibody directed against mouse macrophage and lymphocyte Fc receptors. *J. Exp. Med.* 1979;150(September):580–596.
 175. Van Rooijen N, Sanders A. Kupffer cell depletion by liposome-delivered drugs: Comparative activity of intracellular clodronate, propamidine, and ethylenediaminetetraacetic acid. *Hepatology.* 1996;23(5):1239–1243.
 176. Janes PW, Saha N, Barton W a., et al. Adam meets Eph: An ADAM substrate recognition module acts as a molecular switch for ephrin cleavage in trans. *Cell.* 2005;123(2):291–304.
 177. Kisanuki YY, Hammer RE, Miyazaki J, et al. Tie2-Cre Transgenic Mice: A New Model for Endothelial Cell-Lineage Analysis in Vivo. *Dev. Biol.* 2001;230(2):230–242.
 178. Samuelsson a, Towers TL, Ravetch J V. Anti-inflammatory activity of IVIG mediated through the inhibitory Fc receptor. *Science.* 2001;291(5503):484–486.
 179. Nieswandt B. Targeting of platelet integrin alphaIIb beta3 determines systemic reaction and bleeding in murine thrombocytopenia regulated by activating and inhibitory Fc gamma R. *Int. Immunol.* 2003;15(3):341–349.
 180. Muller AJ, Baker JF, DuHadaway JB, et al. Targeted disruption of the murine Bin1/Amphiphysin II gene does not disable endocytosis but results in embryonic cardiomyopathy with aberrant myofibril formation. *Mol. Cell. Biol.* 2003;23(12):4295–4306.
 181. Severs J, Robenek H, Shi HAO, Munster D-. Effects of calcium on the migration and recruitment foam cells of macrophages. 491–501.
 182. Nunes P, Demaurex N. The role of calcium signaling in phagocytosis. *J. Leukoc. Biol.* 2010;88(1):57–68.
 183. Feske S. Calcium signalling in lymphocyte activation and disease. *Nat. Rev. Immunol.* 2007;7(9):690–702.
 184. Beyersdorf N, Braun A, Vögtle T, et al. STIM1-independent T cell development and effector function in vivo. *J. Immunol.* 2009;182(6):3390–7.
 185. Braun A, Gessner JE, Varga-Szabo D, et al. STIM1 is essential for Fc gamma receptor activation and autoimmune inflammation. *Blood.* 2009;113(5):1097–104.
 186. Gwack Y, Srikanth S, Oh-Hora M, et al. Hair loss and defective T- and B-cell function in mice lacking ORAI1. *Mol. Cell. Biol.* 2008;28(17):5209–22.
 187. Vig M, DeHaven WI, Bird GS, et al. Defective mast cell effector functions in mice lacking the CRACM1 pore subunit of store-operated calcium release-activated calcium channels. *Nat. Immunol.* 2008;9(1):89–96.
 188. Feske S, Gwack Y, Prakriya M, et al. A mutation in Orai1 causes immune deficiency by abrogating CRAC channel function. *Nature.* 2006;441(7090):179–185.

-
189. Kim-Kaneyama JR, Miyauchi A, Lei XF, et al. Identification of Hic-5 as a novel regulatory factor for integrin α IIb β 3 activation and platelet aggregation in mice. *J. Thromb. Haemost.* 2012;10(9):1867–74.
 190. Cheli Y, Jensen D, Marchese P, et al. The Modifier of hemostasis (Mh) locus on chromosome 4 controls in vivo hemostasis of Gp6^{-/-} mice. *Blood.* 2008;111(3):1266–1274.
 191. Rathore VB, Okada M, Newman PJ, Newman DK. Paxillin family members function as Csk-binding proteins that regulate Lyn activity in human and murine platelets. *Biochem. J.* 2007;403(2):275–81.
 192. Lei X-F, Kim-Kaneyama J, Arita-Okubo S, et al. Identification of Hic-5 as a novel scaffold for the MKK4/p54 JNK pathway in the development of abdominal aortic aneurysms. *J. Am. Heart Assoc.* 2014;3(3):e000747.
 193. Rolli-Derkinderen M, Toumaniantz G, Pacaud P, Loirand G. RhoA phosphorylation induces Rac1 release from guanine dissociation inhibitor alpha and stimulation of vascular smooth muscle cell migration. *Mol. Cell. Biol.* 2010;30(20):4786–96.
 194. Aslan JE, McCarty OJT. Rho GTPases in platelet function. *J. Thromb. Haemost.* 2013;11(1):35–46.
 195. Kimura K, Ito M, Amano M, et al. Regulation of Myosin Phosphatase by Rho and Rho-Associated Kinase (Rho-Kinase). *Science (80-)*. 1993;273:245–248.
 196. Palazzo a F, Cook T a, Alberts a S, Gundersen GG. mDia mediates Rho-regulated formation and orientation of stable microtubules. *Nat. Cell Biol.* 2001;3(8):723–729.
 197. Karsten CM, Pandey MK, Figge J, et al. Anti-inflammatory activity of IgG1 mediated by Fc galactosylation and association of Fc γ RIIB and dectin-1. *Nat. Med.* 2012;18(9):1401–1406.
 198. Li F, Smith P, Ravetch J V. Inhibitory Fc Receptor Is Required for the Maintenance of Tolerance through Distinct Mechanisms. *J. Immunol.* 2014;192(7):3021–3028.
 199. Takai T. Roles of Fc receptors in autoimmunity. *Nat. Rev. Immunol.* 2002;2(8):580–592.
 200. Bolland S, Ravetch J V. Spontaneous Autoimmune Disease in Fc γ RIIB-Deficient Mice Results from Strain-Specific Epistasis. *Immunity.* 2000;13(2):277–285.
 201. Li F, Ravetch J V. Apoptotic and antitumor activity of death receptor antibodies require inhibitory Fc receptor engagement. *Proc. Natl. Acad. Sci.* 2012;109(27):10966–10971.
 202. Kam T, Song S, Gwon Y, et al. Fc γ RIIb mediates amyloid- β neurotoxicity and memory impairment in Alzheimer's disease. *J. Clin. Invest.* 2013;123(7):2791–2802.
 203. White A, Beers S, Cragg M. Fc γ RIIB as a Key Determinant of Agonistic Antibody Efficacy. *Fc Recept. SE - 16.* 2014;382:355–372.
 204. Nagelkerke SQ, Kuijpers TW. Immunomodulation by IVIg and the Role of Fc-Gamma Receptors: Classic Mechanisms of Action after all? *Front. Immunol.* 2014;5(January):674.
 205. Schwab I, Nimmerjahn F. Intravenous immunoglobulin therapy: how does IgG modulate the immune system? *Nat. Rev. Immunol.* 2013;13(3):176–189.
 206. Miettinen HM, Rose JK, Mellman I. Fc receptor isoforms exhibit distinct abilities for coated pit localization as a result of cytoplasmic domain heterogeneity. *Cell.* 1989;58(2):317–327.
 207. Mammadova-Bach E, Ollivier V, Loyau S, et al. Platelet glycoprotein VI binds to polymerized fibrin and promotes thrombin generation. *Blood.* 2015;126(5):683–692.
-

-
208. Gardiner EE, Karunakaran D, Shen Y, et al. Controlled shedding of platelet glycoprotein (GP)VI and GPIb-IX-V by ADAM family metalloproteinases. *J. Thromb. Haemost.* 2007;5(7):1530–1537.
 209. Simard JM, Tarasov K V, Gerzanich V. Non-selective cation channels, transient receptor potential channels and ischemic stroke. *Biochim. Biophys. Acta.* 2007;1772(8):947–57.
 210. Barrère-lemaire S, Combes N, Sportouch-dukhan C, et al. Morphine mimics the antiapoptotic effect of preconditioning via an Ins (1 , 4 , 5) P 3 signaling pathway in rat ventricular myocytes. 2008;505:83–88.
 211. Djuric S, BaMaung N, Basha A, et al. 3, 5-Bis (trifluoromethyl) pyrazoles: a novel class of NFAT transcription factor regulator. *J. Med.* 2000;43:2975–2981.
 212. Machlus KR, Italiano JE. The incredible journey: From megakaryocyte development to platelet formation. *J. Cell Biol.* 2013;201(6):785–96.
 213. Varga-Szabo D, Braun a, Nieswandt B. Calcium signaling in platelets. *J. Thromb. Haemost.* 2009;7(7):1057–66.
 214. Safari F, Suetsugu S. The BAR domain superfamily proteins from subcellular structures to human diseases. *Membranes (Basel).* 2012;2(1):91–117.
 215. Kashiwagi H, Tomiyama Y. Pathophysiology and management of primary immune thrombocytopenia. *Int. J. Hematol.* 2013;98(1):24–33.

6 Appendix

6.1 Abbreviations

[

[Ca²⁺]_i. Intracellular Ca²⁺ levels

#

β-ME. β-mercaptoethanol

A

ACD. Acid citrate dextrose

ADAM. A disintegrin and metalloproteinase

ADP. Adenosine diphosphate

AEC. 3-amino-9-ethylcarbazole

APS. Ammonium persulfate

Arp2/3. Actin-related proteins 2/3

ASA. Acetylsalicylic acid

ATP. Adenosine triphosphate

B

BAR. Bin1, amphiphysin and yeast RVS167/161 proteins

BCR. B cell receptor

BIN. Bridging integrator

BSA. Bovine serum albumin

C

Ca²⁺. Calcium

CaLDAG-GEFI. Ca²⁺ and diacylglycerol-regulated guanine-nucleotide-exchange factor I, Ca²⁺ and diacylglycerol-regulated guanine-nucleotide-exchange factor I

cAMP. Cyclic adenosine monophosphate

CD. Cluster of differentiation

Cdc42. Cell division control protein 42 homolog

cGMP. Cyclic guanosine monophosphate

CLEC-2. C-type lectin receptor 2

CMV. Cytomegalovirus

CRACM1. Calcium release-activated calcium modulator 1

CRP. Collagen-related peptide

CV. Column volume

CVX. Convulxin

D

DAG. Diacylglycerol

DAPI. 4',6-diamidino-2-phenylindole

DC. Dendritic cell

DIC. Differential interference contrast

DMSO. Dimethyl sulfoxide

DNA. Deoxyribonucleic acid

dNTP. Deoxynucleotide triphosphates

E

ECL. Enhanced chemiluminescence

ECM. Extracellular matrix

EDTA. Ethylenediaminetetraacetic acid

EGTA. Ethylene glycol tetraacetic acid

ELISA. Enzyme-linked immunosorbent assay

ER. Endoplasmic reticulum

ESC. Embryonic stem cell

ESI. Electrospray ionization

et al. Et alii

F

FcR. Fc receptor

FcRγ. Fc receptor γ

Fg. Fibrinogen

FITC. Fluorescein-isothiocyanate

FSC. Forward scatter

G

GAP. GTPase-activating protein

GAPDH. Glycerinaldehyd-3-phosphat-Dehydrogenase

GDI. Guanine nucleotide-dissociation inhibitor
 GEF. Guanine nucleotide-exchange factor
 GP. Glycoprotein
 GPCR. G protein-coupled receptors
 GTP. Guanosine-5'-triphosphate

H

h. hour
 HEPES. 4-(2-hydroxyethyl)-1-piperazine-ethanesulfonic acid
 Hic-5. Hydrogen peroxide-induced clone-5
 HPLC. High performance liquid chromatography
 HRP. Horseradish peroxidase

I

IF. Immunofluorescence
 IgG. Immunoglobulin G
 IHC. Immunohistochemistry
 IP₁. Inositol-1-phosphate
 IP₃. Inositol-3,4,5-trisphosphate
 ITAM. Immunoreceptor tyrosine-based activation motif
 ITIM. Immunoreceptor tyrosine-based inhibitory motif
 ITP. Immune thrombocytopenia
 IVIG. Intravenous immunoglobulin

K

kDa. Kilo Dalton
 KO. Knockout
 KOMP. Knockout Mouse Project

L

LAT. Linker of activated T cells
 LIM. Lin11, Isl-1 and Mec-3
 LSEC. Liver sinusoidal endothelial cell

M

mDia1. Mammalian diaphanous 1
 MFI. Mean fluorescence intensity
 MK. Megakaryocyte
 MLC. Myosin light chain

MOPS. 3-(*N*-morpholino)propanesulfonic acid
 MS. Mass spectrometry

N

n.d.. Not detectable
 n.s.. Non significant
 nano-LC-ESI-MS/MS. Nano-scale liquid chromatographic electrospray ionization tandem mass spectrometry
 NO. nitric oxide

O

OCS. Open canalicular system
 Orai1. Calcium release-activated calcium modulator 1

P

PAGE. Polyacrylamide gel electrophoresis
 PAK. p21-activated kinases
 PAR. Protease-activated receptors
 PBS. Phosphate-Buffered Saline
 PCR. Polymerase chain reaction
 PE. Phycoerythrin
 PF. Platelet factor
 PFA. Paraformaldehyde
 PGI₂. Prostacyclin
 PI3K. Phosphatidylinositol-3-kinase
 PIP₂. Phosphatidyl-inositol-4,5-bisphosphate
 PKC. Protein kinase C
 PLC. Phospholipase C
 PLL. Poly-L-lysine
 Plt. Platelet
 PM. Plasma membrane
 PRP. Platelet rich plasma
 PS. Phosphatidylserine
 PVDF. Polyvinylidene fluoride

R

Rap1. Ras-proximate-1
 RBC. Red blood cell
 RC. Rhodocytin
 RGD. Arginine-glycine-aspartic acid
 RhoA. Ras homolog gene family, member A
 RIAM. Rap1-GTP-interacting adaptor molecule

RNA. Ribonucleic acid
ROCE. Receptor-operated calcium entry
ROCK. Rho-associated protein kinase
RT-PCR. Reverse transcription polymerase chain reaction

S

SAM. Sterile α -motif
SC. STIM1-C-tail affinity column
SD. Standard deviation
SDS. Sodium dodecyl sulfate
SEM. Standard error of the mean
SERCA. Sarcoplasmic/ER Ca²⁺ ATPase
SFK. Src family kinases
sIC. Soluble immune complex
SLE. Systemic lupus erythematosus
SOC channel. Store-operated calcium channel
SOCE. Store-operated calcium entry
STIM1. Stromal interaction molecule 1

T

TAE. TRIS-Acetate-EDTA
TBS. TRIS buffered saline
TCR. T cell receptor
TEM. Transmission electron microscopy

TEMED. N,N,N',N'-Tetramethylethylenediamine
TF. Tissue factor
TG. Thapsigargin
TGF β 1. Transforming growth factor β 1
Tln. Talin
TMB. 3,3,5,5-tetramethylbenzidine
tMCAO. Transient middle cerebral artery occlusion
TP. Thromboxane-prostanoid receptor
Tregs. Regulatory T cells
TRIS. Tris(hydroxymethyl)aminomethane
TRP. Transient receptor potential
TTC. 2,3,5-triphenyltetrazolium chloride
TxA₂. Thromboxane A₂

U

U46. U46619

V

vWF. von Willebrand factor

W

WAVE. WASP-family verprolin homologous protein
WBC. White blood cell
WT. Wild-type

6.2 Acknowledgements

The work presented here was accomplished in the group of Prof. Dr. Bernhard Nieswandt at the Department of Experimental Biomedicine, University Hospital and the Rudolf Virchow Center for Experimental Biomedicine, University of Würzburg. During the period of my PhD work between October 2011 and April 2016, many people helped and supported me. I would like to express my thanks to the following people:

- My supervisor, Prof. Dr. Bernhard Nieswandt, for giving me the opportunity to perform my PhD thesis in his laboratory, for his constant support, his enthusiasm and great scientific ideas. The gathered experience is irreplaceable for my future professional life.
- PD Dr. Heike Hermanns for critical discussion, helpful support for the BIN2 project and for reviewing my thesis.
- Prof. Dr. Christoph Kleinschnitz for critical discussions during the annual reports and for reviewing my thesis.
- Prof. Dr. Manfred Gessler for chairing my doctorate procedure and my thesis defense.
- The team of the Graduate School of Life Sciences for organizing and offering the transferable skill courses and the coordination of the PhD study program.
- The Bio-Imaging Center (Rudolf Virchow Center) for providing technical infrastructure and support.
- Dr. Katharina Remer for dealing with the bureaucracy of the mouse business
- Our technicians and the animal care takers from RVZ and ZEMM for the effort to keep our laboratories and the animal facilities running.
- Dr. Sebastian Dütting, Dr. David Stegner and Dr. Attila Braun for the commitment to our joint projects, their continuous support, helpful comments and suggestions.
- Simon and Viola, the best table neighbors in the world.
- “Team Bulgaria” (Deya, Sarah, Judith, Carsten) for critical discussions and tons of funny moments.
- The “*in vivo* ladies” for the fruitful collaborations.
- All present and former members of the Nieswandt lab, who have not been mentioned here by name, but spent their time and shared their knowledge with me, for the stimulating and supporting working atmosphere as well as for the great social intercourse and many fun moments besides work and for proofreading this thesis.
- Last, my beautiful girlfriend Kerstin, my parents and my brother. You always supported me, were there for me and kept my life in balance.

6.3 Curriculum vitae

PERSONAL DETAILS

Name: Michael Popp



RESEARCH AND PROFESSIONAL EXPERIENCE

- 11/2011 – 04/2016 PhD student in the group of Prof. Dr. Bernhard Nieswandt, Chair of Vascular Medicine and Rudolf-Virchow-Center for Experimental Biomedicine (Julius-Maximilians-University, Würzburg, Germany)
- 04/2011 – 10/2011 Scientific assistant, Medial Clinic and Polyclinic II, University Hospital of Würzburg, Germany
Immunological analyses of regulatory T-cells
- 04/2010 – 02/2011 Diploma thesis, Institute for Clinical Biochemistry and Pathobiochemistry, University Hospital of Würzburg, Germany
“Transgenic expression of the signal peptide of human dihydrolipoamide-dehydrogenase in a murine mouse model” in the laboratory of Prof. Dr. M. Zimmer

EDUCATION

- 10/2008 – 04/2009 Erasmus student exchange programme, Institute of Microbiology and Molecular Genetics, University of Salamanca, Spain
Advanced practical courses in the laboratory of Prof. Dr. J.M. Fernández-Abalos
- 10/2005 – 02/2011 Studies in biology, Julius-Maximilians University, Würzburg, Germany
Majors: Biotechnology, Genetics and Pathobiochemistry
Degree: Diploma in Biology (Dipl. Biol.)
- 09/1996 – 07/2011 A levels (Abitur), Siebold-Gymnasium, Würzburg, Germany
Majors: Biology and Latin

Würzburg, April 2016 _____

6.4 Publications

Stegner D*, Kraft R*, Hofmann S*, Kraft P, Herrmann AM, Popp S, Michaelis M, **Popp M**, Schuhmann MK, Post A, Kleinschnitz C, Braun A, Meuth SG, Lesch KP, Stoll G, Nieswandt B. Orai2 mediates capacitive Ca²⁺ entry in neurons and critically contributes to hypoxic neuronal cell death. *Submitted*.

**these authors contributed equally.*

Stegner D, **Popp M**, Lorenz V, Gessner JE, Nieswandt B. Liver sinusoidal endothelial cells process antibody opsonized platelets through the inhibitory Fc γ receptor IIB in mice. *Submitted*.

Popp M, Thielmann I, Nieswandt B, Stegner D. Normal Platelet Integrin Function in Mice Lacking Hydrogen Peroxide-Induced Clone-5 (Hic-5). *PLoS One*. 2015;10(7):e0133429.

6.5 International Conferences

2nd EUPLAN Conference; Le Bischenberg, France; 24.09.-26.09.2014.

Michael Popp, Sebastian Dütting, Deya Cherpokova, Paquita Nurden, Georg Krohne, Cord Brakebusch and Bernhard Nieswandt

Oral presentation: Redundant functions of RhoA and Cdc42 in platelet function and biogenesis.

XXIV International Society on Thrombosis and Haemostasis (ISTH) Congress; Amsterdam, The Netherlands; 29.06.-04.07.2013.

Michael Popp, Deya Cherpokova, Sebastian Dütting, Paquita Nurden, Georg Krohne, Cord Brakebusch and Bernhard Nieswandt

Oral presentation: Redundant functions of RhoA and Cdc42 in platelet biogenesis.

6.6 Affidavit

I hereby confirm that my thesis entitled “Mechanisms of platelet activation and receptor regulation in genetically modified mice” is the result of my own work. I did not receive any help or support from commercial consultants. All sources and/or materials applied are listed and specified in the thesis.

Furthermore, I confirm that this thesis has not yet been submitted as part of another examination process neither in identical nor in similar form.

Würzburg, April 2016 _____

6.7 Eidesstattliche Erklärung

Hiermit erkläre ich an Eides statt, die Dissertation „Mechanismen der Thrombozytenaktivierung und Rezeptorregulation in genetisch veränderten Mäusen“ eigenständig, d.h. insbesondere selbständig und ohne Hilfe eines kommerziellen Promotionsberaters, angefertigt und keine anderen als die von mir angegebenen Quellen und Hilfsmittel verwendet zu haben.

Ich erkläre außerdem, dass die Dissertation weder in gleicher noch in ähnlicher Form bereits in einem anderen Prüfungsverfahren vorgelegen hat.

Würzburg, April 2016 _____